# Utilization of Coal Fly Ash and Grape Waste to Remove Toxic Metal Ions in Mining Waste Waters

by

Emmanuel Appiah-Hagan

A thesis submitted in partial fulfillment
of the requirements for the degree of
Doctor of Philosophy (PhD) in Materials Science

The Faculty of Graduate Studies
Laurentian University
Sudbury, Ontario, Canada

**THESIS DEFENCE COMMITTEE/COMITÉ DE SOUTENANCE DE THÈSE**
**Laurentian Université/Université Laurentienne**
Faculty of Graduate Studies/Faculté des études supérieures

| | |
|---|---|
| Title of Thesis<br>Titre de la thèse | Utilization of Coal Fly Ash and Grape Waste to Remove Toxic Metal Ions in Mining Waste Waters |
| Name of Candidate<br>Nom du candidat | Emmanuel Appiah-Hagan |
| Degree<br>Diplôme | Doctor of Philosophy |
| Department/Program<br>Département/Programme | Materials Science |
| Date of Defence<br>Date de la soutenance | September 15, 2017 |

**APPROVED/APPROUVÉ**

Thesis Examiners/Examinateurs de thèse:

Dr. Nelson Belzile
(Co-Supervisor/Co-directeur(trice) de thèse)

Dr. Yuwei Chen
(Co-Supervisor/Co-directeur(trice) de thèse)

Dr. Louis Mercier
(Committee member/Membre du comité)

Approved for the Faculty of Graduate Studies
Approuvé pour la Faculté des études supérieures
Dr. David Lesbarrères
Monsieur David Lesbarrères
Dean, Faculty of Graduate Studies
Doyen, Faculté des études supérieures

Dr. Gaixia Zhang
(External Examiner/Examinateur externe)

Dr. Ming Cai
(Internal Examiner/Examinateur interne)

**ACCESSIBILITY CLAUSE AND PERMISSION TO USE**

# Abstract

In recent years, the studies of a variety of inexpensive adsorbents as alternative to the expensive activated carbon have received a lot of attention. The purpose of my research was primarily focused on the modification of Thunder Bay coal fly ash, the characterization of the pristine and modified fly ash and the application of modified fly ash for removal of metal ions from mine wastewater. Adsorption by grape wine material (GWM) was also investigated though not completed.

Modification at low and elevated temperatures with 2.0 M NaOH yielded improvement in surface area, pore volume and cation exchange capacity. However, low-temperature modification was pursued leading to very efficient adsorbents named TBRM and TBFZ compared to the original fly ash named TB. The modified and unmodified fly ash was characterized using different techniques including ICP-OES, X-ray diffraction, specific surface analysis (Brunauer-Emmet-Teller), particle size distribution analysis and scanning electron microscopy. Surface area analysis revealed an increase of specific surface area from 1.24 (TB) to 64.34 (TBRM) and 68.98 (TBFZ) $m^2/g$, respectively. Likewise, porosity was also induced in the modified fly ash. Cation exchange capacities were determined as 1.94, 23.48 and 29.23 meq/g for TB, TBRM and TBFZ, respectively. SEM-EDS and XPS were employed to confirm the adsorption of metal cations on the surface of the adsorbents.

The performance of TBRM and TBFZ for the removal of $Cu^{2+}$, $Pb^{2+}$, $Ni^{2+}$, $Cr^{3+}$, $Co^{2+}$ and $Cd^{2+}$ from a synthetic cocktail solution (SCS) and tailing pond water (TPW) was compared to that of TB. Results indicated TBRM and TBFZ were more efficient in both SCS and TPW. A batch method was used to study the influential parameters of the adsorption process including contact time, pH effect, and kinetics and adsorption isotherms. Column studies were done to compliment the batch mode approach. Regeneration of TBFZ revealed a possible 3-cycle application.

The equilibrium data were generally modeled by the Langmuir and Freundlich models. Also, the pseudo-second order model was found to explain the adsorption kinetics most effectively. Thermodynamic studies of $Ni^{2+}$ and $Cu^{2+}$ with TBFZ in SCS revealed that the adsorption process was spontaneous although endothermic with a decrease in entropy.

The most efficient adsorbent TBFZ was converted into innovative concrete foam composite material TBFZ:FA:BA 0.22:0.33:0.45, for adsorption studies. Preliminary studies revealed a removal of more than 95 % of $Cu^{2+}$, $Pb^{2+}$, $Ni^{2+}$, $Cr^{3+}$, $Co^{2+}$ and $Cd^{2}$ in both SCS and TPW after 6 h of contact. However, the regeneration of TBFZ:FA:BA 0.22:0.33:0.45 was inefficient and further investigation ought to be carried out.

Overall, the results indicate a significant potential of the modified Thunder Bay fly ash as an inexpensive and effective adsorbent for the removal of toxic metals from mine wastewater.

**Keywords**: coal fly-ash, adsorption, tailing pond water, metal ions

**Acknowledgements**

My thanks first go to the Almighty God for giving me the courage, wisdom and strength to undertake this work. My special thanks go to my supervisors: Drs Yuwei Chen, Nelson Belzile and Louis Mercier for their immense contribution in making their research laboratories available, and the equipment and instruments needed for this project. Their keen interest in this research and their supervision resulted in its successful completion. They also spent time reading through this thesis and making the appropriate corrections and recommendations. To Dr. Chen, Belzile and Mercier, I am very grateful.

My appreciation also goes to these organizations: Vale Canada Limited, NSERC (Natural Sciences and Engineering Research Council of Canada), Corfo (Chilean Research Organization), Codelco Mines Chile, Ontario Power Generation, the City of Greater Sudbury and Laurentian University for their financial and material support in diverse ways which made the research possible.

I am also greatly indebted to Dr. William Zhe and Mark C. Cormier at the Willet Green Miller Centre Sudbury and Fisher Wavy Company, respectively. Dr. William provided assistance for the analysis of the morphology and crystalline phases of the materials via SEM and XRD while Mark supplied the bonding and foaming agents applied in the formulation stage. I also wish to thank Dr. Babak Fotoohi for teaching me how to use the ASAP 2010. I am very grateful to him.

I am also grateful to Drs Eugene Ben-Awuah and Fidelis, Daniel Ankomah and Bright Affum for their support and advices in diverse ways for making my studies a success. My special thanks also go to my colleague in the research laboratory, Xiao Yu for her support throughout the research period.

I wish to thank the entire staff of the Department of Chemistry and Biochemistry especially Luc Beaudet, Paul Guerin, Francois Brunet and Adam Walli who helped in one way or the other to make this work a success.

My thanks also go to my mother, Mrs. Matilda Appiah-Hagan and my wife, Mrs. Alberta Appiah-Hagan for their prayers and unfettered support throughout the studies. Their support is immeasurable. My appreciation goes to my siblings, Mrs Otoo, Mrs Addo, Joseph, Gaddiel,

Thomas, Theophilus and Kingsley whose love, encouragement, material and moral support gave me the courage and strength to pursue this program. I am grateful to them.

I am very grateful to my kids: Emmanuel, Lois and Gaddiel for their patience and cooperation during my extended stay away from home during the research.

**Scientific Contributions**

My studies have led to the formulation of a composite material that could be scaled up industrially for the removal of toxic metal ions from mine waste water. My research revealed the ability of the modified fly ash through column studies to remove metal ions from seepage mine waste water. Hitherto, most adsorption studies were conducted with only powdered fly ash. However, an innovation has been developed which has proven effective.

Communications at international conferences have been delivered including:

1. Yu, Xiao; Appiah-Hagan, Emmanuel; Chen Yu-Wei; Belzile, Nelson. 2016. Studies and comparison of the adsorption efficiency of coal fly ash and drinking water sludge for the removal of As(V), Se(IV), Mo(VI) and Cr(VI) from sulfide tailing pond waters**.** 1st International Conference on Sustainable Water Processing, Stiges, Spain.
2. Appiah-Hagan, Emmanuel; Yu, Xiao; Chen Yu-Wei; Belzile, Nelson. 2016. Investigation on the potential of coal fly ash as an effective adsorbent of toxic metals in industrial mining waste waters**.** 1st International Conference on Sustainable Water Processing, Stiges, Spain.
3. Appiah-Hagan, Emmanuel; Yu, Xiao; Chen Yu-Wei; Belzile, Nelson and Louis Mercier. 2015. Hydrothermally modified Thunder-Bay fly ash for the removal of metal ions from mine tailings. 98th Canadian Chemistry Conference and Exhibition, Ottawa, Canada.
4. Appiah-Hagan, Emmanuel; Yu, Xiao; Chen Yu-Wei; Belzile, Nelson and Louis Mercier. 2015. Hydrothermally modified Thunder-Bay fly ash and sludge for the removal of metal (loids) from mine tailings. Mining and Environment 2015 International Conference, Laurentian University, Sudbury, Canada.

Papers for publication are in preparation:

1. Appiah-Hagan, E. *et al.* Modified coal fly ash as an effective adsorbent for metals in mine effluents. *Water Air Soil Pollution.*
2. Chen, Y.-W., Yu, X., Appiah-Hagan, E. Pizarro, J., Arteca, G.A., Mercier, L. & Belzile, N. Utilization of drinking water sludge and modified coal fly ash as efficient adsorbents of metals and metalloids. *Journal of Environmental Management.*

## Table of Contents

# List of Tables

# List of Figures

# Abbreviation and Acronym list in alphabetic order:

AFS: Atomic fluorescence spectroscopy;

AMAS method: ammonium acetate saturation method;

ASTM: American Association for Testing and Materials;

BA: bonding agent

CEC: Cation Exchange Capacity;

DOC: dissolved organic carbon;

FA: foaming agent

FAAS: flame atomic absorption spectroscopy;

FT-IR; Fourier Transform Infra-red spectroscopy;

GAAS: graphite furnace atomic absorption spectroscopy;

GWW: Grape wine waste;

HDPE: high density polyethylene;

HTB ($CO_3$)150/4: hydrothermal treatment in 2.0 M $Na_2CO_3$ at 150 $^oC$ for 4 h;

HTB (OH)150/4: hydrothermal treatment in 2.0 M NaOH at 150 $^oC$ for 4 h;

ICP – OES: Inductively coupled plasma – optical emission spectroscopy;

LALLS: Low Angle Laser Light Scattering

Micromeritics ASAP 2010: Micromeritics (Accelerated Surface Area and Porosimetry System) 2010;

PTFE: polytetrafluoroethylene;

SCS: synthesized cocktail solution;

SEM – EDS: scanning electron microscopy – energy dispersive x-ray spectroscopy

TB: Thunder Bay coal fly ash;

TBMW(OH)100/0.5: hydrothermal modification with microwave oven in 2.0 M NaOH at 100 $^oC$ for 0.5 h;

TBMW(OH)150/1: hydrothermal modification with microwave oven in 2.0 M NaOH at 150 $^oC$ for 1 h;

TPW: tailing pond water;

DW: Deionized water;

WAC: water absorption capacity;

XRD:  X-ray diffraction;

# Chapter 1

# 1. Introduction

Although 70 % of the Earth's surface is covered by water, only 3 % is freshwater, and two-thirds of this water is lodged in glaciers, therefore unavailable for immediate use. According to a Food and Agricultural Organization report, about 62 % of irrigated area is supplied from surface water and 38% from groundwater **[1]**. Groundwater provides about 50 % of water to global population and thus 2.5 billion people depend on groundwater for daily water needs **[2].** However, it is estimated that 20 % of the World's aquifers is over-used, or damaged as a consequence of land subsidence and intrusion of salt water **[3]**. It is reported that about 1.2 billion people live in areas where water is physically scarce. The total number of people without access to improved drinking water globally is now 663 million – the first time the number has fallen below 700 million **[4]**. It is projected that by 2030, the World is likely to be hit by a 40% global water deficit as result of climate change scenario **[2]**. Scarcity of water could lead to serious water shortage, and crisis. Apart from influence from climate change, the other factors that cause water scarcity include: urbanization, population growth, industrialization, increases in production and consumption, conflict and pollution.

## 1.1 Water pollution by toxic organic and inorganic substances and common treatment methods

With the economic development and industrialization in more countries in the world, many industrial wastes are produced during those processes. How to reuse those waste materials and enhance their potential value becomes an important topic among both industrial and academic worlds. At the same time, water pollution becomes an ever-pressing problem. Water pollution can be caused by both organic and inorganic substances. The organic pollutants include pesticides, food processing waste, petroleum hydrocarbons, pharmaceutical wastes, and paints, dyes of textile and leather industries, toxic volatile gases emitted or discharged from chemical and plastic manufactures, cleaning utilities. These organic pollutants can cause potential health effects including damage to the liver, kidneys, reproductive system, nervous system, gastrointestinal disturbances and cancer **[5]**. Inorganic pollutants in water are often involving metal ions and anions of non-metals and metalloids. Although some metals and metalloids such as copper (Cu), cobalt

(Co), selenium (Se), iron (Fe), manganese (Mn), vanadium (V), strontium (Sr) and zinc Zn are essential to living organisms in very low concentration range, they become toxic when their level exceed their optimal levels **[6]**. Most sources of inorganic pollution are associated to metal mining and smelting, construction material extracting, electroplating, battery manufacturing, land fill leachate, acid drainage of abundant mines, coal powered electrical generation plants, the rejected circuit board, and so on. The most environmentally concerned metals include cadmium (Cd), lead (Pb), mercury (Hg), copper (Cu), chromium (Cr), nickel (Ni), silver (Ag), beryllium (Be) and zinc (Zn). These metals are generally presented as cations in their dissolved forms. The most concerned metalloids are arsenic (As), selenium (Se), antimony (Sb), bismuth (Bi), and tellurium (Te). They can be in multi-chemical valences in natural conditions and present as anions in their dissolved forms. Once these metals and metalloids present in ionic form, they are soluble in water, therefore they become bioavailable and can be assimilated by biological species. Some such as mercury and selenium can be bio-accumulated, even bio-signified in aquatic food webs. Toxicity of some metals can be acute and cause vomiting, blood poisoning, liver and kidney damage, nerve system break down and so on. They can also cause chronic damage to living species. For this reason, governments around the world have established norms for their concentrations in waters of various types according to their toxic levels to biological species. For instance the U.S. Environmental Protection agency (US EPA) has established the limits of these hazardous metals in drinking water such as 1.3 mg/L for Cu, 0.015 mg/L for Pb, 0.01 mg/L for As, 0.005 mg/L for Cd and 0.1 mg/L for Cr, etc. **[7]** .

To breakdown organic pollutants, chemicals such as hydrogen peroxide ($H_2O_2$), ozone ($O_3$), sodium hypochlorite (NaOCl) and chlorine dioxide ($ClO_2$) are applied. When organic pollutants can be oxidized to carbon dioxide ($CO_2$) and water, it is called a complete oxidation. A complete oxidation is not always requested, if a pollutant can be broken down to a non – toxic form. Many other techniques have been developed to treat organic pollutants produce in different processes, and the techniques include electrochemical methods, photo-catalysis and advance oxidation processes **[8]**. Apart from the above destructive techniques, organic pollutants can also be removed by coagulation and coagulation with filtration processes **[9]**.

The most widely used and most effective technique for the removal of metal and metalloid pollutants from waste water in industry is probably chemical precipitation since it is a simple

process and easy to operate **[10]**. However, large quantities of sludge are generated and must be treated before being discharged into the environment. The presence of complexing agents in the waste water may also inhibit metal hydroxide precipitation **[10]**. Another disadvantage associated with precipitation is the presence of amphoteric metals/metalloids, which will create problems since a pH for one element may not be ideal for another present in the same waste water. The chemicals commonly used are calcium hydroxide ($Ca(OH)_2$) and sodium hydroxide (NaOH). The coagulants such as alum, iron salts and organic polymers are also used to improve the efficiency of metal removal from the waste water **[11]**. Sulfide has also been employed in the precipitation of metal ions. The advantages of sulfides precipitation are: (1) there are no amphoteric problems in sulfides precipitate; (2) solubility of metal sulfides are usually much lower compared to their hydroxide counterparts; (3) sludge produced from sulfides show better thickening and dewatering characteristics compared to those formed from hydroxide. The disadvantages of the technique include the potential risks of producing toxic $H_2S$ fumes in operation when pH become low, more complicated operation process, disposal metal sulfides and higher cost **[11]**. They also form colloidal precipitates resulting in settling or filtration issues. Organic chelating agents have been used to enhance precipitation and coagulation of precipitates in aqueous solutions. Some of the most widely used and effective chelating agents are trimercaptotriazine, potassium/sodium thiocarbonate and sodium dimethydithiocarbamate **[12]**. Ion exchange is also used to remove ionic pollutants from water. In this case, ion exchange resins are specific to pollutant ions in question. The most common cation exchangers are strongly acidic resins with sulfonic acid groups ($-SO_3H$) and weakly acid resins with carboxylic groups (-COOH). At an appropriate pH, protons on the carboxylic and sulfonic groups are dissociated and targeted metal ions are grafted **[11]**. Advantages of ion exchange method include high treatment capacity, high removal efficiency and fast kinetics **[13]** .The major disadvantage of applying ion exchange resins is the fouling of the resin by organic matter and iron present in the water.

Adsorption is used to remove organic and inorganic pollutants from wastewater. Adsorption is a phenomenon which occurs at the surface of a material called adsorbent when an adsorbate in a solution comes into contact with the adsorbent. This results in an increase in concentration of the adsorbate on the surface due to an interaction between the solid and the dissolved species **[8]**. There are two kinds of adsorption: physical adsorption (physisorption) and chemical adsorption (chemisorption) **[14]**. In physical adsorption, the forces of attraction between

adsorbate and adsorbent are Van der Waal's forces. This force of attraction is very weak; therefore, this type of adsorption can be reversed. In chemical adsorption, the attraction between adsorbate and adsorbent are similar as chemical bond. Thus, the adsorption cannot be reversed easily. The advantages of adsorption technique include the flexibility in design and operation, and re-usability of adsorbents **[11]**. Like other techniques, adsorption also face disposal problem once it can no longer be reused **[15**].

The cost of adsorbent is an important concern. The most widely used adsorbents are activated carbon (AC), zeolites and silica gel. Among these, activated carbon is the preferred choice due to high efficiency and high surface area. However, activated carbon is an expensive material with its price as $300 - $5000 US/ton. The cost of natural zeolites is also usually more than $100 per ton. For companies that produce a large quantity of waste water, this cost is certainly a huge burden.

One of the major environmental problems confronting the world today is the continuous and high production of toxic substances loaded with water because of industrial processes and increasing population. The major sources of discharge include mining sector, battery industry, textile, paint, petroleum refining, wood processing, electroplating, pigment manufacture, electronic boards, pesticides and herbicides, as well as the photography and printing industries **[16-18]**. Treatment of wastewater with effective method and acceptable cost is a pressing demand in wastewater management. The next section will summarize the recent studies on the removal of organic and inorganic pollutants from wastewater by various sources of fly ash.

### 1.2 Fly ash in wastewater treatment studies

In recent years, the studies on a variety of low-priced materials as alternatives to the expensive activated carbon have received a lot of attention. The reasons for the shift in research interests are threefold: to minimize the cost in wastewater treatment operation, to maximize the values of used materials and to reduce the environmental impact caused by waste material produced in manufacturing processes. The most commonly studied low-cost adsorbents include fly ash, sludge of drinking water treatment plant, clay, agricultural waste or biomass, low-cost composite materials and other industrial wastes.

Due to its chemical and physical properties, fly ash produced after combustion of coal can be used for many different purposes. Because of its richness in silica, alumina and iron oxide, it can be used as a material resource to replace cement in construction of road and land stabilization. Depending on its size, it could be employed as an abrasive for surface scouring and polishing. It could also be used as fillers for road building and in plastic making to enhance its strength. It is also used as ceramic raw material and to make bricks and glass. As an abundant resource, fly ash is also applied in activities related to agricultural purposes, such as land reclamation. Wang and Wu (2006) have reviewed the application of fly ash as a low cost adsorbent **[19]**.

Coal Combustion Products (CCP) include bottom ash, fly ash, and flue gas desulphurization (FGD) gypsum (the residue of sulfur and lime added to reduce the emission of $SO_2$ gas **[20]**. The stocks of CCPs continue increase due to the increasing demand for electricity worldwide. Statistics available indicate that the world production of CCPs 2010 is 780 billion tons, with China, USA and India as the top producers **[21]**.

According to Statistics Canada, fly ash comprises the majority of annual CCPs production with 62.06 %, with bottom ash, gypsum and the rest being 31.1, 3.92 and 2.94%, respectively. As concern to the reuses of CCPs, a statistics by Natural resources Canada showed that flue gas desulphurization (FGDG ) gypsum is 100% reused, but fly ash and bottom ash reutilization is only 28 and 9%, respectively **[22]**. Effectively reusing these valuable resources is not only to solve an environmental problem, but also can take its economic advantage.

### 1.3 Chemical and physical properties of fly ash

The main composition of fly ash includes oxides of silicon, aluminum, calcium, iron, magnesium and to a smaller extent sodium and potassium. This makes fly ash a very alkaline material. An empirical formula for fly ash based on certain major elements is proposed below **[23]**:

$$Si_{1.0}\,Al_{0.45}\,Ca_{0.51}\,Na_{0.047}\,Fe_{0.039}\,Mg_{0.020}\,K_{0.013}\,Ti_{0.011}$$

Fly ash can be categorized as class C and class F. Class C is produced in burning of sub-bituminous and lignite coals and usually contains more lime (15-30%). Class F is produced in burning of anthracite coal and contains less than 7% of lime content and has more silica, alumina and iron oxide **[23]**. The chemical composition of fly ash is close to those in clays and construction materials. Class F fly ash is considered a good candidate as a low-cost adsorbent.

Fly ash has a characteristic spherical shape as demonstrated in **Figure 1.1**. Fly ash particles are generally small, ranging from few micrometers to few tenths of nanometers, and most of them are in less than 1μm in diameter. Because of their generally small sizes, fly ash possesses large specific surfaces; therefore, it has potential to be a good adsorbent.

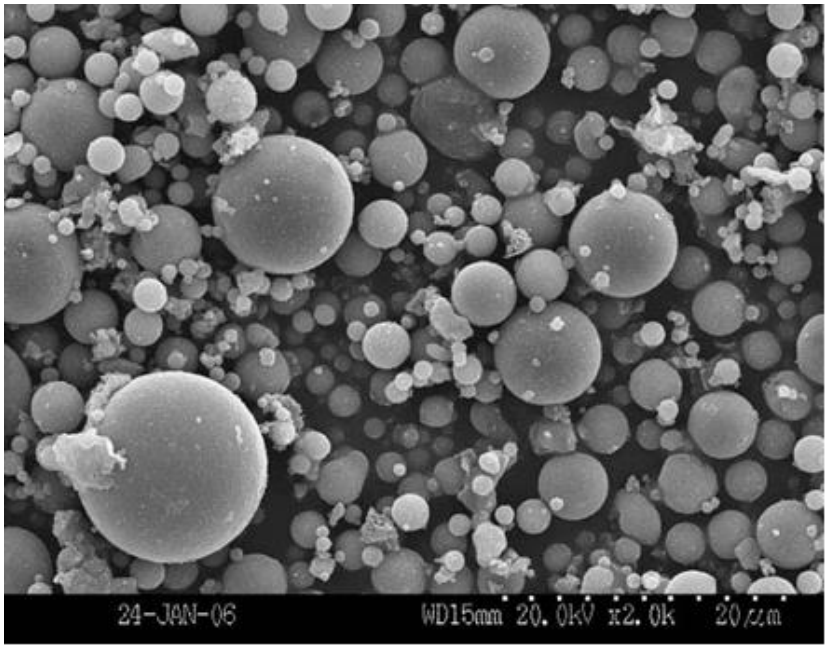


**Figure 1.1 SEM photo of coal fly ash.**

### 1.4 Removal of organic pollutants using fly ash

The properties of an adsorbent, includes: equilibrium time, removal efficiency, maximum adsorption capacity, etc. These properties are strongly related to how and under what conditions a study is conducted. However, many of the previous works have not carefully presented essential

experimental conditions which brings significant confusion and puzzling to readers. The more detailed experimental conditions, results and conclusions are given in a separate table below.

Toxic organic pollutants have created a myriad of environmental concerns. The most common organic pollutants includes: persistent organic pollutants (POP) such as polychlorinated biphenyls (PCBs), polychlorinated dibenzo-dioxins and dibenzofurans (PCDDF/Fs), and organo-chlorine pesticides (OCPs) like hexachlorobenzene (HCB) or dichloro-diphynyl-trichloroethane (DDT) **[8]**. The studies related to the removal of organic pollutants from wastewater by fly ash are limited.

Fly ash used in studies varies in their origin, some are coal fly ash **[24-27]** and the other are from bagasse **[28-29]**. Coal fly ash used in some studies are deeply modified such as those by Dash et al. **[24]**, where calcination with sodium hydroxide at 550–600 $^{o}$C followed by intensive neutralization and grafting with polyethylenimine (PEI) was applied. The surface phenomenon of the adsorbent (CFA-PEI) has been studied in detail. Duta and Visa **[26]** have modified their coal fly ash with FAw: $TiO_2$ = 3:1 (FAw stands for the washed fly ash and sized to 20 – 40 μm), then grafted a cationic surfactant hexadecyltrimethylammonium bromide (HTAB). With this material (denoted as FAA-DCS), they compared removal mechanisms of a mixed dye system of Bemacid Blue N-TF (BB) and Bemacid Red N-TB (BR) under visible and UV ($\lambda_{max}$ 365 nm) light exposure. The authors stated that the dyes were first adsorbed on the FAA-DCS, then the $TiO_2$ played a catalyzer role to promote the breakdown of dyes under a UV irradiation. They found the adsorption efficiency of the dyes as dependent on the morphological structure and surface charge of substrates and the adsorption kinetics influenced by the flexibility of dye molecules. Addition of $H_2O_2$ did not promote the breakdown of the dyes.

Both Singh **[25]** and Nollet et al. **[27]** used non – modified coal fly ash in their studies, however the latter have their fly ash washed with distilled water for 24 h and dried before being used. The former studied the potential of fly ash to adsorb pesticides (atrazine AT, metolachlor M1 and metribuzin M2,) from water and the latter investigated the removal of polychlorinated biphenyls PCBs (2,3,4-trichlorobiphenyl, TCB and 2,20,3,30,4,5,6-heptachlorobiphenyl, HeCB). Singh **[25]** found that the adsorption equilibria were reached quickly for all tested pesticides. The adsorption isotherm fitted well with both Langmuir and Freundlich models and calculated $q_m$

differed greatly from each other. Increase of the adsorbent mass increased the percentage removal of pesticides, but reduced the adsorption capacity. The size of adsorbent does not clearly affect the adsorption efficiency. Nollet et al. **[27]** found that pH (2–10) does not affect adsorption of TCB and HeCB, whereas the presence of other ionic species generally reduced the adsorption of the PCBs. The kinetics of adsorption is dependent on the initial concentration ($C_{int.}$), the lower $C_{int.}$, the faster the equilibrium was reached. Usually it took 24h to have 80 – 97 % of PCBs being removed. However, without indicating under what initial concentration of adsorbate used in the study, the results seem inconclusive, as it is known that an adsorption capacity of a material should be done with an increasing concentration of adsorbate and fixed amount of adsorbent. The adsorption fit well with first order kinetics model at both low and high concentrations for TCB and HeCB. The Freundlich model fits well for both TCB and HeCB, but the Langmuir model fits well for only HeCB. As Singh, Nollet also observed a drop in adsorption capacity as an increased dose of adsorbent. The maximum adsorption capacities of adsorbent ($q_m$) to TCB and HeCB are undecided, as the adsorption of the material to these compounds are not saturated because the tested concentration ranges of TCB and HeCB were not high enough.

The fly ash from bagasse was studied by Deokar et al. **[28]** to remove the herbicide 2,4-dicholorophenoxyacetic acid (2,4-D). Unlike regular coal fly ash, the fly ash used in their studies contains 47.4 % of carbon which makes the material behavior partially as an active carbon. In their investigation, the batch tests were applied to study the affecting factors. The study found that the adsorption equilibrium was fast to reach, but the removal % drops as the $C_{init.}$ increased. A lower pH was preferred for 2,4-D adsorption due to a positive charge of the adsorbent when its pH is lower than its $pH_{zpc}$. It was found that the larger particles have higher surface area and higher adsorption efficiency, which can be explained by their higher carbon: silica ratio and higher surface area. This material behaved like active carbon. The packed bed tests were also carried to examine the effects of $C_{init.}$, flow rate and bed height on the herbicide removal on the packed bed system. The model fittings on the packed bed system were discussed. Gupta and Ali **[29]** used bagasse fly ash to remove pesticides DDD [2,2-Bis(4-chlorophenyl)-1,1-dichloroethane] and DDE [1,1- Bis (4-chlorophenyl) -2,2-dichloroethene]. The solubility of these compounds in water is less than few tenth of micrograms. The bagasse was first soaked in hydrogen peroxide solution (60 $^{o}$C, 24 h), then dried and ground to desired particle sizes. The chemical composition of the so-prepared

material was dominated by $SiO_2$ (61 %) and $Al_2O_3$ (15 %); the loss in ignition was 18 % and pH strongly influenced adsorption of DDD and DDE and was optimized at pH 7. Unfortunately, the authors have ignored many critical conditions, e.g. there was no mention either the two pesticides were studied as a mixed or in a separated system, or on the initial concentration and volume used in kinetic studies. Furthermore, constantly using mg/g, rather than removal percentage, to express the effects of studied parameters on removal of pollutants at equilibrium is confusing when so many basic parameters were not given.

The detailed experimental conditions and conclusions of these studies are given in **Table 1.1**. To shorten text, the following symbols will be used in the table hereafter. **B** – batch study; **PB** – packed bed study; **A** – adsorbate name, $\mathbf{W_{ad}}$ – mass or mass concentration of adsorbent used to determine adsorption kinetics or isotherm study in batch study; $\mathbf{C_{init.}}$ – initial concentration of adsorbate in a kinetic study; $\mathbf{C_{qm}}$– concentration of adsorbate used in qm determination; **V** – volume (mL) in a batch study; **pH** – the optimal pH used in a study; **T** – optimal temperature ($^oC$) in a study; **t** – time (min) needed to reach an adsorption equilibrium; $\mathbf{R_m\%}$ - removal percent of adsorbate with $C_{init}$; $\mathbf{q_m}$ – maximum removal capacity of studied material; **LM** – Langmuir Model fitting; **FM** – Freundlich model fitting; **KAM** – kinetic adsorption model. **S** – stirring; **NA** – information is not available. When a parameter is not given, it means that there was no mention or unclear in the reference.

**Table 1.1 Summary of the experimental conditions and conclusions of the studies on removal of organic pollutants with fly ash.**

| Adsorbent type | Experimental conditions | Results | Refs |
|---|---|---|---|
| Polyethethyle-nimine grafted coal fly ash (CFA-PEI)<br><br>Batch study | **A**: dyes Malachite green MG, reactive red RR2 separately;<br>Kinetic studies:<br>$C_{init.}$ =100 ppm (MG or RR2);<br>$W_{ad}$= 40 mg (MG), 25 mg(RR2);<br>T= 35 $^oC$, 40 $^oC$; t = 40 min (MG), 50 min (RR2); Stirring 105 rpm.<br><u>maximum adsorption ($q_m$)</u>:<br>$W_{ad}$ = 40 mg (MG); 25mg(RR2);<br>$C_{qm}$ = 100 ppm-275 ppm (RR2); 100 ppm -250 ppm (MG); T= $35^0C$ (MG); 40 $^oC$ (RR2) ;t = 40 min | Rm = 97.5 mg/g (RR20; 95.25 mg/g (MG); pH=8 (MG) and 4 (RR2); $q_m$=174.8mg/g (MG, 316.8mg/g (RR2,).<br>T affects ads<br>MG & RR2 fit well to LM and pseudo-$2^{nd}$ order KAM. Reusable.<br>Similar to ion exchange mechanism | **[24]** |

| | | | |
|---|---|---|---|
| | (MG); 50 min (RR2) ; Stirring 105 rpm for both; | | |
| Non-modified coal fly ash<br><br>Batch study | **A**: herbicides atrazine AT, metolachlor M1, metribuzin M2, separately,<br>kinetic study:<br>$C_{init.}$ = 10mg/L; $W_{ad}$ = 0.5g; t = 1440 min; V = 10 mL, T= room, stirring.<br>maximum adsorption ($q_m$):<br>$C_{qm}$ = 2.5 – 500 mg/L (M2); 2.5-200 mg/L (M1); 2.0-10.0 mg/L (AT), $W_{ad}$=0.2g (AT), 1.0 g (M1 or M2), V =10 mL, t =120 min, T=room, Stirring. | Rm%=97 (AT), 91 (M1), 89 (M2); $q_m$ (mg/g) by LM=3.3(AT), 1.0(M1), 0.2(M2); $q_m$(mg/g) by FM=0.38 (AT), 0.28(M1), 0.2(M2). | **[25]** |
| Coal fly ash – $TiO_2$ – cationic surfactant HTAB (FAA-DCS)<br><br>Batch study | **A**: dyes Bemacid Blue N-TF BB and Bemacid Red N-TB BR, mixed:<br>kinetic study: $C_{init.}$ = 50 mg/L each; $W_{ad}$=0.5 g; V=50.0 mL; T= 22 $^oC$; t=50 min.<br>photo catalysis by $TiO_2$: $\lambda_{max}$ =365 nm irradiation t=240 min, the rest are the same. Stirring. | adsorption kinetic study: Rm%=75 (BR), 18 (BB); pH=10.6 (non-adjusted)<br>photo catalysis by $TiO_2$:<br>Rm% (dark) =80 (BR), 20 (BB);<br>Rm% ($\lambda_{max}$365 nm) =93(BR), 78(BB). $TiO_2$ alone inefficient;<br>FAA-DCS has a negatively charged surface. Best fit to pseudo-2$^{nd}$ order KAM. | **[26]** |
| Fly ash of bagasse<br><br>Batch study | **A**: Polychlorinated biphenyls: 2,3,4-trichlorobiphenyl (TCB), 2,2,3,3,4,5,6-heptachlorobiphenyl (HeCB)<br>kinetic study:<br>$C_{init}$ = 250 µg/L (TCB); 125 µg/L (HeCB; $W_{ad}$ = 5 g/L (TCB & HeCB), t = 300 min, T= 25 $^oC$; pH=7.0 Stirring NA.<br>maximum adsorption ($q_m$):<br>$C_{qm}$=250 – 2500 µg/L (TCB); 125 – 1000 µg/L (HeCB), t=24h, T=25$^oC$. | kinetic study:<br>Rm%= 97 (TCB); 97 (HeCB);<br>maximum adsorption:<br>$q_m$ = 0.38mg/g (TCB), 0.23 mg/g (HeCB)<br>$\Delta H^0$ = -15.70 kJ/mol (TCB); 40.47 kJ/mol (HeCB);<br>LM fit HeCB better than TCB; | **[27]** |
| Fly ash of bagasse (BFA)<br><br>Batch study (**B**) | A: herbicide 2,4dicholorophenoxyacetic acid 2,4-D.<br>kinetic study: $W_{ad}$=1.0 g, V=25 mL, t =360 min (50 mg/L), 720 min | Rm%=97 (50 mg/L), 50(400 mg/L); pH 3.5; when $W_{ad}$> 1.0 g, R% did not improve. Fits LM better than FM. $q_m$(mg/g) by LM: 5.63 (30 $^oC$), 6.40 (45 $^oC$), 7.14 | |

| | | | |
|---|---|---|---|
| Packed-bed (**PB**) | (400 mg/L), T=30 $^{o}$C. Stirring NA. <u>maximum adsorption ($q_m$)</u>: $C_{qm}$ = 50-400 mg/L, $W_{ad}$ = 1.0g, V = 25 mL, T=30 $^{0}$C, t = 720 min **PB:** IDΦ=1.2 cm; Length=6.5 cm; T 30±2 $^{o}$C; $C_{init.}$:50 mg/L; flow rate:1.2 mL /min; pH 3.5 | (55$^{o}$C) **PB:** R%: 37.04. The deactivation kinetic model fit best on this packed-bed system among all other tested models. | **[28]** |
| Bagasse socked in $H_2O_2$<br><br>Batch study **(B)**<br><br>Packed – bed **(PB)** | **A**: pesticide DDD and DDE <u>kinetic study:</u> **B:** $W_{ad}$=5 g/L; T=30$^{o}$C, pH 7.0; t=80min; Stirring <u>maximum adsorption ($q_m$)</u>: $C_{qm}$ = 2.0 – 30.0 mg/L; pH 7.0; T= 30 $^{0}$C; t = 80 min (DDD & DDE) **PB:** $C_{init.}$ = 22µg/L (DDD and DDE) IDΦ =2cm, no bed height info. | **B:** $q_m$=7.69µg/g (30$^{0}$C), 7.61µg/g (40$^{0}$C), 7.54 µg/g (50$^{0}$C) - DDD); 6.67µg/g (30$^{0}$C), 6.60µg/g (40$^{0}$C), 6.53 µg/g (50$^{0}$C) -DDE); exothermal adsorption; particle size does not affect adsorption; foreign ions dropped adsorption. Fit LM better than FM. **PB:** when flow rate>1mL/min, removal efficiency dropped linearly. Wash with 5% NaOH, precondition with 1M $HNO_3$, reused 10 times. | **[29]** |

### 1.5 Fly ash to remove toxic elements

The studies on using fly ash to remove toxic elements from water are mainly focused on metal ions. In most cases, the studied toxic metals are positively charged in the studied system, but some are negatively charged anions such as $Cr_2O_7^{2-}$, $AsO_2^{-}$ and $AsO_4^{3-}$. Banerjee et al. **[30]** applied impregnated fly ash (FA) to remove $Hg^{2+}$ and $Cr_2O_7^{2-}$ from aqueous solutions. The FA was first treated in 500 mL of 0.01 M NaOH solution for 24 h at 26 ± 2 $^{o}$C, then was filtered and washed 3 times with distilled water. This FA was then soaked in 500 mL of 0.1 M $Al(NO_3)_3$ (IFAAl) or 0.1 M $FeCl_3$ (IFAFe) for 24 h at 26 ± 2$^{o}$C. The reagent solution was removed and the impregnated sample was washed and dried at 26 ± 2 $^{o}$C, then dried at 100 ± 2 $^{o}$C again. Fly ash was sieved to average particle diameter of 100 µm before the impregnation. Fourier transform analysis showed a formation of Si-O$Al^{2+}$ after the impregnation. Impregnated fly ash had a better efficiency for both Hg(II) and Cr(VI) compared to the original. The formation of extra Al- or Fe- hydroxide layers around the fly ash was responsible for the increased adsorption efficiency. The study showed a 90 % removal in 100 mL of 7.6 mg/L Cr(VI) (pH 3.5) in an electroplating waste water by 0.5 g of IFAAl. However, the modified fly ash was unstable under a hot dilute acidic condition without

further specification. As observed by Banerjee et al. **[30]**, pH strongly affects the adsorption of Cr(VI) by FA. A strong pH condition favored the adsorption and this is probably due to the protonation of silanol– OH functional groups which made the surface positively charged. The adsorption of $Cr_2O_7^-$ occurred due to the electric attraction between the adsorbent and adsorbate. A novel thiol modified coal fly ash (CFA-SH) has been applied by Dash et al. **[31]** to remove toxic metal ions ($Hg^{2+}$& $Cd^{2+}$) from water. The non-magnetic components part of coal fly ash (CFA) was calcined with NaOH (1:1.2) for 4 h at 550 $^oC$ and NaOH was neutralized by refluxing concentrated HCl for 15h (MCAF). Thiol functional groups on 3-mercaptopropyltrimethoxysilane (MPTS) was then grafted onto the calcined fly ash (CAF-SH). The surface area was increased from 62.79 $m^2\ g^{-1}$ for CFA to 105.72 $m^2\ g^{-1}$ for surface modified CFA. The rapid drop of surface area in CFA-SH (58.30 $m^2/g$) suggests an effective coating of MPTS on the fly ash since $N_2$ gas used in the surface measurement interact much weakly with the coating material. The deprotonation of –SH group strongly affects the chemical adsorption of $Hg^{2+}$ and $Cd^{2+}$ and the optimal pH is 8. The adsorption efficiency gradually drops by 20 % after 4 cycles of adsorption/desorption cycles for both $Hg^{2+}$ and $Cd^{2+}$. The adsorption test indicated a better affinity for $Hg^{2+}$ than $Cd^{2+}$ on the CFA-SH. It is necessary to indicate that the maximum adsorption capacity based on the Langmuir model and extracted from the experimental data show a great gap. The optimal adsorption temperature was 34 and 39 $^oC$ for Cd and Hg, respectively. Higher than this temperature, the removal percentage dropped, probably due to the decomposition of coating material MPTS. It is unfortunate that the authors have not presented any results with non-modified CFA, therefore the advantages of thiol grafting cannot be discussed. Hui et al. [32] prepared zeolite 4A from coal fly ash for the removal of $Co^{2+}$, $Cr^{3+}$, $Cu^{2+}$, $Ni^{2+}$ and $Zn^{2+}$. Their method involved boiling 30g of fly ash with 300 mL of 2 M NaOH at 100 $^0C$ for 2 h stirring at 300 rpm. The molar ratio $SiO2/AlO_3$:$Na_2O/SiO_2$: $H_2O/Na_2O$ of the filtered solution was adjusted to 1.64:8.09:56.51 by the addition of 100 mL of aluminum solution to control the molar ratio for synthesis of pure zeolite 4A. At 25 $^oC$, this solution was stirred (500 rpm) for 30 min and further heated at 90 $^oC$ for 1.5 h. The solution was finally subjected to further heating at 95 $^oC$ for 2.5 h. The synthesized zeolite 4A was washed for 24 h at 25 $^0C$ with 1M NaOH prior to adsorption test. The residual fly ash was concerted to NaP1 zeolite according to the studies. Comparing the surface areas of the fly ash, zeolite 4A (synthesized) and zeolite 4A (commercial) reveal an increment from 1.38 to 54.82 $m^2/g$ while commercial zeolite 4A had 71.41 $m^2/g$ due to smaller particle size. Kinetic studies indicates that 90 % of all metal ions

were removed within 60 min at pH 3 while at pH 4, a 90% removal was attained within 30 min indicating the dependence of removal on pH. The same sorption sequence was observed for commercial and synthesized 4A zeolites in the order Cu > Cr > Zn > Co > Ni during isotherm studies. The authors compared the adsorption efficiency of synthesized to the commercial zeolite; a comparison with the original fly ash would have been better. In addition, the experimental $q_m$ values should have been provided for comparison with calculated $q_m$ as these values reveal many differences. The fly ash used by Ulatowska et al. **[33]** was a product of combustion of lignite and biomass. The removal of As(III) from a synthesized aqueous solution was compared between the pristine fly ash (FA) and an agglomerated fly ash (AFA). The agglomeration was done simply by using water as a binder agent (200 g FA, 110 mL water, mixed for 1 h, cured for 1 week). Only the size 2.5 – 5.0 mm of agglomerates was used. The authors found that the influence of pH on adsorption of As(III) fluctuates without a defined trend. Therefore, the adsorption test was done in a pH given by the tested adsorbents, i.e. pH 10.4 – 11.5 and 8.5 – 10.75 for FA and AFA, respectively. The authors indicated that the pristine FA has a higher adsorption capacity to As(III), but AFA is more convenient in application. The major problem occurred in the work is the quantity of adsorbent used in kinetic and adsorption isotherm studies were too high, which makes an adequate estimation of maximum adsorption capacity impossible. The given $q_m$ in **Table 1.2** are extracted from the experimental results conducted in selecting an optimal adsorbent mass where the values correspond to the highest adsorption of As were given.

Nascimento et al. **[34]** modified a fly ash sample based on Plackett–Burmann experimental design ($2^{5-2}$ fractional factorial design), in which 8 different combinations of experimental conditions were tested with a variable of NaOH concentration (2.0 and 5.0 M), hydrothermal temperature (100, 150 $^{o}$C), treatment time (0.5, 6.0 h), Al/Si ratio (0.51, 1.0) and solid/liquid ratio (1/6, 1/8). The adsorption of $Mn^{2+}$, $Zn^{2+}$, $Cu^{2+}$ and $Pb^{2+}$ was studied with this material. Using Cu and Mn in the primary test, the authors found that increasing hydrothermal temperature and time can more significantly improve the adsorption properties among the tested parameters. The author also concluded, based on the results of these two elements, that the adsorption efficiency of hydrothermally treated fly ash is increased 2 – 25 times of non – modified fly ash. It needs to be noticed that their definition on adsorption capacity presented in their Table 2 is in fact the removal percentage in each concentration of Mn and Cu and given time, therefore, this term is misleading. Second, due to an unstable chemical property of $Mn^{2+}$ in an oxygenated condition, the $Mn^{2+}$ should

be converted to $Mn^{4+}$ rapidly. Furthermore, the authors claimed that the adsorption of capacity of the treated material toward the tested metal ions was Pb > Cu > Zn > Mn. However, it is more accurate to use the expression with number of moles of adsorbate /g of adsorbent. In this case, the order should be Cu > Pb > Mn > Zn.

It should be indicated that in papers related to the fly ash adsorption, many problems are involved. A very common problem is the lack of the necessary description of experimental conditions. An equilibrium time in adsorption is closely associated to an initial concentration of adsorbate and adsorbent in a studied system. When these conditions are altered, the adsorption equilibrium time will be changed. For this reason, the equilibrium time used in determine $q_m$ (maximum adsorption capacity) should be the time that corresponds to the maximum concentration of a studied adsorbate. It is noticed that this condition has been reported in many papers. Similarly, adsorption capacity should be done with an extend range of concentration of an adsorbate, until the plateau of $q_m$ *vs.* $C_e$ or $C_{init.}$ (the concentration of adsorbate in suspension at equilibrium and in initial condition respectively). Unfortunately, very often $q_m$ was done by randomly selected concentration by investigators. For instance, in the study of $Pb^{2+}$ and $Cu^{2+}$ by non – modified fly ash, Alinnor **[37]** reported the kinetic study without given important conditions involved in the experiment, such as the concentrations of adsorbate and adsorbent, the volume, etc. We can only guess that the concentration 6.5 mg/g in their Figure 1 could be 6.5 mg of Cu and Pb in 1.0 g of adsorbent system before the adsorption was initiated. If it is so, what is the volume used in the study? Without the volume of the solution, the concentrations of both adsorbent and adsorbate are still unknown. Apart from the mentioned problem, the interpretation of pH effect on adsorption is completely wrong. In a simple single ionic solution, the pH to make $Pb^{2+}$ precipitate is 6.61 at 10 mg/L and 5.72 at 600 mg/L, and to $Cu^{2+}$ is 8.11 (10 mg/L) and 7.11 (600 mg/L). Although the initial concentration of adsorbate is not given, it is easy to speculate that the "metal adsorbed" is removed by formation of precipitation at a pH > 8.

Adsorption studies using fly ash as an adsorbent for metallic ion removal are difficult task because fly ash is a basic material. When it is placed into an aqueous system, the water become alkaline and the pH of the studied system is subjected to a constant shift toward a high pH condition

as the OH- releases gradually from the fly ash. This situation is well reflected in the study conducted by Luo et al. **[38]**.

**Table 1.2 Summary of the recent studies on inorganic pollutant removal with fly ash.**

| Adsorbent type | Experimental conditions | Results | Refs |
|---|---|---|---|
| Fly ash (FA), Impregnated with $Al(NO_3)_3$ (IFAAl), impregnated with $FeCl_3$ (IFAFe)<br><br>Batch study | **A**: Cr(VI), Hg(II), individual system;<br>kinetic study:<br>$C_{init}$ (Cr): 5.0 mg/L (pH2.0); (Hg), 30 mg/L<br>Wad = 1.0g, V = 300 mL (Cr), 500 mL (Hg). t = 30 min (Cr), 20 min (Hg). T=30 $^oC$. Stirring 100 rpm.<br>maximum adsorption ($q_m$):<br>$W_{ad}$ = 0.1g, V = 100 mL; T = 30$^oC$; $C_{qm}$= 2-10 mg/L (Cr), 20-40 mg/L (Hg)<br>t = 1h; stirring 100 rpm. | For Cr adsorption (pH 2.0):<br>$q_m$ = 1.1 mg/g ( FA), 1.50 mg/g (IFAAl), and 1.23 mg/g (IFAFe)<br>For Hg adsorption (pH5.8):<br>10.1 mg/g (FA), 11.40 mg/g (IFAAl) and 12.30 mg/g (IFAFe)<br><br>Hg(II) and Cr(VI) fit well to LM.<br>Endothermic adsorption for Hg and Cr(VI | **[30]** |
| Thiol grafted fly ash (CFA-SH)<br><br>Batch | **A**: $Hg^{2+}$, $Cd^{2+}$; individual system;<br>kinetic study:<br>$C_{init.}$=200 mg/L ($Hg^{2+}$or $Cd^{2+}$); V=25.mL; $W_{ad}$= 35mg (Hg), 50mg (Cd); T= 40$^oC$ (Hg), 35$^oC$ ($Cd^{2+}$); t = 50 min (Hg), 60min (Cd); Stirring 100rpm.<br>maximum adsorption ($q_m$):<br>$C_{qm}$ = 90–280mg/L; Wad, V, t, T, rpm are the same as above. | Kinetic study:<br>Rm%: 91% (Hg), 74% (Cd)<br>experimental $q_m$ (mg/g):<br>Cd: 72.3, Hg: 132.0<br>LM fitting $q_m$ (mg/g):<br>Cd: 106.4, Hg: 361.01,<br>$Hg^{2+}$ & $Cd^{2+}$ fit well to LM and pseudo-2$^{nd}$ order KAM. | **[31]** |
| Modified fly ash<br><br>(zeolite 4A)<br><br>Commercial zeolite 4A | **A:** Co $^{2}$+, $Cr^{3+}$, $Cu^{2+}$, $Ni^{2+}$ and $Zn^{2+.}$ (mixed)<br>kinetic study:<br>$C_{init}$ = 50 and 100 mg/l; $W_{ad}$= 0.1g; T= 25 $^oC$; V= 100 mL; t = 240 min; stirring 600 rpm.<br>maximum adsorption ($q_m$):<br>$C_{qm}$= 50-300 mg/L; $W_{ad}$= 0.5g; T=25 $^0C$; V = 100 ml; t= 240min; stirring = 600 rpm | Kinetic study:<br>% $R_m$ = > 90 for all metal ions at both pH 3 and 4 for 50 and 100 mg/L of solution.<br>LM fitting $q_m$ (mg/g):<br>For prepared zeolite:<br>$Co^{2+}$:13.72, $Cr^{3+}$ : 41.61, $Cu^{2+}$: 50.45, $Ni^{2+}$:8.96, $Zn^{2+}$:30.80<br>Commercial zeolite 4A:<br>$Co^{2+}$:11.52, $Cr^{3+}$:45.29, | **[32]** |

| | | | |
|---|---|---|---|
| | | $Cu^{2+}$:53.45, $Ni^{2+}$:7.90, Zn $^{2+}$:31.58. Co $^{2}$+, $Cr^{3+}$, $Cu^{2+}$, $Ni^{2+}$ and $Zn^{2+}$. Fit well to LM and Co $^{2}$+, $Cr^{3+}$, $Cu^{2+}$, $^{+}$ and $Zn^{2+}$. Fit pseudo 2nd order KAM whiles $Ni^{2+}$ fit to pseudo 1st order KAM. | |
| Fly ash (FA) and agglomerated Fly ash (AFA)<br><br>Batch | **A**: As(III)<br>$C_{init.}$, Only the ratios between adsorbent: std solution were given.<br>T= 25°C; t =1440 min; Stirring NA.<br>pH 10.4 – 11.5 (FA), 8.5 – 10.75 (AFA) | $q_m$= 13.5mg/g (FA), 5.7 mg/g (AFA);<br>Adsorption fits well to LM (FA), to FM (AFA);<br>Adsorption kinetics fit well to 2nd order KAM for FA and AFS. $\Delta H^0$ = 30 kJ/mol (agglomerate) | **[33]** |
| Hydrothermally modified fly ash<br><br>Batch | **A**: Zn, Cu, Mn & Pb; mixed system<br><br>Maximum adsorption ($q_m$)<br>$C_{qm.}$ = 100 – 3000mg/L; V = 50 mL; $W_{ad}$= 0.5g; T= 25 °C; t = 120 min; pH 4-5, Stirring 180 rpm. | Experimental $q_m$ (mg/g): Mn:38.35, Zn:39.7, Cu:64.4, Hg:145.2;<br>LM fitting $q_m$ (mg/g): Mn: 60.4, Zn: 59.2, Cu: 76.9; Pb: 194.7. Cu, Pb, Mn & Zn fit well to both LM & FM.<br>Mechanism is ion exchange | **[34]** |

### 1.6 The objectives of the current studies

My research is primarily focused on the modification of Thunder Bay coal fly ash, the characterization of the pristine and modified fly ash and the application of modified fly ash for removal of metal ions from mine wastewater.

Although several studies have been conducted regarding the application of fly ash for the removal of metal ions, the methods applied present several limitations. The modification are highly energy consuming and, very few ions are studied either singly or mixture of two, three or four with very few comprising five ions. The modified fly ash is mostly applied in the powdered form in most investigations. In many investigations, thermodynamic properties which are very critical are also not addressed. The question of regeneration of adsorbent is also not attended to in most studies. Adsorption studies are mostly restricted to batch mode experiments.

***The specific objectives of this research were to:***

(1) Modify Thunder Bay coal fly ash through a cold temperature methodology
(2) Characterize the pristine and modified fly ash
(3) Investigate conditions affecting adsorption of metal ions ($Cu^{2+}$, $Pb^{2+}$, $Cr^{3+}$, $Cd^{2+}$, $Co^{2+}$ and $Ni^{2+}$), including pH, contact time and initial concentration.
(4) Select the most efficient adsorbents for conversion into an innovative concrete foam for adsorption studies.
(5) Evaluate the performance of the concrete foam regarding adsorption
(6) Investigate the reusability of the most efficient adsorbent

Investigate the applicability of the most efficient adsorbent in column studies.

# Chapter 2

## 2. Experimental and methodology on coal fly ash and grape waste

The objective of this study was to investigate the potential application of fly ash as a low-cost adsorbent for the removal of metal ions, more specifically $Cu^{2+}$, $Pb^{2+}$, $Cr^{3+}$, $Cd^{2+}$, $Co^{2+}$ and $Ni^{2+}$ from mine wastewater. To maximize its adsorption capacity, different modification processes of a coal fly ash sample were designed and results were compared. The pristine and modified coal fly ash samples were characterized and their merits and problems in preparation as well as their adsorption properties were compared. The optimal preparation was decided in further studies. The pH conditions of a fly ash system alone and in presence of each metal ion solution were investigated first in order to minimize the possibility of formation of metal hydroxides during the adsorption studies. Other adsorption properties such as the quantity of adsorbents, adsorption kinetics and effect of temperature on adsorption were investigated. The maximum adsorption capacity of a given adsorbent for each metal ion were also studied in both synthetic water samples and mine waters. The adsorption kinetic models were also examined. To estimate the potential application of fly ash, column studies and adsorption/desorption cycles of the material were also examined. To enhance its applicability in real environmental systems, some preliminary studies on fly ash powder molding were also conducted.

### 2.1 Source of fly ash

The Thunder Bay fly ash denoted as (TB) throughout this thesis was obtained from the Northwest Thermal Ontario Power Generation Plant located near Thunder Bay, a plant that was responsible for approximately half the electricity generation for the province of Ontario, Canada. The Thunder Bay generation station used Powder River Basin coal from USA. The use of coal to produce electricity has been stopped since 2013, but the fly ash remaining on site has been a great environmental hazard. The fly ash was shipped to the laboratory in air tight metallic containers and was kept at room temperature for further analysis.

## 2.2 Instrumentation and equipment

- Atomic fluorescence spectrometer for Se and As measurements: PS Analytical Excalibur Millennium system;
- Boosted hollow cathode lamp: Super lamp by Photron, Australia;
- Ball mill for sample grinding: Spex mixer / mill Industries Inc, Metuchen, N. J., U.S.A;
- Centrifuge in sample washing: Beckman Coulter TM, Avanti TM J-20 XPI, rotor JLA 8.1000, serial No. 05U1435;
- Centrifuge for preparation of testing samples: Sigma 112 Martin Christ & Michael Christ West Germany;
- Flame atomic absorption spectrometer for metal measurements: Perkin Elmer Analyst 400;
- Graphite furnace atomic absorption spectrometer for metal measurements: Perkin Elmer Analyst 600;
- Ionic chromatography for anion analysis in tailing water: Dionex DX 500, equipped with a GP 40 gradient pump, an Ion Pac AF9HC4mm pre-column, an Ion Pac AS9HC4mm anion column, an ASRS Ultrall 4mm bifer membrane suppressor and a conductivity detector;
- Microwave oven for fly ash modification: Microsynth microwave Labstation, Milestone, Italy;
- Microscope for morphological studies: Scanning electron microscopy (JSM-6400) equipped with 6 energy dispersive X-ray detectors ((INCAX – Sight Oxford Instrument);
- Particle analyzer for particle size distribution studies: Mastersizer 2000 version 5.22;
- pH meter: Accumet pH 25 meter;
- Sonicator for sample washing: Fisher Scientific FS60, 100W, 42 kHz ± 6%;

- Surface analyzer for surface studies: Micromeritics ASAP 2010, Folio Instrument Inc.;
- Peristaltic pump for column adsorption study: LSAMTEC-MV pump system, Cole-Parmer Instrument company, Chicago, U.S.A;
- Water bath and shaker with a thermostat: Gyratory water bath shaker, model G76, New Brunswick Scientific;
- X – ray diffractometer for mineralogical study: XRD 2000 instrument from Scintag Inc.
- Filter paper for fly ash washing: Ahlstrom: Cat. No 6010-0900, grade 601, size 9 cm;
- Brucker Alpha FT-IR model 11774075, Germany.
- 30 TON PRESS C-30, Research & Industrial Instruments Company, London England.
- Tyler Rotap testing sieve shaker, the W.S. Tyler of canada Limited, St. Catherine,ON.
- X-Ray photoelectron spectroscopy (XPS, VG ESCALab 3 MARK II), using non-monochromated Al Kα radiation (1486.7 eV)

### 2.3 Fly ash modifications

The fly ash used in control tests (**TB**) and the fly ash forms after modification were all subjected to grinding with a ball mill for 5 min in order to ensure homogeneity of the samples. Several fly ash modification procedures are given below.

#### 2.3.1 Hydrothermal modification in 2.0 M NaOH at 150 $^{o}$C for 4 h (HTB (OH) 150/4)

A 15.0 g portion of the pristine fly ash was placed in a 1.0 L heavy duty polytetrafluoroethylene (PTFE) bottle and 150 mL of 2.0 M NaOH (sodium hydroxide beads, Fisher Scientific, purity > 95%, $Na_2CO_3$ as the remaining impurity) was added with a stirring bar into the slurry. The PTFE bottle was sealed and placed in a glycerol heating bath and heated while mixing at 150 $^{o}$C for 4 h. The whole reactor was thermally insulated with glass wool and fiber pads. (**Figure 1.1**). After reaction, the sample was allowed to cool down. The cooled slurry was then filtered through a 2.5 µm membrane to remove the basic solution. The residue was washed by passing through deionized water (DW) until the pH of the final washing elute was around 10.5,

which happened after around 3.0 L of DW. The modified sample was dried under vacuum overnight. The sample was homogenized with ball mill and stored in a zipped plastic bag until future use. The sample was named as HTB (OH) 150/4.

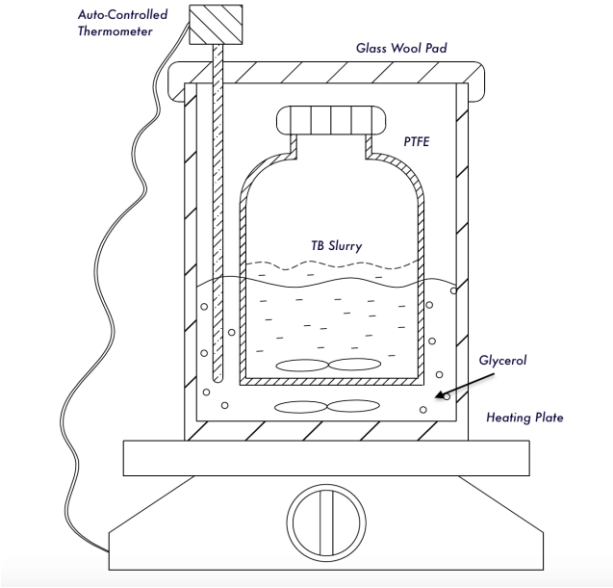


**Figure 2.1 Diagram of the hydrothermal reactor used for fly ash modification.**

### 2.3.2 Hydrothermal modification in 2.0 M $Na_2CO_3$ at 150 ºC for 4 h (HTB ($CO_3$) 150/4)

Another 15.0 g of the pristine fly ash was placed in a 1.0 L PTFE bottle and 150 mL of 2.0 M $Na_2CO_3$ (sodium carbonate, Fisher Scientific, Caledon Canada, Reagent Grade) was added. The rest of procedure was the same as in section 2.3.1. The pH of final washing elute was around 8.4 after a 3.0 L of DW. The sample was dried under vacuum overnight and homogenized with ball mill. It was stored in a zipped plastic bag for future use. The sample was named as HTB ($CO_3$) 150/4.

### 2.3.3 Hydrothermal modification with microwave oven in 2.0M NaOH at 100 ºC for 0.5h (TBMW (OH) 100/0.5)

Two 5.0 g aliquots of the pristine fly ash were placed into a high-density polyethylene vessel HDPE and 50.0 mL of 2.0 M NaOH solution was added and the lid tightened. The reactor was placed into a microwave oven. The heating program was set as the following: Step1: room

temperature to 100 ºC in 5 min; Step 2: 100 ºC for 30 min; Step 3: cooling in 3–5 min. When the vessel was thoroughly cooled down, the slurry of each aliquots was filtered through a 2.5 µm filter paper. The pH of final washing elute was around 10.7 after 3.0 L of DW washing. The samples were dried under vacuum overnight. The two aliquots of samples were mixed and homogenized by ball mill and stored in zipped plastic bag for future use. This sample was labeled as TBMW (OH) 100/0.5.

### 2.3.4 Hydrothermal modification with microwave oven in 2.0 M NaOH at 150 ºC for 1 h (TBMW (OH) 150/1)

Two 5.0 g aliquots of the pristine fly ash were placed into a high-density polyethylene vessel HDPE and 50.0 mL of 2.0 M NaOH solution was added and the lid tightened. The samples were subjected to microwave oven treatment with the following program: Step1: room temperature to 150 ºC in 5 min; Step 2: at 150 ºC for 60 min; Step 3: cooling in 3-5 min. When the vessel was thoroughly cooled down, the slurry of each aliquot was filtered through 2.5 µm. The pH of final elute was 10.7 after 3.0 L DW washing. Dried samples were mixed and homogenized, then stored in a zipped bag for future use. The sample was labeled as TBMW (OH) 150/1.

### 2.3.5 Hydrothermal modification with microwave oven in 2.0 M NaOH at 150 oC for 1 h and with sonication washing (TBMW (OH) 150/1/so)

In this sample preparation, the microwave oven treatment of the sample was exactly the same as described in section 2.3.4. The slurry of each aliquot was washed by filtering through 2.0 L DW first and then the solid material was transferred to a glass beaker and sonicated for 5 min in 250 mL for 4 times with fresh DW each time. The pH of the final washing solution was pH 8.9. The sample was dried under vacuum overnight and the two aliquots were mixed and homogenized by ball mill, then stored in a zipped bag for future use. The sample was labelled as TBMW (OH) 150/1/so.

### 2.3.6 Fly ash modification in 2.0 M NaOH at room temperature (TBRM)

For this modification, 50.00 g of TB was placed in a 1.0 L high density polyethylene (HDPE) vessel and 500.0 mL of 2.0 M NaOH was added and placed in the laboratory. The mixture was shaken by hand three times per day (morning, afternoon and evening) to ensure a good contact of NaOH with the fly ash. After seven days, the liquor was removed and the sample was washed

several times with centrifugation until a stable pH of 10.80 was obtained. Each washing involved the addition of 500.0 mL of deionized water and a shaking step on a gyratory shaker for 10 min at 120 rpm. The washing solution was removed with a centrifugation at 6000 rpm or 8983 G for 20 min at 4 $^{o}$C. A total of 5.0 L of DW was used for washing. The sample was dried in oven at temperature between 50–60 $^{o}$C and homogenized with a ball mill. The sample was stored in an airtight plastic bottle for further analysis. This sample was labeled as **TBRM.**

### 2.3.7 Fly ash modification with freezing and thawing cycles in 2.0 M NaOH (TBFZ)

Finally, 50.00 g of TB was weighed into a 1.0 L HDPE bottle and 0.5 L of 2.0 M NaOH was added. The bottle was placed in a freezer at -15 $^{o}$C. After 21 h, the frozen sample was allowed to thaw and placed back in the freezer. The thawing was performed within 2-3 h in warm water. The sample was subjected to the freezing and thawing cycle for seven days, after which the sample was washed several times with deionized water by centrifugation until pH was stabilized at 10.6 as described above. The sample was dried in the oven at between 50–60 $^{o}$C. The dried sample was homogenized with a ball mill. The powdered sample was stored in airtight plastic bottles for future study. The dried sample was labeled as **TBFZ.**

## 2.4 Mineral and physical characterization of fly ash samples

The mineral composition of non-modified and modified fly ash samples, their surface phenomena and their particle size distribution and porosity were studied by means of X-ray Diffraction (XRD), Laser Particle Sizer, Scanning Electron Microscopy – Energy Dispersive X-ray spectroscopy (SEM – EDS) and Particle Surface Analyzer.

### 2.4.1 Mineralogical studies by X-ray Diffraction

The mineralogical composition of fly ash samples was determined by XRD. The cobalt (Co) cathode X–ray generator working at 40 kV and 20 mA was used as an X–ray source. $CoK_{\alpha}$ radiation ($\lambda = 1.789$ Å) was collimated and projected to a sample. The wavelength of $CoK_{\alpha}$ should be at the same magnitude to the spacing of planes (d) in a crystal lattice. Under this condition, a crystalline substance can act as a three–dimensional diffraction grating. A full scan of 2θ angles ranging from 10 to 70$^{o}$ with an increment of 0.05$^{o}$ was performed. The constructive interference

of X–ray occurs only when the relationships between X–ray, λ and the unit space of a crystal mineral satisfies the Bragg's law:

$$n\lambda = 2d \sin\theta \qquad [2.1]$$

where n is an integer, λ is the wavelength of the incident x-rays on the material, d is the atomic lattice space (d-spacing) and θ is the angle of diffraction between the incident rays and lattice planes. The XRD spectra were interpreted by matching with a data base spectrum on a High score plus software. A 0.2 g sample was used in the analysis.

### 2.4.2 Adsorbent morphological studies

The surface morphology of the samples was visualized using a scanning electron microscope equipped with energy dispersive X–ray probes. A small amount of sample was dispersed on a glass slide by using ethanol as a solvent for dispersion. A two-face carbon tape was placed on the slide and a small amount of the powdered sample was dispersed in a drop of ethanol in a ceramic container. A drop of the prepared mixture was then placed on the carbon tape on the glass slide and allowed to dry before the sample was analyzed.

### 2.4.3 Surface area and porosity studies of fly ash samples

The characterization of surface area and porosity of adsorbent was done by a surface analyzer; a 0.3-0.5 g sample was weighed precisely and degassed for 6–7 h at 110 $^{o}$C. The $N_2$ adsorption-desorption isotherm was measured for each sample at 77 K (-195 $^{o}$C) for 8–9 h. The surface area and pore volume were calculated from the isotherms using the Brunaur, Emmet and Teller (BET) model.

### 2.4.4 Particle size distribution

The particle size distribution was done with a Malvern particle analyzer at the Vale ITSL; Powder Characterization Lab. Results were compiled using the Mastersizer 2000 software version 5.22.

## 2.5 Chemical characterization and analytical methods

### 2.5.1 Chemical characterization of pristine Thunder Bay fly ash (TB)

The chemical composition measurement of TB was done in the Vale Analytical Laboratory in Sudbury, Ontario, Canada. The sample was fused in sodium peroxide and analyzed by inductively coupled plasma – optical emission spectroscopy (ICP–OES).

### 2.5.2 Trace metal concentrations in pristine and modified TB samples

To obtain precise concentrations of trace metal concentrations in the pristine (TB) and modified fly ash adsorbents (TBRM and TBFZ), graphite furnace and flame atomic absorption spectroscopy (GFAAS and FAAS) techniques were employed in the determination of Cd, Co, Cr, Cu, Fe, Mn, Mo, Ni, Pb and Zn. Atomic fluorescence spectroscopy (AFS) was used to determine metalloids As and Se. Selenium and arsenic super lamps were employed in each determination.

A two-stage microwave digestion was conducted before any measurement where a 0.2500 g of sample was weighed precisely and transferred into a 100 mL Teflon microwave digestion vessel, followed by 6.0 mL of 15 M $HNO_3$ and 2.0 mL of 12 M HCl. The vessel was closed and the sample was digested with the microwave digestion program below: (1) from the room temperature to 85 $^oC$ in 5 min, then to 150 $^oC$ in 5 min and stay at 150 $^oC$ for 20 min. The sample was allowed to cool down thoroughly. An additional 2.0 mL of 28 M HF was added and the sample was further digested at 210 $^oC$ for additional 30 min with a preheating from room temperature to 85 $^oC$ in 4 min, and from 85 $^oC$ to 210 $^oC$ in 10 min. The sample was completely digested except for some white $CaF_2$ precipitate. The digest was then transferred into a Teflon beaker to completely remove any remaining HF. The digest was then diluted to 50.0 mL in a HDPE volumetric flask and filled to scale. The sample was stored in a HDPE bottle in a refrigerator. The acids used in the digestion were all analytical grade by Fisher Scientific.

The analytical wavelength for each element were Cd 228.0 nm, Co 240.73 nm, Cr 357.87 nm, Cu 324.74 nm, Fe 248.7 nm, Mn 280.0 nm, Mo 313.3 nm, Ni 232.0 nm, Pb 283.31 nm and Zn 214.3 nm, respectively.

### 2.5.3 Metal and element measurements in adsorption studies and chemical characterization of tailing pond water (TPW).

Chemicals used in analytical calibrations were standard solutions of 1000 ppm (mg/L) for atomic absorption standards purchased from the following sources: Lead standard in 3% $HNO_3$, Ricca Chemical Company, Arlington, Texas, 76012 with Cat. No. APB1KN-500; Cobalt AA Co 2 in 2-5% $HNO_3$, SCP Science, Lots SC 8215889; Cadmium in 4% $HNO_3$, SCP Science, CAS #142-001-485; Chromium in 4% HCl, with CAS #146-002-245; Nickel in 4% $HNO_3$, with CAS #140-001-285; Copper in 4% $HNO_3$, with CAS #140-001-295.

The chemicals used in adsorption experiments were all prepared from nitrate salts of the metals: cadmium(II) nitrate tetra-hydrate ($Cd(NO_3)_2.4H_2O$), 98.5%, Alfa Aesar, Johnson Matthey Company, CAS #10022-68-1; lead(II) nitrate anhydrate ($Pb(NO_3)_2$) 100.6%, Fisher Scientific, CAS #10022-68-1. The following chemicals were bought from ACROS organics, New Jersey, U.S.A : cobalt(II) nitrate hexa-hydrate ($Co(NO_3)_2.6H_2O$) 99%, CAS #10026-22-9; chromium(III) nitrate nona-hydrate ($Cr(NO_3)_3.9H_2O$) 99% CAS #7789-02-8; copper nitrate(II) tri-hydrate ($Cu(NO_3)_2.3H_2O$) 99%, CAS #10031-43-3 and nickel(II) nitrate hexa-hydrate ($Ni(NO_3)_2.6H_2O$) 99% CAS #13478-00-7. All chemicals were ACS certified. To avoid the deliquescence of the salts, the samples were stored in double zipped bags and stored in a refrigerator immediately after usage. All 100.00mL stock solutions of 10,000 mg/L of metal were prepared individually in 0.01M of nitric acid, depending on the purpose of experiments. The stock solutions were stored in high density polyethylene bottles in a refrigerator. In each batch of experiment, either mixed or single metal solutions were prepared the same way as with the presence of adsorbent was prepared as a control sample. The concentration of each metal measured in this sample was as an initial concentration $C_{init.}$ and the removal percentage was calculated based on this value. Analytical wavelengths for the six studied adsorbates (Cd, Co, Cr, Cu, Ni and Pb) were given in section 2.5.2.

The Vale tailing pond is immersed under water and occupies a surface area of 27 $km^2$. For this work, 25 liters of tailing water was collected on Oct. 26, 2015 before it enters the liming station. This water was called tailing pond water (TPW). As soon as the water sample was transported in the laboratory, the pH of the sample was measured and two 50 mL aliquots of water sample were obtained, one filtered through a 0.2µm membrane and another without filtration. Each water sample was acidified with 1.00 mL of 15 M $HNO_3$. The dilution factor was 1.02 after

acidification. These two samples were serviced for metal ion determination. Another aliquot of tailing water was filtered and the filtrate was stored in a glass vessel for anion analyses by ion chromatography. The analytical flow rate was 1.0 mL/min and injection loop was 25 µL. The remaining TPW was stored in a refrigerator for future use.

### 2.5.4 Determination of the cation exchange capacity (CEC) of adsorbents with the Kjeldahl Method

CEC is defined as the number of cations (metallic ions or protons) that a soil sample can adsorb. It is usually expressed as the millimole of mono-charged cation (such as $H^+$) that can be held in 100 grams of a sample. In this study, the CEC determination is based on the method described by Kitsopoulos **[35]**. The analytical method is based on the principle of replacing all adsorbed cations of a sample with a concentrated solution of ammonium acetate ($NH_4Ac$). The adsorbed $NH_4Ac$ is then released in a basic solution in boiling condition so that all $NH_3$ which is then sent and collected in a receiver that is contained in an excess and precise amount of acidic solution. An acid-base reaction thus happens in the receiver. After distillation, the remaining acid in the receiver is determined by titration. By calculating the difference of acidity in the receiver, the CEC value can be found (Kjeldahl for organic Nitrogen determination). The method is called the ammonium acetate saturation (AMAS) method.

Briefly, 3.00 g of each sample was quantitatively transferred into a 50 mL centrifuge tube and 30.0 mL of 1.0 M ammonium acetate $NH_4Ac$ was added (Fisher Scientific, analytical grade). The samples were set in a water bath shaker at 120 rpm for 17 h at 22–25 $^oC$. The samples were then centrifuged for 20 min at 2500 rpm. The solid was washed with 8.0 mL of 99 % (v/v) 2–propanol by shaking horizontally for 10 min and centrifuging for 20 min. This washing procedure was repeated 5 times to eliminate any remaining $NH_4Ac$. The samples were dried in the oven at 50 $^oC$ for 24 h. The Kjeldahl distillation apparatus consisted of a long–necked reactor glass flask (250 mL) and a receiver glass flask (250 mL), connected by a condenser with cold water. In the receiver, a 20 mL aliquot of a standardized 0.10 M HCl solution was placed (in excess) and the receiver was tightly connected to one end of the condenser; 0.10 g of the dried sample was precisely weighed and transferred into the reactor followed by 0.50 g of granular zinc as boiling stone. An aliquot of 20 mL of 0.1 M NaOH was swiftly added and the whole system was connected immediately (**Figure 2.2**). The reactor was heated by a heating mantle and the

mixture was allowed to boil for about 1 h and cooled thoroughly before disconnecting the joints. The condenser was rinsed with a small volume of DW and allowed to drain into the receiver. The remaining molar concentration of HCl in the receiver was determined by titration with a previously standardized NaOH solution, using Bromocresol Green as an indicator. All chemicals used in this experiment were analytical grade. Sodium carbonate (99.999 %) was dried at 170 $^{o}$C for 1 h before being used to prepare the primary standard solution.

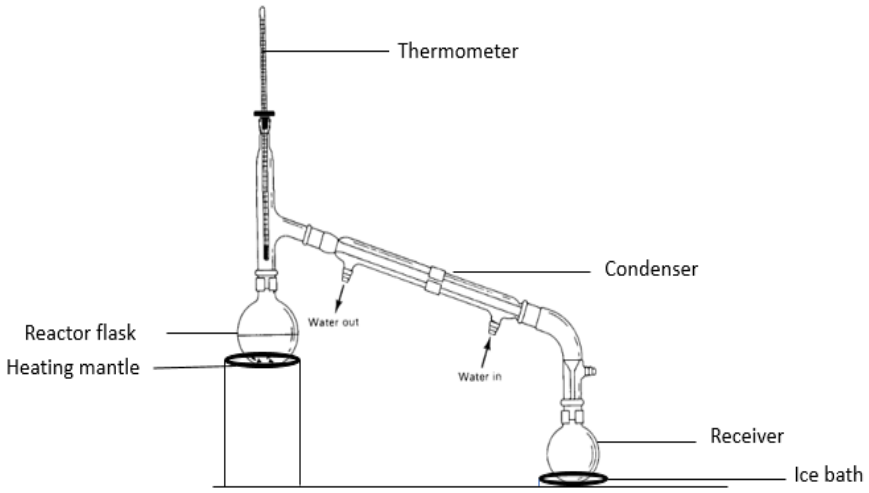


**Figure 2.2 Diagram of the Kjeldahl distillation setup for the determination of cation exchange capacity (CEC) with the ammonium acetate saturation (AMAS) method.**

The related chemical reactions in the AMAS method are given below:

(1) Replacement of cations adsorbed on the sample surface by $NH_4Ac$:

$$\equiv M + NH_4^+ \rightarrow \equiv NH_4 + M^{n+} \quad [2.2]$$

(2) Release of $NH^{4+}$ from the sample during Kjeldahl distillation:

$$\equiv NH_4^+ + NaOH \rightarrow \equiv Na^+ + NH_3 + H_2O \quad [2.3]$$

(3) Neutralization reaction in the receiver:

Step one: $NH_{3(g)} \rightarrow NH_{3(aq)}$ [2.4]

Step two: $NH_{3(aq)} + HCl \rightarrow NH_4^+ + Cl^-$ [2.5]

(4) Titration to determine the quantity of remaining HCl:

$$HCl_{remained} + NaOH_{standardized} \rightarrow H_2O + NaCl \quad [2.6]$$

The cation exchange capacity (meq/100g of adsorbent) in a sample can be calculated as:

$$CEC = \{[(C_{HCl} * V_{HCl}) - (C_{NaOH} * V_{NaOH})] / \text{sample weight}\} * 100g \text{ sample} \quad [2.7]$$

Here, $C_{HCl}$ and $V_{HCl}$ are the initial concentration of standardized HCl and its volume placed in the receiver before the reaction started; $C_{NaOH}$ and $C_{NaOH}$ are the standardized NaOH and its volume consumed in the titration. The unit of CEC is expressed as a number of millimole of mono charged cations that can be held by 100 g of sample (meq = milliequivalent).

### 2.5.5 Determination of total dissolved carbon (DOC) in formulated fly ash

In this study, a piece of 5.00 g of formulated TBFZ cylinder chunk was placed in a conical flask and 500.0 mL of either Millipore water or TPW was added. The flasks were sealed with parafilm and placed on the shaker at 120 rpm at a temperature of 22±1 $^{o}$C; 50.0 mL of each the solutions were pipetted after 1, 7 and 21 days and filtered through a 0.22µm membrane after measuring pH. The solutions were poured into glass bottles and stored at 6 $^{o}$C in the refrigerator for 20 h before being transferred to the freezer (-15 $^{o}$C) until further analysis. All glass vessels were subjected to a 150 $^{o}$C heating to remove any organic carbon prior usage. For sampling bottles, the aluminum foil was used to eliminate any contact of water with the rubber lid. The samples were analyzed by Testmark Laboratories in Sudbury, Ontario, Canada, with standard method for TOC analysis. A blank sample was carried out to check potential presence of deionized water.

## 2.6 Experimental design on fly ash

### 2.6.1 Investigation of potential elemental release from the adsorbing materials

To investigate the potential metal release from the studied adsorbents, 0.500 g of TB, TBRM and TBFZ was weighed and introduced into different polypropylene tubes to which 50.00 mL of deionized water was introduced before being set on the shaker at a speed of 120 rpm and temperature 22 ± 2 $^{o}$C. An aliquot of 1.00 mL of supernatant was collected at 1, 4, 8, 24, 72, 168 and 240 h. The samples were subjected to constant horizontal shaking during all test periods except during sampling. The sample was centrifuged at 15,000 rpm for 5 min and 0.95 mL of supernatant

was carefully pipetted after centrifugation and acidified to 2.0 % $HNO_3$. The concentrations of concerned element were determined with GFAAS.

The pH of the studied systems was controlled within the first 4 h (TB 4.50 - 7.70, TBRM 4.60 - 7.78, and TBFZ 4.51 - 7.80). After 4 h, the pH of these samples was allowed to evolve freely according to the alkaline nature of the adsorbents.

### 2.6.2 Studies of acid-base properties on fly ash

To understand the acid-base properties of fly ash adsorbents used in this study, 0.500 g of pristine fly ash (TB) or modified fly ash samples (TBFZ and TBRM) was soaked in 50.0 mL of deionized water, or in a 50.0 mL of the mixed 6 metallic ion solutions at 50.0 mg/L each (synthesized cocktail solution - SCS) . The suspension in a polypropylene tube was shaken constantly at 120 rpm at 22±1 $^oC$. The pH of each of the studied system was measured at given time until 6 h after which small particles were removed by centrifugation at 2000 rpm for 5 min.

### 2.6.3 Effect of pH on the adsorption of metal ions

To study the pH effect on the adsorption of metal ions by the studied materials, a cocktail solution containing 50.0 mg/L of each of the ions was prepared by precisely pipetting certain volume of each stock solution. The wished pH range of 2.30 - 11.50 was adjusted with 0.1 M NaOH or 0.2 M $HNO_3$ and the volume of solution was fixed at 50.0mL. Then, 0.500 g of adsorbent (TB, TBFZ or TBRM) was introduced in a 50 mL of polypropylene tube and subjected to a horizontal shaking for 2 h at 120 rpm (22±1 $^oC$). At the end of each test, the sample was then centrifuged for 20 min at 2000 rpm. The supernatant was then filtered through a 0.22 µm membrane and acidified to 2 % $HNO_3$ in 25.00 mL before analysis by FAAS.

During the two hours of adsorption test, the pH of adsorption system was monitored and adjusted to keep a constant pH value. The total spiked acid or base solutions were accounted for in the calculation of removal percentage. Usually the volume of additional acid and base spiked in pH adjustment was less than 0.8 mL. An aliquot of the identical cocktail solution without adsorbent was performed along with other the samples as a control and the concentrations of the metal ions measured in this solution are considered to be $C_{init}$.

The removal percentage by adsorbent was calculated based on the following equation:

$$\text{Removal \%} = \frac{C_{init.}V_{init.} - C_{final} * V_{final}}{C_{init.} * V_{init.}} * 100 = \frac{C_{init.} - C_{final} * d.f.}{C_{init.}} * 100 \qquad [2.8]$$

$C_{init.}$ and $V_{init.}$ stand for the initial concentration and volume of the adsorbate in the system, $C_{final}$ and $V_{final}$ stand for the final concentration and volume of the adsorbate; d.f. stands for dilution factor (d.f. = $V_{final}/V_{init.}$).

### 2.6.4 Adsorption kinetic studies

In the preliminary studies with hydrothermal modified samples (HTB(OH)150/4, TBMW (OH)150/1/so, TBMW($CO_3$)150/1), the experiments were only done in the synthesized cocktail solution (SCS). In these studies, a cocktail solution of 50.0 mL with 6 metal ions at 50.0 mg/L each was prepared in a 50.0 mL volumetric flask and transferred into a polypropylene tube. A 0.500 g of hydrothermally modified adsorbent was introduced in the cocktail solution. The sample was subjected a constant horizontal shaking. An aliquot of 1.00 mL of supernatant was taken at a given time between 5 and 120 min. The sample was centrifuged at 15,000 rpm for 5 min and 0.95 mL of supernatant was carefully pipetted and acidified to 2.0% $HNO_3$. The sample was stored in a refrigerator for future analysis by FAAS. In these tests, the pH of the adsorption system was not controlled. However, the pH evolution previously performed in various fly ash systems could provide a reference.

Adsorption kinetics tests of metal ions on TB, TBFZ and TBRM were done using both synthesized cocktail solution (SCS) and tailing pond water (TPW). In the first set of experiments, 150.0 mL of cocktail solution containing 6 metal ions at 50.0 mg/L each was prepared in deionized water and placed into a glass Erlenmeyer flask, then 1.50 g of adsorbent was introduced and the flask was sealed with a parafilm. The sample underwent horizontal stirring immediately. At a given time between 10 and 360 min, 1.50 mL of supernatant was pipetted, centrifuged (15,000 rpm, 5 min) and 1.40 mL of supernatant was collected and acidified (2.0% $HNO_3$) for analysis by FAAS. During the adsorption period, the pH of the adsorption system was monitored and adjusted to avoid pH overshooting beyond the formation of precipitates for all elements, except for Cr.

The experimental procedure in the studies of adsorption kinetics of metals in the tailing pond water (TPW) was the same as in deionized water, except that an additional 50.0 mg/L of each of the 6 metal ions were pipetted in the TPW. In this case, the $C_{init.}$ should be the sum of the

concentrations of a spiked metal ion and that of the original TPW as well. The pH of the studied systems was controlled as close as possible in both TPW and SCS media.

The adsorption kinetics property was established by plotting the removal % by an adsorbent against the adsorption time. The kinetic model fittings were based on these data.

### 2.6.5 Adsorption isotherm studies and maximum adsorption determination

In this study, 0.500 g of adsorbent (TB, TBFZ, or TBRM) was introduced into a 50.0 mL of the various concentrations of a single metal ion solution prepared in deionized water. During each study, the pH of each studied adsorption system was controlled as close as possible to the optimal condition to that particular metal ion as established in the experiments described in section 2.6.3. Since the pH for precipitation was progressively decreasing with increase in pH as shown in **Table 3.6**, the pH for the adsorption isotherm test for each metal ion was selected such that, it was less than the pH for the highest concentration. The sample underwent a 2-h adsorption in presence of a horizontal stirring (120 rpm) at 22±1 $^{o}$C. At the end of adsorption period, the sample was first centrifuged for 20 min at 2000 rpm, then filtered through a 0.22 µm Millipore membrane, acidified to 2.0% $HNO_3$ and stored for analysis by FAAS. The concentration of given metal ions ($C_e$) was determined by FAAS and the quantity of adsorbed metal ion per gram of adsorbent at a given initial concentration ($q_e$) was calculated based on the equation below:

$$q_e = \frac{(C_{init.} - C_e * d.f.) * V}{Wt} \qquad [2.9]$$

Here, $C_{init.}$ and $C_e$ are initial and final concentrations of an adsorbate in aqueous phase (mg/L), d.f. is the dilution factor due to pH adjustment during the adsorption period; V is the initial volume of adsorption system (mL), Wt is the weight of adsorbent used in the study (g); $q_e$ is the quantity of adsorbed metal ions per gram of adsorbent (mg/g).

Isotherms for each metal ion were constructed by plotting $q_e$ against $C_e$. The model fittings were also based on that set of data. From that set of data, a maximum adsorption capacity of an adsorbent to an adsorbate could be estimated based on the adsorption isotherms obtained experimentally.

The same study was also performed using tailing pond water (TPW) as matrix with an addition of spiked metal ion. In this case, $C_e$ represents the sum of the initial TPW concentration and the spiked component.

### 2.6.6 X-ray photoelectron spectroscopy of adsorbed Cu, Ni and Pb on TBFZ

The surface properties of TB and of TBFZ before and after adsorption of Cu, Ni and Pb were analysed by X-Ray photoelectron spectroscopy (XPS, VG ESCALab 3 MARK II), using non-monochromated Al Kα radiation (1486.7 eV). The C 1s peak (BE = 285 eV) was used as the reference line to accurately determine the positions of other spectral lines. Data were analysed using Casa XPS software (2.3.15 Version). The instrument resolution was 0.8 eV. Solutions containing individual cations (400 mg/L for $Ni^{2+}$, 500 mg/L for $Cu^{2+}$ and 600 mg/L for $Pb^{2+}$) were put in contact with 0.500 g of TBFZ7 for 2 h each at the optimal pH conditions for each metal. After centrifugation and filtration, the solids were dried and sent for analysis.

### 2.6.7 Studies on adsorption thermodynamics of Cu and Ni on TBFZ

The thermodynamic properties of adsorption were conducted only with Ni and Cu. For those, 50.0 mL of Ni or Cu ionic solutions with a concentration range (50–500 mg/L) were prepared and a 0.500 g of adsorbent TBFZ was introduced. The samples were subjected to a horizontal stirring for 2h at temperatures of 20, 30, 40 and 50±1 $^{o}$C, respectively. The pH of the studied system was periodically checked and adjusted (usually 3–4 times) to avoid the formation of precipitates. After two hours, the samples were centrifuged first (2000 rpm, 20 min) and filtered (0.22 µm). The filtrate was acidified to 2% $HNO_3$ and stored for analysis by FAAS. The dilution factor due to pH adjustment was taken into consideration.

Isotherms were generated from the data at the different temperatures and maximum adsorption capacities were calculated based on the Langmuir model. The thermodynamic information of the adsorption process for Cu and Ni was extracted.

### 2.6.8 Studies on the reusability of TBFZ powder

The potential reusability of the adsorbent material was assessed by repeating the adsorption leaching cycle three times. In this study, a 50.0 mL cocktail solution of 6 metal ions containing 50.0 mg/L each was prepared and 0.500 g of TBFZ powder was introduced. The sample was

subjected a horizontal shaking (120 rpm) for 6 h. The sample was centrifuged (2000 rpm, 20 min). The supernatant was filtered, acidified to 2.0 % $HNO_3$ and stored for analysis by FAAS. The removal fraction $R_m$ was calculated according to equation **[2.8]**. To the solid fraction, an aliquot of 25 mL DW was added and the sample was hand shaken. The sample was centrifuged and supernatant was rejected. The washing process was repeated once. The washed sample was dried at 70 $^oC$ overnight. The dried sample was weighed and an aliquot of 0.5 M HNO3 was added in a solid/liquid ratio of 1/100. The acid extraction of adsorbed metals was performed under a horizontal shaking for 1.0 h. The leachate was filtered and stored for future analysis by FAAS. This remaining solid was subjected to two more consecutive cycles.

In a parallel study, the recovered adsorbent after acid leaching was reconditioned by soaking it in a 10.0 mL of 2.0 M NaOH overnight and then washed with 25.0 mL DW twice.

Because the sample size became smaller after each consecutive cycle, the volume of solution for adsorption and desorption of each cycle was identical as 1:100 solid and liquid ratio, although the volume used in each consecutive cycle become smaller. Also since acid leaching (desorption) of metals was not always 100%, the metal loading for each test was corrected by considering the quantity of remaining metals in previous test. The removal ($R_m$) and leaching (Lch) ratios were calculated according to the following equations:

<u>In the first cycle</u>:

$$R_{m1} = \frac{(C_{init.} * V_{ad1.} - C_{adl.} * V_{ad1.})}{(C_{init.} * V_{ad1.})} * 100 = \frac{(C_{init.} - C_{ad1.})}{C_{init.}} \quad [2.10]$$

$$L_{lch1.} = = \frac{C_{lch1.} * V_{lch1.}}{[R_{m1} * C_{init.} * 1.]} \quad [2.11]$$

Here, $R_{m1}$ and $L_{lch1}$ are removal and leaching fraction in the first cycle. $C_{init.}$, $C_{ad1}$ and $V_{ad1.}$ stand for the concentration of a metal in the initial cocktail solution which was unchanged in all tests, the concentration of a metal ion remaining in the solution after 6 h adsorption and volumes used in the first adsorption test respectively. $C_{lch1}$ and $V_{lch1}$ are the concentration and volume in the first leaching test. $V_{ad1} = V_{lch1}$.

In the second cycle:

$$R_{m2} = \frac{(C_{init.} * V_{ad2.} - C_{ad2.} * V_{ad2.})}{\{C_{init.} * V_{ad2.} + [(1 - L_{lch1.}) * R_{m1} * C_{init.} * V_{ad1.}]\}} \quad [2.12]$$

$$L_{lch2.} = \frac{(C_{\boldsymbol{lch2}} * V_{lch2})}{(C_{init.} * V_{\boldsymbol{ad2}.} - \boldsymbol{C_{ad2}} * V_{ad2.})} = \frac{\boldsymbol{C_{lch2.}}}{(\boldsymbol{C_{init.}} - \boldsymbol{C_{ad2.}})} \quad [2.13]$$

Here, $R_{m2}$ and $L_{lch2}$ are removal and leaching fraction in the second cycle. The other signs stand for the same meaning and the number 2 stands for the related parameters in the 2nd cycle. $V_{ad2} = V_{lch2}$. The possible remaining of metal ion after the first acid leaching was ignored in the $L_{lch2}$ calculation.

In the third cycle:

$$R_{m3} = \frac{(C_{init.} * V_{ad3.} - C_{ad3.} * V_{ad3.})}{\{C_{init.} * V_{ad3.} + [(1 - L_{lch2}) * (C_{init.} * V_{ad2.} - C_{ad2} * V_{ad2.}]\}} \quad [2.14]$$

$$L_{lch3} = = \frac{(C_{lch3} * V_{lch3})}{(C_{init.} * V_{ad3} - C_{ad3} * V_{ad3})} = \frac{C_{lch3}}{(C_{init.} - C_{ad3})} \quad [2.15]$$

Here, $R_{m3}$ and $L_{lch3}$ are removal and leaching fractions in the third cycle. The other signs stand for the same meaning and the number 3 stands for the related parameters in the 3rd cycle. $V_{ad3} = V_{lch3}$. The possible remaining of metal ion after the second acid leaching was ignored in $L_{lch3}$ calculation.

### 2.6.9 Studies on metal removal with column system

In this study, 5.00 g of adsorbent was packed in a glass column having an internal diameter of 48 mm, an external diameter of 52 mm and a height of 200 mm. The outlet of the column was evenly padded with a dense layer of glass wool (1.05 g) to retain the adsorbent. The glass wool was wet and compacted with DW first and 5.00 g of TB or TBFZ was loaded on the top of the glass wool; 500.0 mL of cocktail solution of 6 metal ions in a concentration of 50 mg/L each was prepared. The flow rate was controlled by a peristaltic pump. The effect of flow rate was investigated at 2.1 and 4.2 mL/min; 10.0 mL of eluent was collected in a glass cylinder at a given time. The eluent was transferred into a 14-mL polypropylene tube and centrifuged at 2000 rpm for

20 min. The pH of each eluent sample was measured and the supernatant was filtered through a 0.22 µm membrane, the filtrate was acidified to 2.0 % $HNO_3$ and stored for analysis by FAAS. The procedure was performed under a flow rate 2.1 and 4.2 mL/min. At 2.1 mL/min flow rate, a new aliquot of eluent was collected at every 10 min; at 4.2 mL/min rate at every 7 min until all 500.0 mL of the cocktail solution was passed. Some eluent was discarded between each new sample collection.

### 2.7 Preliminary studies on TBFZ formulation, characterization and adsorption

#### 2.7.1 TBFZ formulations

To prepare a mixture of TBFZ and the bonding agent (BA), 20.00 g of the freeze modified fly ash was mechanically mixed with 40.00 g of BA in a beaker and it was denoted as TBFZ-BA.

For the first formulation, 20.00 g of a foaming agent FA was mixed thoroughly with 11.0 mL of DW to generate a slurry-foam first, then 20.00 g of the TBFZ-BA mixture was added to the slurry-foam and mixed by hand using a glass rod, first and then a rheostat controlled mixer was then used to mix the TBFZ-FA-BA slurry and produce a homogeneous paste. The paste was poured into an open ended 50 mL polypropylene centrifuge tube and allowed to cure at room temperature (23±1 $^oC$) for 7 days. The cured material was removed from the tube and dried in an oven at a temperature ≤ 70 $^oC$ until constant weight was reached (5 d). The samples were stored in zipped plastic bags for further studies. The chemical composition of the formulation was TBFZ:FA:BA = 0.17:0.50:0.33 and the material was labeled as TBFZ:FA:BA = 0.17:0.50: 0.33**.** For the second formulation, the foaming slurry was prepared by mixing 15.0 mL of DW with 20.00 g of FA, then 40.0 g of the TBFZ–BA was added and hand–mixed first with the FA slurry and followed by a rheostat controlled mixer to produce a homogeneous paste. The paste was poured in to open ended 50 mL polypropylene centrifuge tubes and allowed to cure at room temperature 23±1 $^oC$ for 7 days. The cured formulation was removed from the tubes and dried at ≤ 70 $^oC$ in the oven until constant weight was reached. The material has a chemical composition TBFZ:FA:BA = 0.22:0.33:0.45. The samples were labeled as TBFZ:FA:BA = 0.22:0.33:0.45.

Bonding agent: Portland cement (CAS # 65997–15–1). Main chemical composition is limestone ($CaCO_3$), gypsum ($CaSO_4.2H_2O$), calcium oxide (CaO), magnesium oxide (MgO), quartz ($SiO_2$).

Foaming agent: Master Cell 25 by MASTER BUILDERS SOLUTION, BASF Corporation. CAS # 68439-57-6. The main chemical composition are Sulfonic acids, C14-C16 alkane hydroxyl, C14-C16- alkene, Sodium Olefin sulfonate, Benzene sulfonic acid, dimethyl-, sodium xylene sulfonate.

### 2.7.2 Physical characterization of TBFZ:FA:BA 0.22:0.33:0.45

The physical and mechanical properties of the prepared foaming material was done with only TBFZ:FA:BA = 0.22:0.33:0.45, since formulation one was too soft.

**For density:** The cylindrical shaped foam material was cut into smaller pieces in a diameter: length = 1:2. The sample was then polished with a sand paper to obtain a smooth and flat surface. The diameter and height of each sample were measured with a caliper and the average of three measurements was used in calculation. The mass of each sample was recorded and the density of the material was obtained from the equation below:

$$\text{Density} = \text{mass (g)} / \text{volume (cm}^3\text{)} = \text{mass} / \left( \pi * \frac{D^2}{4} * H \right) \quad [2.16]$$

Here D is the diameter of a cylinder, H is the height.

**For water absorption:** The water absorption of the foaming material was done following the procedure below: A chunk of material (Φ = 2.91 cm, H = 36.6 cm) was soaked in 100 mL of DW for 24 h, then the wet sample was weighed. The sample was dried at ≤ 70 $^{o}$C until the weight became constant and its dry weight was recorded. The water absorption capacity (WAC) of the material can be expressed as relative to sample weight (WAC% (w)) and as relative to sample volume (WAC (v)).

$$\text{WAC\% (w)} = (\text{wet sample weight} - \text{dry sample weight})/\text{dry sample weight} * 100 \quad [2.17]$$

$$\text{WAC (v)} = (\text{wet sample weight} - \text{dry sample weight}) / \left( * \frac{D^2}{4} * H \right) \text{ (g/cm}^3\text{)} \quad [2.18]$$

**For compressive strength:** **The c**ompressive strength is the ability of a specimen to sustain the axial force load. There are three types of specimen that could be used to determine the compressive strength. These are cylindrical, cube or prism. In this study, a cylindrical foaming material (Φ = 2.6 cm, H = 5.8 cm) was polished and subjected to test. The material strength was

determined by a compression machine. The data collected was used to calculate the compressive strength, $f_c$ according to the following formula:

$$f_c = \frac{P}{A} \ (N/m^2) \qquad [2.19]$$

where $f_c$ is the compressive strength, P is the force exerted on a specimen at which the block collapsed, A is the cross-sectional area of the specimen ($A = \pi * D^2/4$).

### 2.7.3 Adsorption and desorption tests with the formulated material

**Adsorption test with formulated materials:** The adsorption kinetics of metal ions on TBFZ:FA:BA = 0.22:0.33:0.45 and TBFZ:FA:BA = 0.17:0.50:0.33 and FA was done using deionized water (DW). However, the kinetics tests of metal ions on TBFZ:FA:BA = 0.22:0.33:0.44 were also done using tailing pond water (TPW). For TBFZ:FA:BA = 0.22:0.33:0.45 and TBFZ:FA:BA = 0.17:0.50:0.33 experiments, 100.0 mL of cocktail solution containing 6 metal ions at 50 mg/L each was prepared in deionized water and placed into a glass Erlenmeyer flask; then 1.00 g of adsorbent was introduced and the flask was sealed with a parafilm. The sample underwent a horizontal stirring immediately. At given times between 5 to 300 min, 1.50 mL of supernatant was pipetted, centrifuged (15,000 rpm, 5 min) and 1.30 mL of supernatant was collected and acidified (2.0 % $HNO_3$) for analysis by FAAS. During the adsorption period, the pH of the adsorption system was monitored and adjusted to avoid pH overshooting beyond that for the formation of precipitates. For FA, a 0.5 g adsorbent was put in contact with 50.0 mL of cocktail in a PP tube and shaken horizontally as above. Between the intervals of 5 to 300 min, 1.0 mL aliquot was taken, filtered and acidified (2.0 % $HNO_3$) for analysis by FAAS; pH was monitored and controlled during the adsorption period to avoid precipitation.

**For the desorption test:** The reusability of the formulated material was assessed by repeating the adsorption – desorption cycle two times. In this study, a 100.0 mL cocktail solution of 6 metal ions containing 50.0 mg/L each was prepared and 1.00 g of formulated material TBFZ:FA:BA = 0.22:0.33:0.45 was introduced. The sample was subjected to a horizontal shaking (120 rpm) for 6 h. The sample was centrifuged (2000 rpm, 20 min). The supernatant was filtered, acidified to 2.0 % $HNO_3$ and stored for analysis by FAAS. The removal fraction $R_m$ was calculated according to equation **[2.8]**. To the solid fraction, an aliquot of 25 mL DW was added and the sample was hand shaken. The sample was centrifuged and supernatant was rejected. The washing process was repeated once. The washed sample was dried at 70 $^oC$ overnight. The dried sample

was weighed and an aliquot of 0.5 M of $HNO_3$ was added in a solid/liquid ratio of 1/100. The acid extraction of adsorbed metals was performed under a horizontal shaking for 6 h. The leachate was filtered and stored for future analysis by FAAS. This remaining solid was subjected to another cycle. In a parallel experiment, the same procedure was followed but 1.0 M $HNO_3$ was used as the desorption agent. Equations **[2.12]** and **[2.13]** were used to calculate the second removal and leached fractions, respectively. In the tests, the pH of the aqueous phase in the adsorption process is not adjusted.

### 2.8 Experimental design and characterization of grape waste material

#### 2.8.1 Treament of graph waste material (GWM)

The graphs used in this test was a red graph, called Ali Cante Spanish grape and purchase from California. About 500 mL of a fermented grape waste (pomace) was collected and dried in the oven at ≤ 70 $^{o}$C for 5 days.The caked but brittle pomace was then milled to produce the powdered biosorbent (GWM). Part of GWW was sieved through standard sieves of sizes < 38, 45, 53, 75, 106, 150 and > 212 µm; 10.0 g of milled samples was placed in a U.S standard testing sieves ranging from 38-212 µm and placed in a rotor to mechanically shake for 10 min. After shaking, various fractions were weighed, recorded and stored in airtight polyethene bags for further analysis.

#### 2.8.2 Fourier Transform Infrared (FTIR) analysis.

The surface chemical characteristics of GWM were obtained by a Brucker Alpha FT-IR model 11774075. Small amount of GWM ( ≈ 0.5 g) of sample was mixed with about 1 g of KBr. A pellet was formed by pressing the fine powdered mixture in a mechanical disc press by applying a pressure of 5 tons in 5 min using a 30-ton press C-30, Research & Industrial Instruments Company, London England. The pellet was then placed on a sample holder and inserted into the FT-IR instrument for analysis. The infra red spectra was collected for interpretation.

#### 2.8.3 Batch adsorption experiment

The experiments were perfomed at 22±2 $^{o}$C with shaking at 120 rpm. The effect of contact time (kinetics), pH and particle size on adsorption were investigated.

#### 2.8.3.1 Effect of pH on adsorption

The effect of pH on adsorption was studied by the addition of 0.500 g of GWM to each of 5 PP tubes containing 50.0 mL of mixed solution with concentration of 50.0 mg/L of each metal ion. The pH of solution was adjusted within a compromised pH range of 2.6-6.8. After shaking for 4 hours, solutions were centrifuged, filtered and the supernatant acidified to 2% $HNO_3$ for instrumental analysis.

#### 2.8.3.2 Effect of particle size on adsorption

In this study, 0.500 g of GWM of size 38, 106, 150 and 212 µmwas put in contact with 50.0 mL of SCS contaning 50.0 mg/L each. The pH of the aqueous phase was adjusted periodically with 0.1M NaOH. The detailed pH adjustment information can be found in **Table 4.3** in **4.2.2**. After shaking for 4 h, solution was centrifuged and filtered through a 0.22 µm membrane; 25.0 mL of filtrate was acidified to 2 % $HNO_3$ for FAAS analysis. The dilution factors in pH were taken into the considerations as described before.

#### 2.8.3.3 Kinetics studies

A 1.00 g sample of GWM was left in contact with 100 mL of mixed metal ion solution of 50 mg/L each in a 125 mL conical flask and shaken for 240 min.The pH of the solution was adjusted by 0.1 M NaOH. The details of the pH adjustment can be found in **Table 4.4** in **4.2.3**. For this, 1.0 mL of mixture was withdrawn at different times and centrifuged. The supernatants were filtered through a 0.22 µm filter. The filtrates were acidified to 2% $HNO_3$ before FAAS analysis.The procedure was repeated for 0.500 g of GWM in 50.0 mL (1:100) solution of concentration at 10.0 mg/L each metal ion. The dilution factors in pH were taken into the considerations as described before.

# Chapter 3

# 3. Results and discussion on fly ash samples

Mine wastewater is known to contain a variety of chemical species including metal cations such as $Cu^{2+}$, $Cd^{2+}$, $Co^{2+}$, $Cr^{3+}$, $Ni^{2+}$, $Pb^{2+}$, $Hg^{2+}$, $Fe^{2+}$, and anions such as $S^{-2}$ , $NO_3^-$, $SO_4^{2-}$, $Cl^-$, $CO_3^{2-}$, etc. These metal and non-metal ions are also proven to create environmental problems, thus requiring to find ways to remove them from the wastewater before being discharged to the natural environment. In this work, the potential of coal fly ash to remove the selected metal ions lead ($Pb^{2+}$), copper ($Cu^{2+}$), chromium ($Cr^{3+}$), cadmium ($Cd^{2+}$), cobalt ($Co^{2+}$) and nickel ($Ni^{2+}$) in mining wastewater was investigated and the adsorption kinetics, capacities and factors influencing adsorption were studied. The possible recycling and moulding of this modified material were also tested.

### 3.1 Mineralogical and physical characterization of coal fly ash samples

#### 3.1.1 Mineralogical studies by X-ray Diffraction.

XRD analysis was carried out to investigate the crystal phases of pristine fly ash (TB) and modified fly ash samples under both low and high temperature with 2.0 M NaOH. **Table 3.1** and **Figure 3.1** present in color codes the identified mineral phases and XRD patterns, respectively. The XRD pattern of TB shows the main crystalline phases are aluminum oxide, silicon oxide, calcium carbonate and sodium aluminum silicate sulfate.

The appearance of aluminum oxide and silicon oxide in the XRD patterns confirms the major chemical composition of fly ash in **Table 3.3** as determined by ICP-OES analysis, which revealed high percentages of aluminum and silicon oxides. It is observed in **Table 3.1** that whereas calcium carbonate and silicon oxide maintained their integrity, all the peaks of aluminium oxide ($Al_2O_3$) had disappeared when treated in high alkaline solution indicating the probable dissolution of $Al_2O_3$ and/or transformation of the aluminum oxide to other minerals (sodium aluminum silicate sulfate, sodium aluminum silicate sulfate hydrate or sodium aluminum silicate hydroxide). Comparing to the pristine fly ash, new crystalline phases (sodium aluminum silicate sulfate hydrate, sodium aluminum silicate hydroxide and iron titanium oxide) were formed in TBRM. The

XRD pattern of TBFZ revealed formation of sodium aluminum silicate sulfate hydrate. Sodium aluminum silicate sulfate also appeared in HTB(OH)150/4 whereas sodium aluminum silicate sulfate hydrate and sodium aluminum silicate hydroxide appeared in HTB($CO_3$)150/4. The newly identified minerals in the modified samples are indication of chemical restructuring within fly ash after treating it with 2.0M NaOH hydrothermally and at low temperature. The crystalline modification were accompanied by increase in surface area **[36]** as shown in **Table 3.2.**

Pristine fly ash was subjected to a continuous freezing and thawing conditions while soaked in 2.0 M NaOH. This freezing and thawing coupled with the corrosive nature of NaOH contributed significantly to the change in the crystal phases as well as to the increase in surface area. Fly ash was also subjected to hydrothermal conditions while soaked in 2.0 M NaOH which revealed similar physical and chemical characteristics to the freezing and thawing conditions. However, during the hydrothermal treatment, we encountered explosions of the reactor due to pressure build-up. Also, the amount of mass that could be produced at a time was small (< 5.0 g) while using high amount of energy. As result the focus was shifted to the low temperature treatment which yielded larger output (approximately 50.0 g) and consumed much less energy. Most of the adsorption experiments were thus based on the pristine TB, TBRM and TBFZ samples.

**Table 3.1 Comparison of mineralogy of TB, TBFZ, TBRM, HTB(OH)150/4 and HTB($CO_3$)150/4 by XRD**

| Color Code | Mineral name | Chemical Formula |
|---|---|---|
| | **TB** | |
| Blue | Sodium Aluminum Silicate Sulfate | $Na_8(SO_4)(Al_6Si_6O_{24})$ |
| Green | Calcium Carbonate | $CaCO_3$ |
| Grey | Silicon Oxide | $SiO_2$ |
| Pink | Aluminum Oxide | $Al_2O_3$ |
| | **TBRM** | |
| Blue | Calcium Carbonate | $CaCO_3$ |
| Green | Sodium Aluminum Silicate Sulfate Hydrate | $Na_8(SO_4)\ (Al_6Si_6O_{24})\ (H_2O)_{0.96}$ |
| Grey | Silicon Oxide | $SiO_2$ |
| Pink | Iron Titanium Oxide | $FeTiO_3$ |
| Light blue | Sodium Aluminum Silicate Hydroxide | $3NaAlSiO_4NaOH$ |
| | **TBFZ** | |
| Blue | Calcium Carbonate | $CaCO_3$ |
| Green | Silicon Oxide | $SiO_2$ |
| Grey | Sodium Aluminum Silicate Sulfate Hydrate | $Na_8(SO_4)\ (Al_6Si_6O_{24})(H_2O)_{0.96}$ |
| Pink | Sodium Aluminum Silicate Sulfate | $Na_8(SO_4)\ Al_6Si_6O_{24}$ |
| | **HTB(OH)150/4** | |
| Blue | Calcium Carbonate | $CaCO_3$ |
| Green | Silicon Oxide | $SiO_2$ |
| Grey | Sodium Aluminum Silicate Sulfate | $Na_8(SO_4)\ (Al_6Si_6O_{24})$ |
| | **HTB($CO_3$)150/4** | |
| Blue | Calcium Carbonate | $CaCO_3$ |
| Green | Silicon Oxide | $SiO_2$ |
| Grey | Sodium Aluminum Silicate Sulfate Hydrate | $Na_8(SO_4)\ (Al_6Si_6O_{24})\ (H_2O)_{0.96}$ |
| Pink | Sodium Aluminum Silicate Hydroxide | $3NaAlSiO_4NaOH$ |

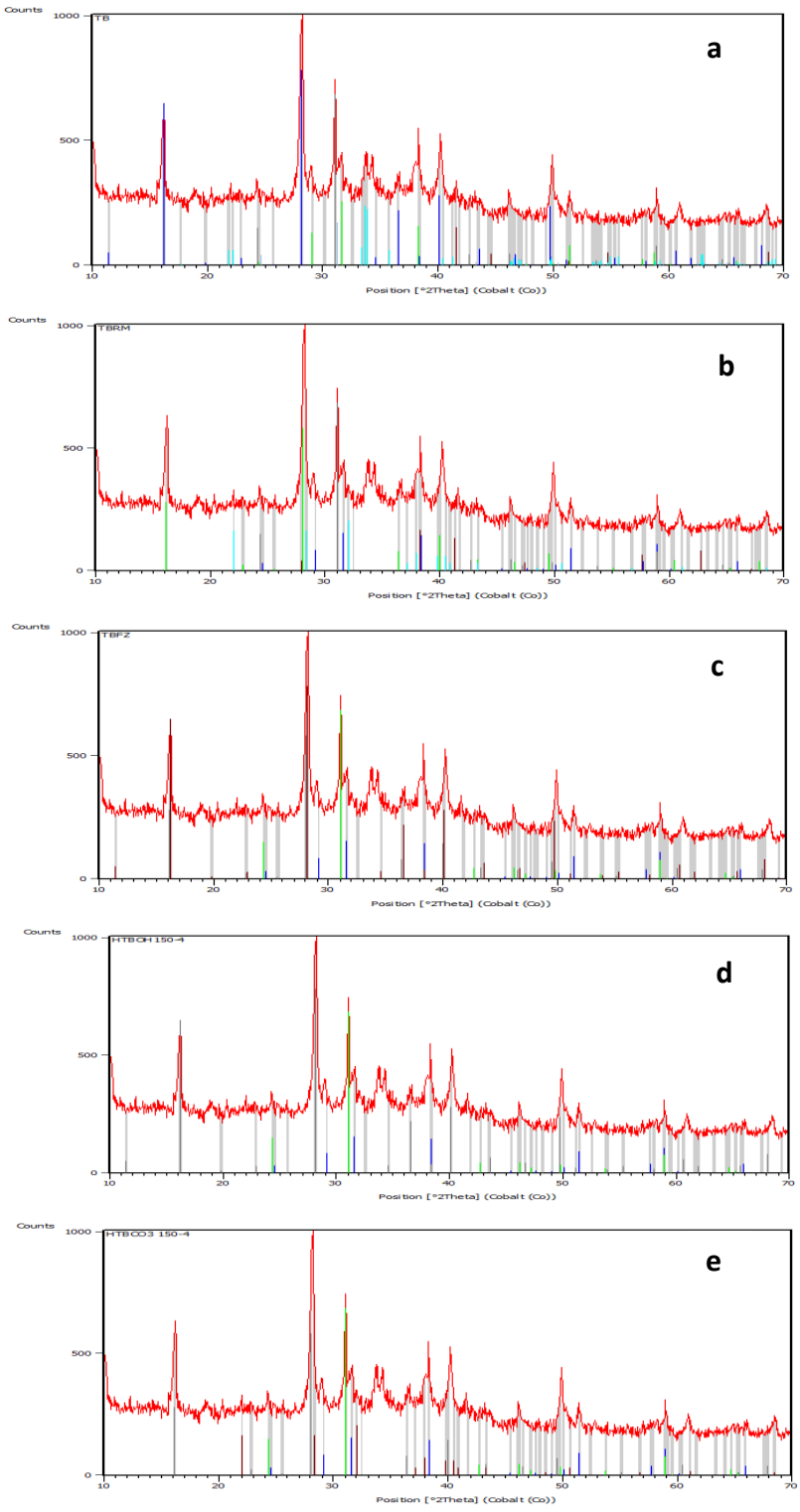


**Figure 3.1 XRD patterns of (a) TB, (b) TBRM, (c)TBFZ, (d) HTB(OH)150/4, (e) HTB(CO3)150/4.**

### 3.1.2 Morphological of adsorbent by SEM

**Figures 3.2** presents the morphological features of TB, TBRM, TBFZ, HTB(OH)150/4, HTB($CO_3$)150/4. **Figure 3.3** is for the SEM of TBFZ:FA:BA = 0.22:0.33:0.45, TBFZ:FA:BA = 0.17:0.50:0.33. **Figure 3.4** presents the SEM images of TB and TBFZ with elemental spectra. The original TB sample in **Figure 3.2(a)** is dominated with spherical shaped particles with varied sizes formed from the rapid cooling of molten products after combustion of coal and clay compounds in original coal **[37]**. By contrast, the morphology of the modified samples in **Figures 3.2 (b-(d)** for TBRM, TBFZ and HTB(OH)150/4 appear cracked, fused, irregular and rough shapes; in **Figure 3.2 (e)** HTB($CO_3$)150/4 appears also rough, irregular and somewhat cube-like in shape. These changes in morphology are beneficial for adsorption as the surface area was increased.

The presence of the activating agent 2.0 M NaOH might have attacked the constituents in the pristine fly ash inducing fusion and roughness. As discussed in **[37]** in a solution with pH > about 9, the silica network had started to dissolve at its interface with the solution. All modified TB also appear porous which was confirmed by the BET analysis. The irregular shaped particles led to an increase in surface area which was corroborated by the $N_2$ adsorption - desorption analysis. **Figure 3.3** is SEM images of two formulated foaming material with different ratios of fly ash, foaming (FA) and bonding (BA) agents (a) TBFZ: FA:BA = 0.22:0.33:0.45 and (b) TBFZ: FA: BA = 0.17:0.50:0.33. Both ratios show morphology that appears irregular in nature and spongy with lots of voids, which are due to the introduction of the FA. The presence of the FA increased the volume of the mixture while giving additional qualities such as light weight which was confirmed by the floating characteristics in water and the density (0.7 $cm^3/g$) of the material. The water absorption percentage also confirms the void nature of the material as prepared and these characteristics contributed significantly to the adsorption properties of the material.

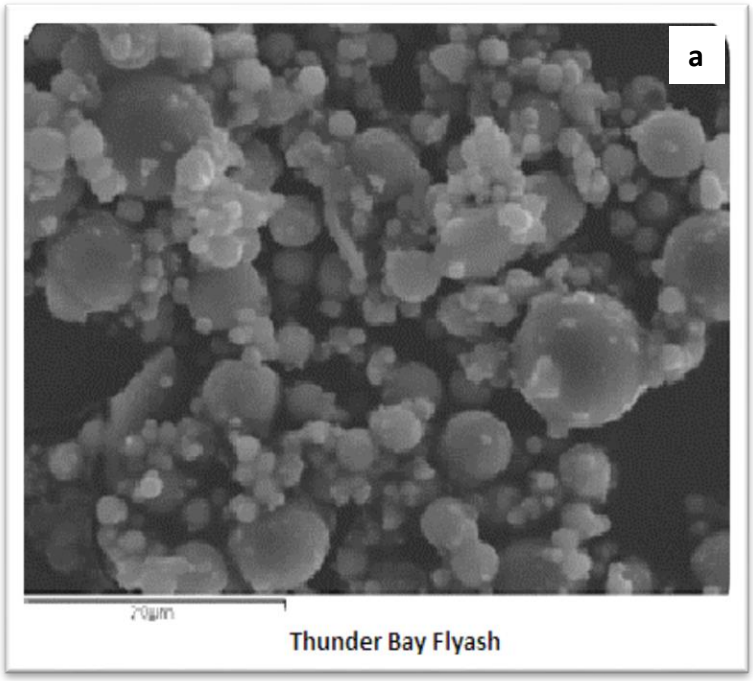
a
20µm
Thunder Bay Flyash

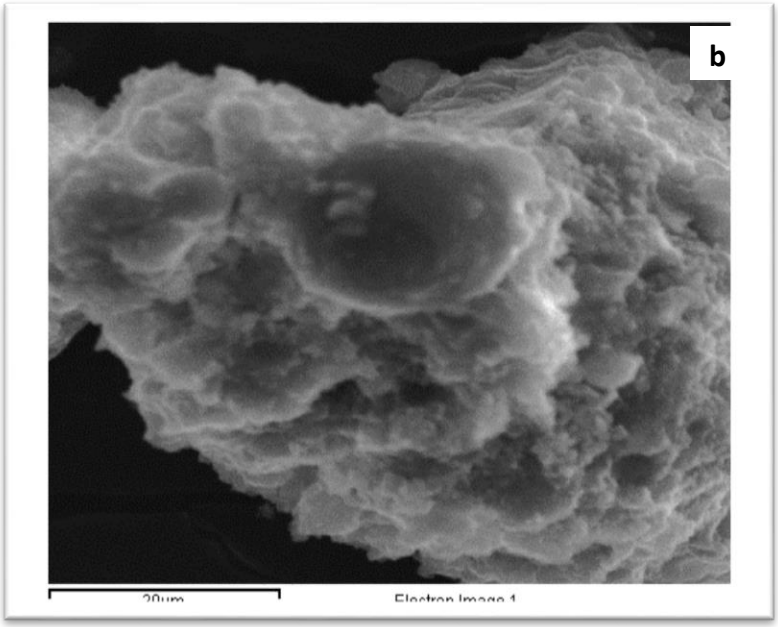
b
20µm
Electron Image 1

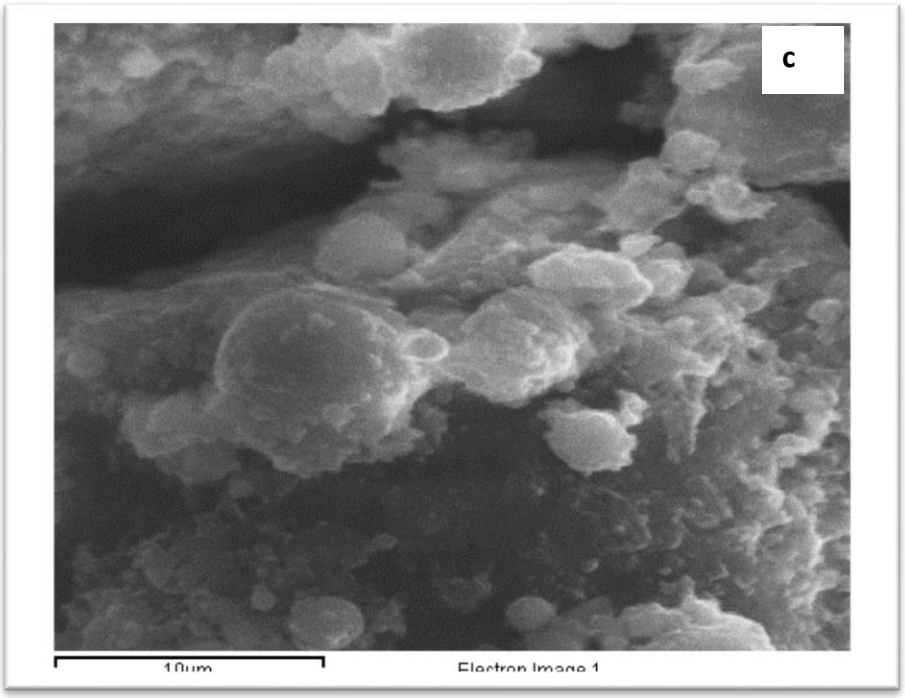
c
10µm
Electron Image 1

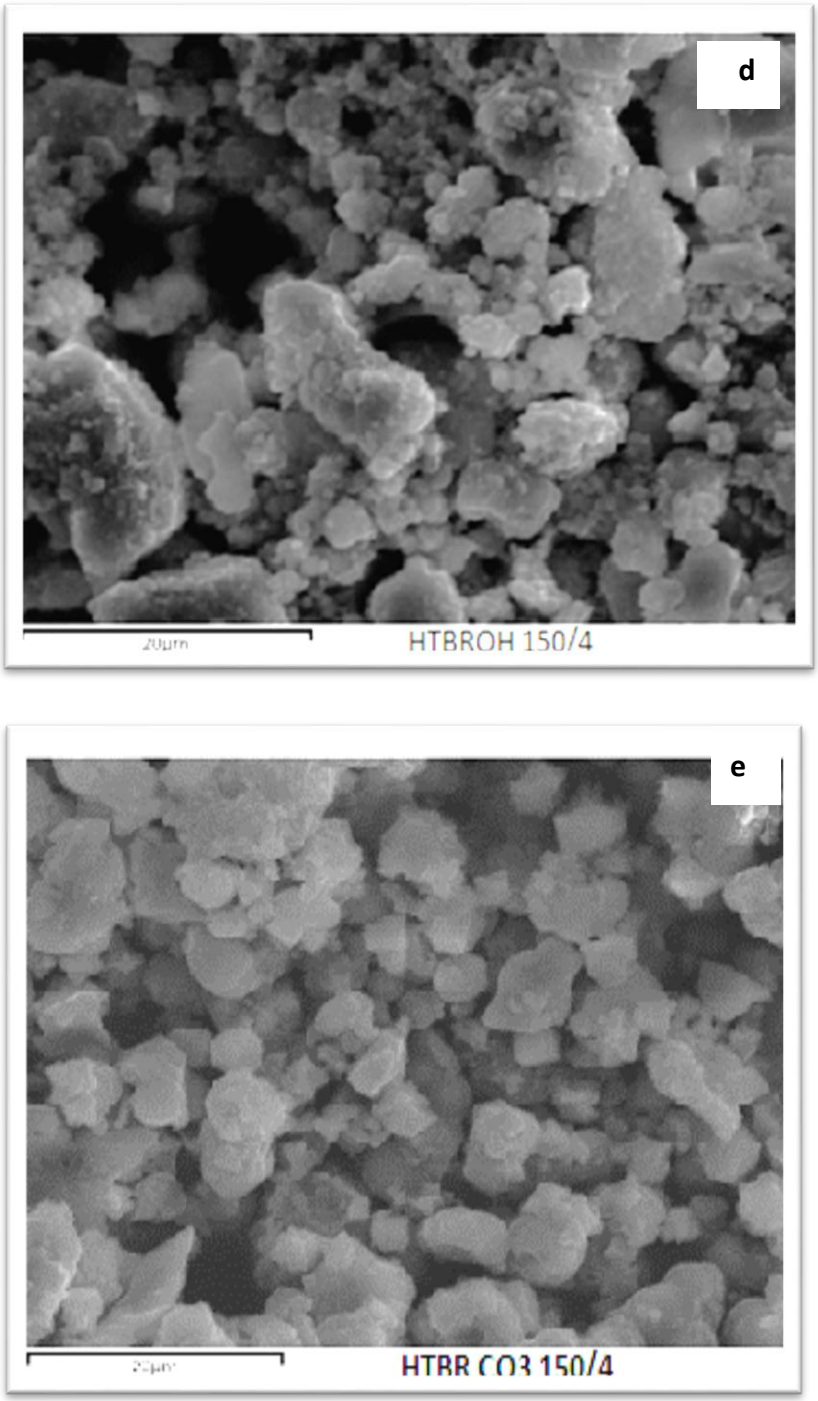


**Figure 3.2 SEM images of (a) TB, (b) TBRM, (c) TBFZ, (d) HTB(OH)150/4 and (e) HTB($CO_3$)/150/4. Scale of 20 µm (a) - (e), except (c)**

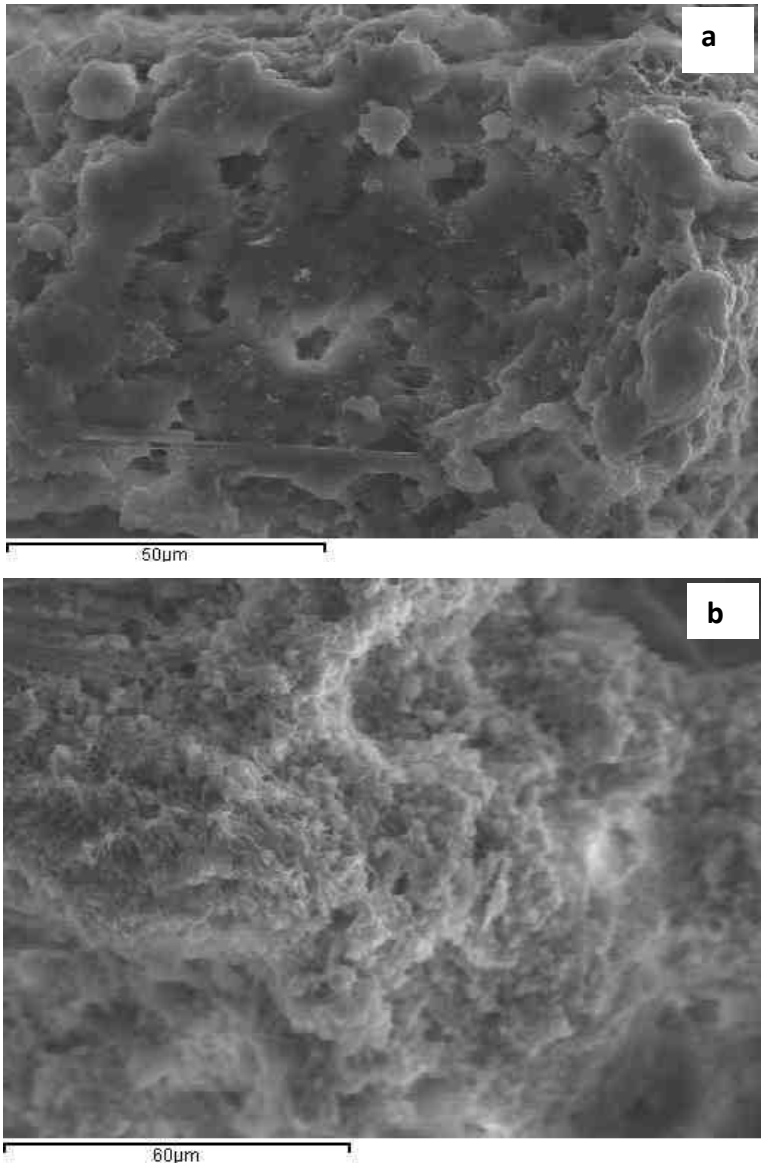


**Figure 3.3 SEM images of (a) TBFZ:FA:BA = 0.22:0.33:0.45 and (b) TBFZ:FA:BA = 0.17:0.50:0.33.**

**Figures 3.4 presents** SEM - EDS data for TB sample and its adsorption of different metals ions. These results confirm the presence of the metals on the solid after adsorption. **Figure 3.5** showed the adsorption of metal ions on the TBFZ surface. Both sets of experiments showed the adsorption did occur on the surfaces of the adsorbents.

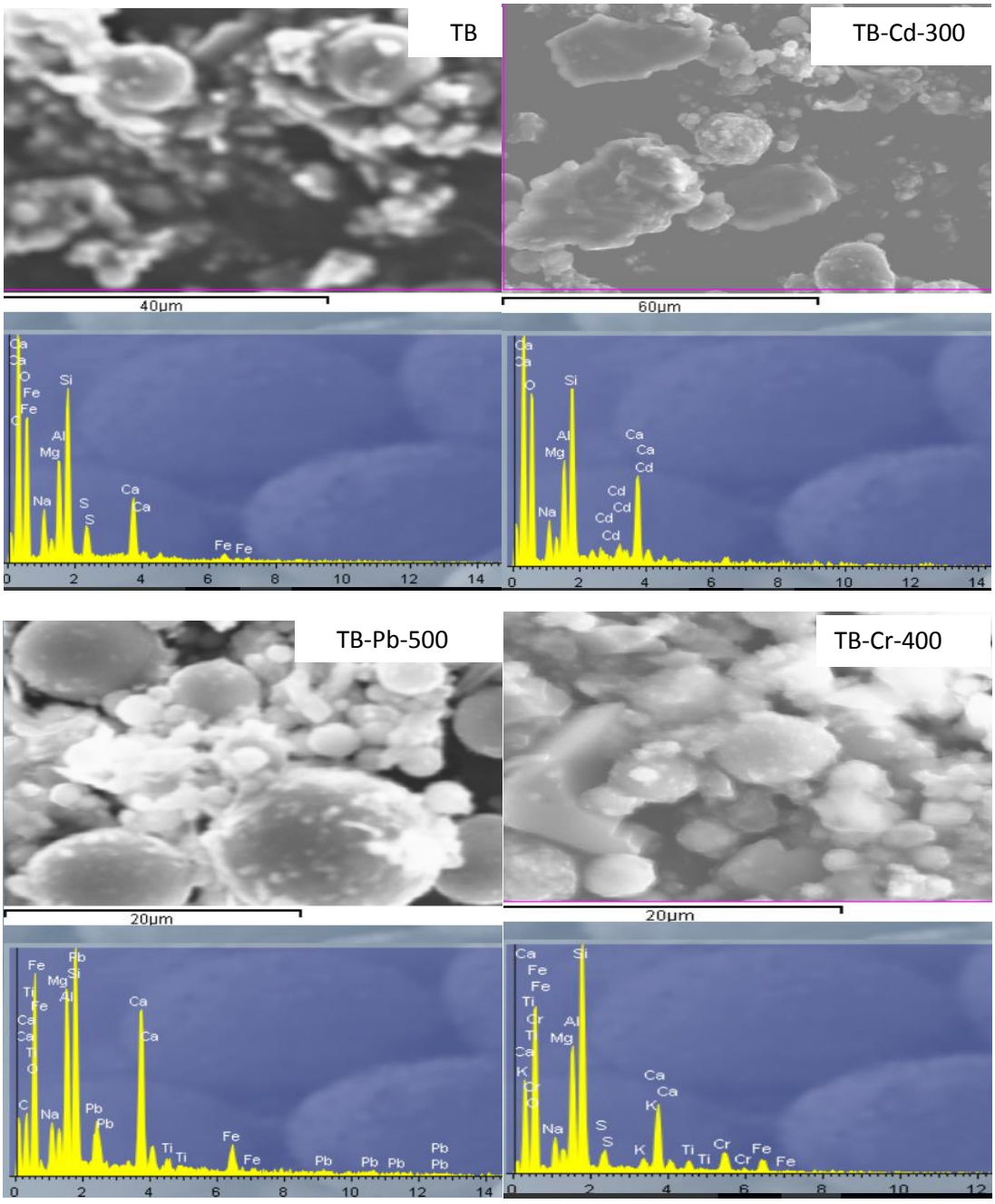


**Figure 3.4 SEM-EDS images of pristine TB, absorbed with 500ppm Pb, with 400 ppm Cr and with 300 ppm Cd (see 2.6.5).**

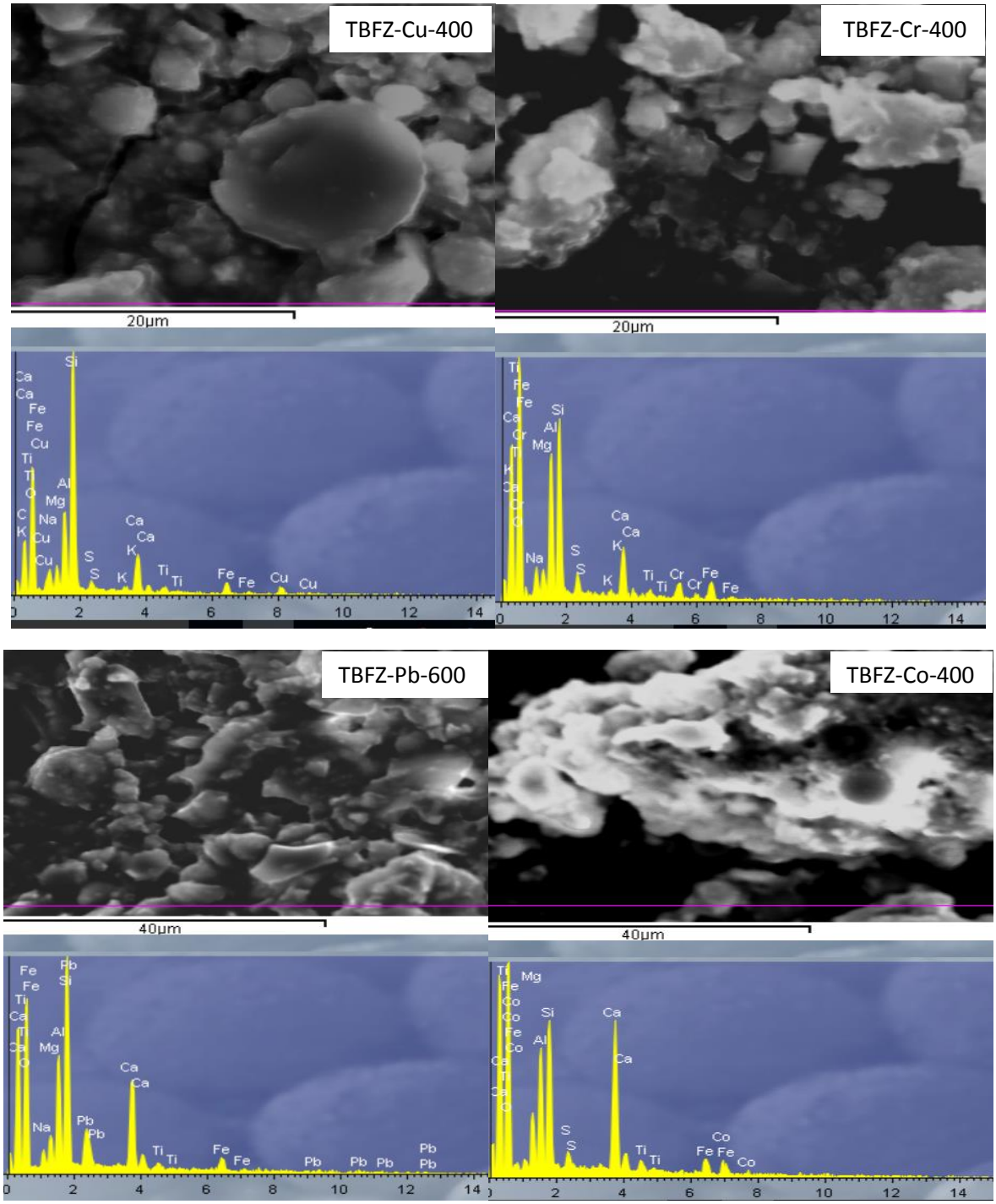


**Figure 3.5 (a) SEM-EDS images of TBFZ-Cu (400 ppm), TBFZ-Cr (400 ppm), TBFZ-Pb (600 ppm) and TBFZ-Co (400 ppm) (see 2.6.5 for experimental details).**

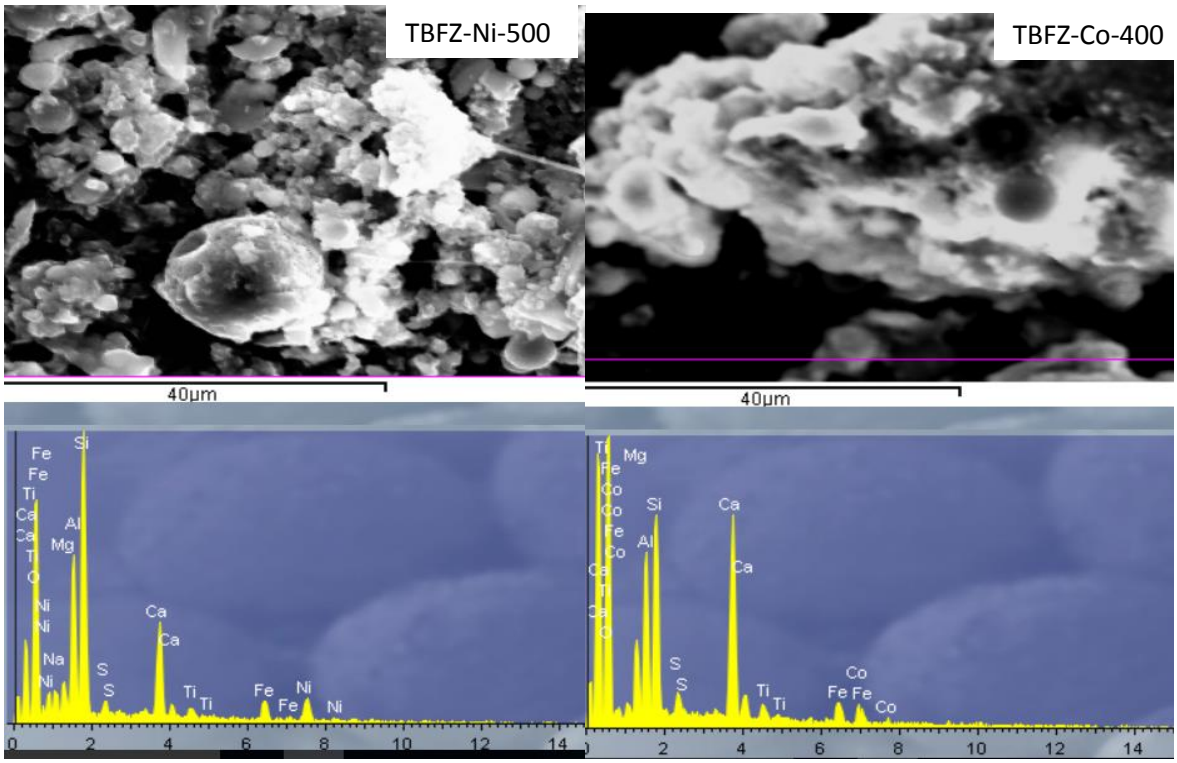


**Figure 3.5 (b) SEM-EDS images of TBFZ-Ni (500 ppm) and TBFZ-Co (400 ppm). (see 2.6.5 for experimental details)**

### 3.1.3 The surface area and porosity of adsorbents

**Table 3.2** shows the comparison of the surface area, pore volume and mean diameter of the pristine sample (TB) and various modified fly ash. The data clearly indicate significant increase in surface areas and pore volumes in fly ash modified under different conditions. With treatments at high temperature, the surface increased by 53 times for HTB($CO_3$)150/4 and 45-folds for HTB(OH)150/4. With a low temperature treatment, the surface area increased to nearly 56 times for TBFZ and 54 times for TBRM. The huge increase in surface area for both TBFZ and TBRM should be translated to much-improved adsorption efficiency and capacity.

During the surface area investigation, it was observed that the BET surface area increased with respect to contact time with 2.0M NaOH solution at room temperature. With contact times of 1, 2, 3 and 4 days, the corresponding BET surface areas were 7.51, 11.19, 18.25 and 25.31 $m^2/g$, respectively; the longer the contact time the better the effect of the activating agent.

**Table 3.2 Surface characteristics of pristine and modified adsorbents**

| Sample ID | BET Surface area | BJH Adsorption Pore Volume | BJH Average pore diameter |
|---|---|---|---|
| Units | ($m^2/g$) | ($cm^3/g$) | (nm) |
| TB (Original) | 1.24 | 0.0035 | NA |
| TBMW(OH)100/0.5 | 12.09 | 0.0234 | 8.27 |
| TBFZ: FA:BA=0.22:0.33:0.45 | 19.48 | 0.0044 | 6.15 |
| TBMW(OH)150/1/So | 41.14 | 0.0844 | 9.07 |
| TBMW(OH)150/1 | 46.66 | 0.0911 | 8.65 |
| HTB(OH)150/4 | 55.66 | 0.1233 | 9.27 |
| HTB($CO_3$)150/4 | 65.95 | 0.1056 | 6.64 |
| TBRM | 67.34 | 0.1557 | 9.45 |
| TBFZ | 68.98 | 0.1547 | 9.19 |

The surface area of the compressed formulated foaming material TBFZ: FA:BA = 0.22:0.33:0.45 was logically lesser compared to the powdered forms of modified fly ash, even though its surface was nearly 16 times that of TB. The lower surface area of other types of modification is attributed to either a lower temperature or shorter reaction time.

The pore volume of the fly ash TB was also remarkably increased after the 2.0 M NaOH treatment, i.e. 35, 30, 44, 44 times for HTB(OH)150/4, HTB ($CO_3$ **)**150/4, TBRM and TBFZ, respectively. The pore diameters presented in **Table 3.2** point to the mesoporous (between 2 to 50 nm) nature of the modified fly ash materials. The pore size distribution was calculated from the nitrogen adsorption using the Barrett-Joyner-Halenda (BJH) model. The results show that modified adsorbents were mesoporous (average pore diameter between 2-50 nm) and this was confirmed by the $N_2$ adsorption-desorption isotherms shown in **Figure 3.6.** The type IV apparent hysteresis loops were observed in the relative pressure $P/P_0$ range of 0.4-0.9.

The quantity of nitrogen adsorption increased significantly at $P/P_0$ of 0.9 suggesting a capillary condensation of nitrogen within the mesoporous material. These hysteresis loops are finger-prints for mesoporous materials. Except for TB, hysteresis was observed in all the modified samples which is a confirmation that samples have been modified with regards to surface area, pore volume and pore size distribution.

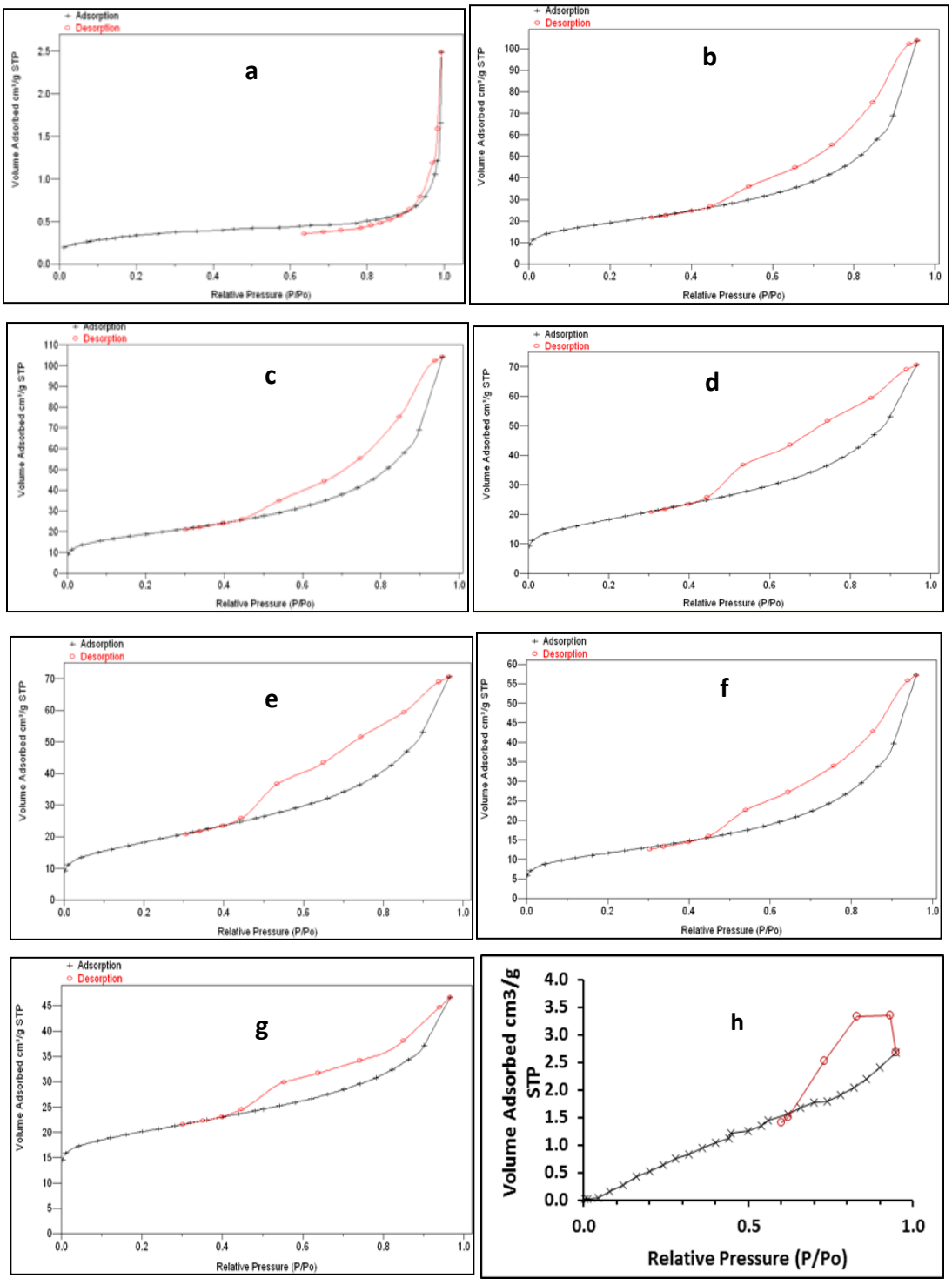


**Figure 3.6 Nitrogen adsorption-desorption isotherms and ore size distribution of (a) TB, (b) TBFZ, (c) TBRM, (d) HTB(OH)150/4, HTB($CO_3$)150/4, (f) TBMW(OH) 150/1/so, (g) TBMW($CO_3$)150/1 and (h) TBFZ: FA:BA 0.22:0.33:0.45.**

### 3.1.4 Particle size distribution

The particle sizing was carried out by Low Angle Laser Light Scattering (LALLS) on the adsorbents. Only the results of the adsorbents used in following tests are presented in **Figure 3.7**. It is observed that the shape of particles distribution of pristine fly ash (TB) is a plateau, with a large percentage of particles in large size range, and that of other treated fly ash samples all have a remarkable peak. The appearance of a high percentages of particles in larger size range for TBRM and HTB(OH)150/4 could be due to the more amorphous property of these treated samples and possible agglomeration of the samples.

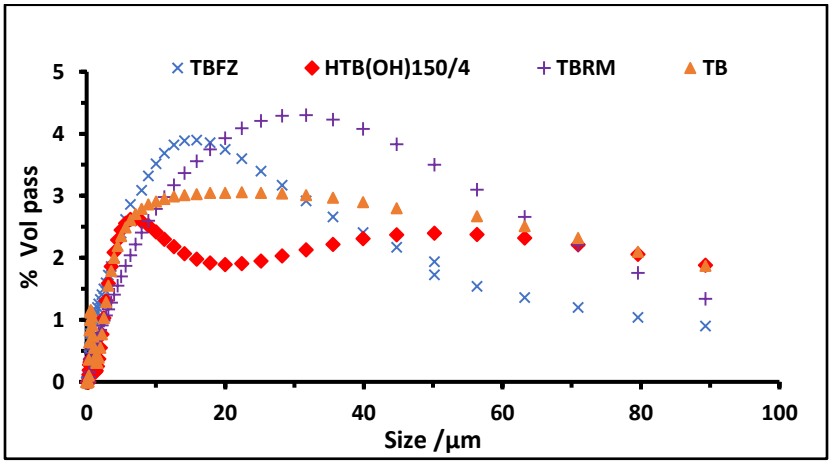


**Figure 3.7. Particle size distribution of TB, TBRM,TBFZ and HTB(OH)150/4.**

From the results of characteristic studies, it is clear that the modified fly ash samples possess a superior surface property due to its much-increased activated surface area. Among those treatment, TBFZ and TBRM are much more attractive than high temperature modification (heating and microwave preparation), thanks to their much lower energy consumption, simpler preparation process and greater productivity in material preparation. In our earlier adsorption studies, it was found that the high temperature treatments of the fly ash did not show any remarkable advantage over the low temperature treatment. For these reasons, in later work, TBFZ and TBRM were used, and TB was used as a control sample.

## 3.2 Chemical characterization of fly ash and mining waste water

### 3.2.1 Main chemical components in pristine Thunder Bay fly ash (TB)

**Table 3.3** shows the chemical composition of the pristine fly ash (**TB**) used throughout the experiments. The amount of $SiO_2$, $Al_2O_3$, CaO and $Fe_2O_3$ were 35.46, 18.16, 15.53 and 10.35%, respectively as assayed by inductively coupled plasma - optical emission spectrometry (ICP-OES) after a sodium peroxide fusion.

**Table 3.3 Chemical composition of pristine fly ash (TB)**

| Chemical compound | $SiO_2$ | $Al_2O_3$ | CaO | $Fe_2O_3$ | MgO | $SO_3$ | $K_2O$ | BaO | $TiO_2$ | $P_2O_5$ | ZnO |
|---|---|---|---|---|---|---|---|---|---|---|---|
| Percentage composition % | 35.46 | 18.16 | 15.53 | 10.35 | 3.68 | 6.49 | 0.74 | 1.32 | 1.15 | 0.25 | 0.09 |

The presence of high percentages of $SiO_2$, $Al_2O_3$, CaO and $Fe_2O_3$ is not surprising because the chemical properties of fly ash are largely influenced by the chemical content of the burned coal. The source of coal was the River Basin and contained high amounts of these elements. The average concentrations of these elements in the coal were in mg/kg as: Al (4531), Si (7471), Ca (5735) and Fe (1886). At high temperature for the combustion of coal these elements present in their ores are converted to their corresponding oxides. The example below shows how zinc blend ore (zinc sulphide) is converted to ZnO by roasting as shown in equation 3.1:

$$2ZnS + 3O_2 \xrightarrow{roasting} 2ZnO + 2SO_2 \qquad [3.1]$$

In this process, zinc sulfide is converted to zinc oxide and $SO_{2(g)}$. A large majority of the trace metals in the form of tiny oxide particles is emitted to the atmosphere in the process.

The leachability of trace metals from pristine TB was tested in deionized water for 10 days. The results showed that there is no measurable amount of trace metals of Pb, Cu, Cd, Cr, Co and Ni (see 2.6.1 for experimental details). The results suggest that the release of tested metal ions from the testing material into testing fluids in the adsorption study is unlikely, and would not be a source of secondary contamination.

The American Association for Testing and Materials (ASTM C618) classifies fly ash to Type C and Type F. For Class C, the sum of the oxides $SiO_2$, $Al_2O_3$ and $Fe_2O_3$ should be in 50 – 70%

wt in a fly ash. For Class F, this sum should be ≥ 70%. Thus, the fly ash TB should belong to Class C. Apart from the valuable materials $SiO_2$, $Al_2O_3$ and $Fe_2O_3$ in TB, there are significant amount of alkaline materials such as CaO, MgO and $K_2O$, which will be beneficial for metal removal, particularly in an acidic medium.

### 3.2.2 Trace metal concentrations in pristine Thunder Bay fly ash (TB) and its modified samples

To assess the concentration of remaining trace elements in TB, TBFZ and TBRM, these samples were subjected to a total digest (see 2.5.2) and the analytical results are presented in **Table 3.4.** The results indicate that Cu, Zn, Ni, Cr and Pb had high amount relative to the other trace elements. While the concentrations of Pb, Cu, Mn, Cd and Fe in modified fly ash sample does not change significantly compared to TB, the concentrations of other elements appear lower after treatment. This can be explained by the chemical properties of these elements: under a highly alkaline condition, Pb, Cu, Mn, Cd and Fe will be in insoluble form of hydroxides, thus remained with the fly ash as a solid phase. The other elements, such as Se, As, Mo and Cr will be present in the dissolved phase as $SeO_3^{2-}$, $AsO_4^{3-}$, $MoO_4^{2-}$ and $Cr_2O_7^{-}$, and thus leave the fly ash. The results show that the 2.0 M NaOH modification can also clean the fly ash material from these undesirable elements. Although the concentrations of Pb, Ni, Zn and Cu were higher than other elements, their concentrations were still quite low for an adsorbent material. As it has been shown earlier, these elements are non-water leachable. It can be concluded that the fly ash TB is a suitable primary low-cost material for adsorption.

**Table 3.4. Trace elements concentrations of testing materials with graphite furnace atomic spectrometry (all in mg/kg).**

| Sample ID | Co | Cd | Mo | Se[b] | As[b] | Pb | Cr | Ni | Zn[a] | Cu | Mn[a] | Fe[a] |
|---|---|---|---|---|---|---|---|---|---|---|---|---|
| **TB** | N.D. | 1.0 | 12.6 | 9.4 | 15.7 | 37.3 | 43.6 | 58.0 | 90.1 | 138.3 | 0.35 | 30.22 |
| **TBFZ** | N.D. | 1.4 | 2.8 | 1.5 | 6.7 | 40.3 | 34.7 | 61.0 | 80.3 | 143.4 | 0.36 | 30.02 |
| **TBRM** | N.D. | 1.3 | 2.7 | 0.9 | 8.6 | 34.4 | 32.8 | 61.1 | 82.3 | 145.4 | 0.36 | 28.17 |

N.D. – Not detectable. The detection limit of Co by GFAAS is 0.40µg/g.

a – the results are produced with FAAS.

b – the results are produced with hydride generation – atomic fluorescence spectrometry (HG – AFS)

### 3.2.3 Chemical characterization of tailing pond water (TPW)

Tailing pond water was collected on the morning of October 26, 2015 from one of the creeks about 3-4 km leading to the water treatment plant of Vale Canada in Sudbury.

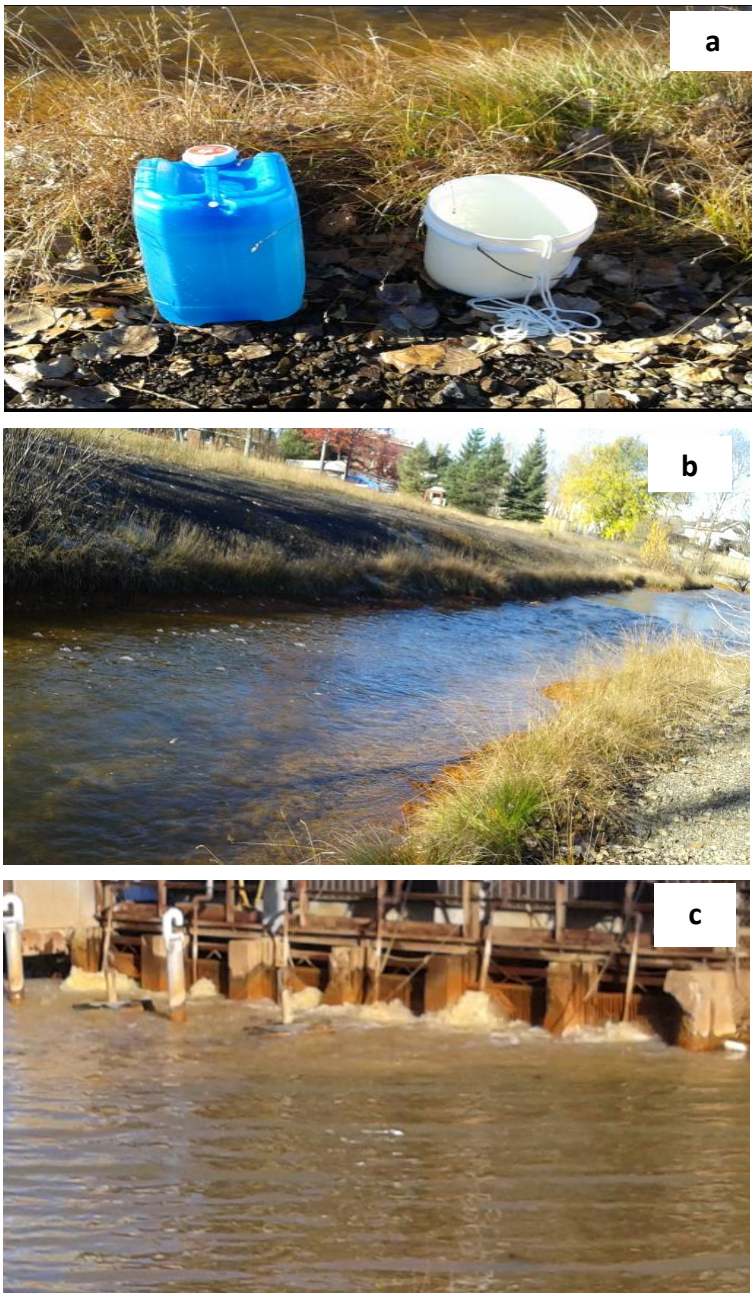


**Figure 3.8 Pictures of (a) Sampling storage containers, (b) sampling creek and (c) the enterance of treatment plant where liming is applied**.

The metals in this mining water is normally treated with large amounts of lime to a desirable pH range 10-11 before being precipitated and discharged into the natural waters. A polymer Fluorine 935 is used in the treatment to assist precipitation and coagulation. **Figure 3.8**. displays the sampling tools and the creek from which water was collected, and the liming station at the entrance of wast water treatment plant. The sampled water was very clear with a pH of 3.36 at the sample collection. However with time, some yellow-brownish precipitates were observed.

The chemical composition of TPW is presented in **Table 3.5**. As seen in **Table 3.5**, one of the elements of interest for this study, Ni had a high concentration of 16024 µg/L or 273.0 µmol/L in the TPW. This is not surprising since the main metals being extracted from the ores are Ni and Cu. The other metals of interest, Cd, Co, Pb and Cr had smaller concentrations. The concentrations of alkali, alkline earth metal and iron ions are high in smelting operations. In TPW, the concentration of sulphate and chloride ions are high. The high content of sulphate is due to the presencce of oxidable sulfide in the ore. As a result of the oxidation of sulfide tailings, sulphuric acid is produced. This is chemical process makes TPW very acidic water.

**Table 3.5 Chemical composition and concentrations of major and minor elements in TPW**

| **Major Cations** | $Na^+$ | $K^+$ | $Ca^{2+}$ | $Mg^{2+}$ | Tot Fe | Tot Mn |
|---|---|---|---|---|---|---|
| (mg/L) | 118.1 | 33 | 375.5 | 82.7 | 66.7 | 1.6 |
| **Major anions** | $F^-$ | $Cl^-$ | $NO^{2-}$ | $PO_4^{3-}$ | $NO_3^-$ | $SO_4^{2-}$ |
| (mg/L) | 0.2 | 127.6 | N. D | 0.3 | 0.7 | 664.2 |

| **Trace elements in the tailing pond water** | | | | | | | | |
|---|---|---|---|---|---|---|---|---|
| Unit | Tot As | Cd | Co | Tot Cr | Cu | Mo | Ni | Pb | Tot Se |
| (µg/L) | 1.1 | 5.2 | 348.5 | 8.3 | 4485 | 0.7 | 16024 | 6.4 | 4.9 |
| (µmol/L) | 0.02 | 0.05 | 5.91 | 0.16 | 70.6 | 0.01 | 273.0 | 0.03 | 0.06 |

Note: the concentration of tested anions (As, Cr, Mo and Se are expressed in mg/L of the mass of each given element and not the formula weight of the given element).

### 3.2.4 Cation Exchange Capacity (CEC) of adsorbents

The cation exchange capacity (CEC) was determined by $NH_4^+$ exchange in cation exchange sites on the pristine and modified fly ash. CEC has direct relation with adsorption capacity of adsorbents and those with higher CEC will retain higher amounts of metal cations upon contact **[38]**. The general principle of the CEC determination based on Kotsiopoulos' method is outlined in section 2.5.4.

The Kjeldahl distillation technique is time consuming and requires practice. However, it has the advantage of minimizing the possible interference compared to other techniques such as the determination of total concentration of all cations. The average values of CEC are presented in **Figure 3.9.** TBFZ had the highest CEC with a value of 29.23 meq/g, followed by TBMW(OH)150/1 and TBRM with values of 23.48 meq/g each, respectively. The least CEC was recorded by TB with a value of only 1.94 meg/g. An increase of about 12 to 15-folds in CEC is very significant to contribute to the adsorption efficiency of an adsorbent. This increase in CEC of all the modified samples can be explained by the work of the strong alkaline solution of 2.0 M NaOH that interacted and corroded the fly ash particles. Although the CECs for the samples with elevated temperature-modification had improved compared to TB by 4, 4 and 12 times for TBMW($CO_3$)150/1, HTB($CO_3$)150/4 and TBMW(OH)150/1, respectively, their CECs are not better than those obtained at low temperature, with 15 and 12 times for both TBFZ and TBRM, respectively. From the results, it can be concluded that the alkalinity of solution and contact play the essential role in the fly ash modification. While temperature may be important, the short time in treatment is unfavorable for this process. This set of data further demonstrates the low temperature treatment with a longer time (7 d), particularly the frozen – thaw cycle, is an optimal process for fly ash modification. It is simple and can take the advantage of a natural Canadian environment. The NaOH liquor can also be reused after adjustment.

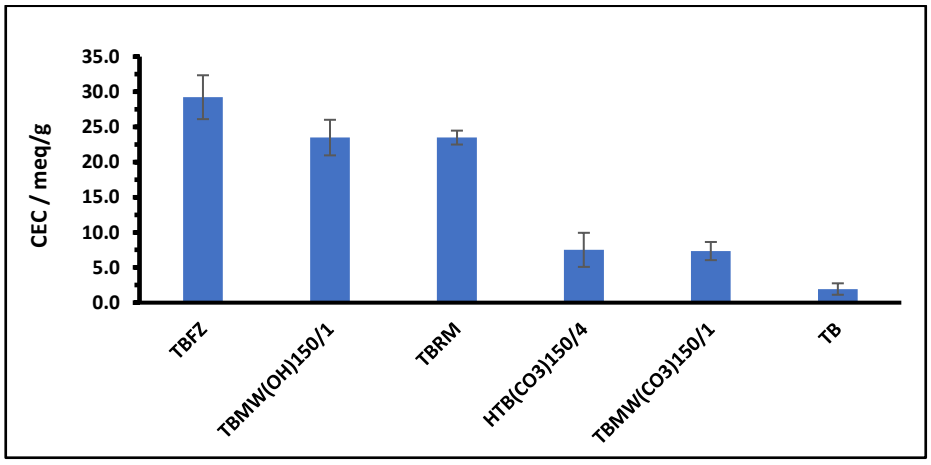


**Figure 3.9 Comparison of CEC of TBFZ, TBMW(OH)150/1, TBRM, HTB(CO3)150/4, TBMW($CO_3$)150/1 and TB. (for experimental details, see 2.5.4.)**

### 3.3 The pH investigation of adsorption systems and its influence on adsorption

In the adsorption studies, the adsorption/removal % is often obtained according to the operation described in equation [2.8], which is based on the determination of an initial and final concentrations of dissolved chemical species in a solution of a studied system. The solutions for analysis are often obtained by centrifugation or filtration to eliminate the solid phase. It is known that many metals can form precipitates at an appropriate pH. In the study of an adsorption properties of an adsorbent for metal ions, it is crucial to control the pH of the adsorption system, if we want to make sure that a metal removal is attributed to adsorption, and not to the formation of metal precipitate. Due to the alkaline nature of the fly ash, it is understandable that it is impossible to control the pH of the material itself, thus the effort was made to understand better the alkaline properties of different types of fly ash in different media and the influence of pH of a solution on metal adsorption.

#### 3.3.1 Studies of acid-base properties of fly ash in DW, synthesized cocktail solution (SCS) and TPW.

To better control pH of the studied adsorption systems in later studies, the pH evolution of different adsorbents in different testing media were conducted first. **Figure 3.10** demonstrates the results of these studies. In **Figure 3.10 (a)** TB, TBFZ and TBRM were immersed in DW and the release of $OH^-$ ions was immediately observed from 5 min until it stabilized at pH 10.70 for TB and 11.50 for TBFZ, respectively. It is noticed that pH of solution in TB system was remarkably lower than the treated fly ash. **Figure 3.10 (b)** shows that in a synthesized cocktail medium, the pH of the solution was lowered to 2.0 from 4.5. With time, pH in a SCS medium gradually increased to 6.7 in TB and 7.7 in TBFZ system, but it was still much lower than in a DW medium. The results indicate that the materials are highly alkaline and that pH adjustment is needed in adsorption test to avoid the formation of precipitates for several metals.

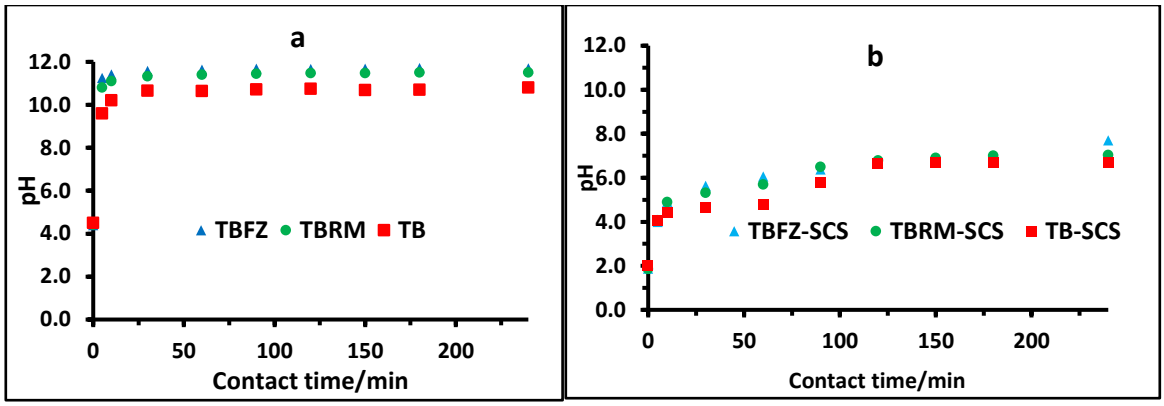


**Figure 3.10 pH evolution of different adsorbents in different media without any pH adjustment, done with 0.50 g adsorbent in 50.0 mL of deionized water (DW) and synthesized cocktail solution (SCS), and a constant shaking of 120 rpm at 22±1 ºC (2.6.2).**

### 3.3.2 Examination of precipitation pH of metal ions by calculations

The pH at which each metal ion would precipitate at a specific concentration was investigated. Since each metal ion would precipitate at a specific pH depending on the solubility product $K_{sp}$ and the concentration of the hydroxide of the metal ion, the critical theoretical pH was calculated. The theoretical pH values at which these metals would precipitate at given concentrations are presented in **Table 3.6.**

**Table 3.6. Calculated theoretical pH for precipitation based on (OH) for metal ions, assuming that the ionic strength can be ignored.**

| Metal (mg/L) | Cd | Co | Ni | Pb | Cu | Cr |
|---|---|---|---|---|---|---|
| 50 | 8.50 | 8.09 | 7.92 | 7.76 | 5.89 | 4.67 |
| 100 | 8.35 | 7.94 | 7.77 | 7.61 | 5.74 | 4.57 |
| 150 | 8.26 | 7.85 | 7.69 | 7.52 | 5.65 | 4.51 |
| 200 | 8.20 | 7.79 | 7.62 | 7.46 | 5.59 | 4.47 |
| 300 | 8.11 | 7.70 | 7.53 | 7.37 | 5.50 | 4.41 |
| **$K_{sp}$ of (OH), I = 0** | **$4.5 \times 10^{-15}$** | **$1.3 \times 10^{-15}$** | **$6.0 \times 10^{-16}$** | **$8.0 \times 10^{-16}$** | **$4.8 \times 10^{-20}$** | **$1.0 \times 10^{-31}$** |

Calculation indicated that the pH required to form a precipitate increase in following order $Cr^{3+} < Cu^{2+} < Pb^{2+} < Ni^{2+} < Co^{2+} < Cd^{2+}$. To avoid precipitation of metal ions, during the adsorption experiments, the values of pH in Table 3.6 were used as a guideline. A 0.1 M NaOH and a 0.2 M

$HNO_3$ solution were used in pH adjustment in the experiments to control pH to below its pH guideline.

### 3.3.3 Effect of pH on adsorption

In this study, the removal %, rather than the adsorption % was used. This is because it is difficult to absolutely exclude possibility of formation of precipitates of metal ions on an alkaline surface of fly ash as it has been mentioned before.

The experimental data showed that pH has a strong influence on the removal of cations from aqueous solutions for all adsorbing materials. As pH increased there was correspoding increase in metal removal as shown in **Figure 3.11**. It could also be observed that the studied metal ions could be classified in two groups. Those that are easily removed even at low pH (Cr, Pb and Cu) and those that are removed at high pH (Co, Cd and Ni). This can be explained by the fact that the second group of elements requires higher pH before they could be precipitated as shown in **Table 3.6**. The pH investigated ranged from 2.9-8.2.

**Table 3.6** demanstrates that Cr, Pb and Cu can be classified as a group of metals easier to be adsorbed at a relatively low pH comparatively to Co, Ni and Cd, although better adsorption of Cu required a higher pH than Cr and Pb did. For the Co, Ni and Cd group, at low pH, their removal % were quite low. However as the pH increased, the removal percentage increased greatly. It is certain that the modified materials have a much better removal efficiency than the pristine fly ash. It is worth to mention that excellent adsorption of Pb has been observed in all materials at a pH much lower than its theoretical pH for precipitation. However, at pH below 7.0, the adsorption for Ni by TB, TBFZ and TBRM was very low. At pH 6.70±0.60, the order of adsorption for the metal ions in TB was $Cr^{3+} > Pb^{2+} > Cu^{2+} > Co^{2+} > Ni^{2+} > Cd^{2+}$. For TBRM and TBFZ, the adsorption order was $Pb^{2+} > Cr^{3+} = Cu^{2+} = Co^{2+} > Ni^{2+} > Cd^{2+}$ and $Pb^{2+} > Cr^{3+} = Cu^{2+} = Co^{2+} = Ni^{2+} > Cd^{2+}$, respectively. Cd is the least adsorbed metal by all adsorbents, probably due to its lowest hydrolysis constant.

The observed preference in adsorption could be attributed to the specifics of the adsorbents and adsorbate. Selectivity sequences have been reported in literature (studies mainly conducted in single solution) for Na-clinoptilolite, natural clinoptilolite and zeolite 4A as: $Cr^{3+} > Cu^{2+} > Zn^{2+} > Cd^{2+} > Ni^{2+}$, **[39]**; $Ba^{2+} > Cu^{2+} > Cd^{2+} = Zn^{2+} > Co^{2+} > Ni^{2+}$, **[40]**; for natural clinoptilolite: $Ba^{2+} > Pb^{2+} > Cd^{2+} > Zn^{2+} > Cu^{2+}$, **[41]**; $Pb^{2+} > Cu^{2+} > Cr^{3+}$, **[42]**; and, $Pb^{2+} > Cr^{3+} > Fe^{3+} > Cu^{2+}$, **[43]**; and for zeolite 4A: $Cu^{2+} > Co^{2+} > Mn^{2+} > Zn^{2+} > Cd^{2+} > Ni^{2+}$, **[44]**.

The low removal of metal ions at lower pH can be attributed to the competition between $H_3O^+$ and metal ions. In addition, the hydroxyl groups (Si-OH and Al-OH, Ti-OH, Fe-OH) on the surface of the adsorbents could be ionized in aqueous solution **[45]**. With increase in pH, dissociation of the hydroxyl groups will be enhanced, therefore creating more anionic sites and hence significant increases in adsorption of metal ions at high pH. Similar results have been reported in the literature **[46-49].** The removal of metal ions could be attributed to adsorption *via* electrostatic attraction, ion exchange and precipitation since $Cr^{3+}$ and $Cu^{2+}$ had their pH of precipitation theoretically exceeded. At pH above the critical value, metal hydroxides will likely be formed leading to precipitation metal ions.

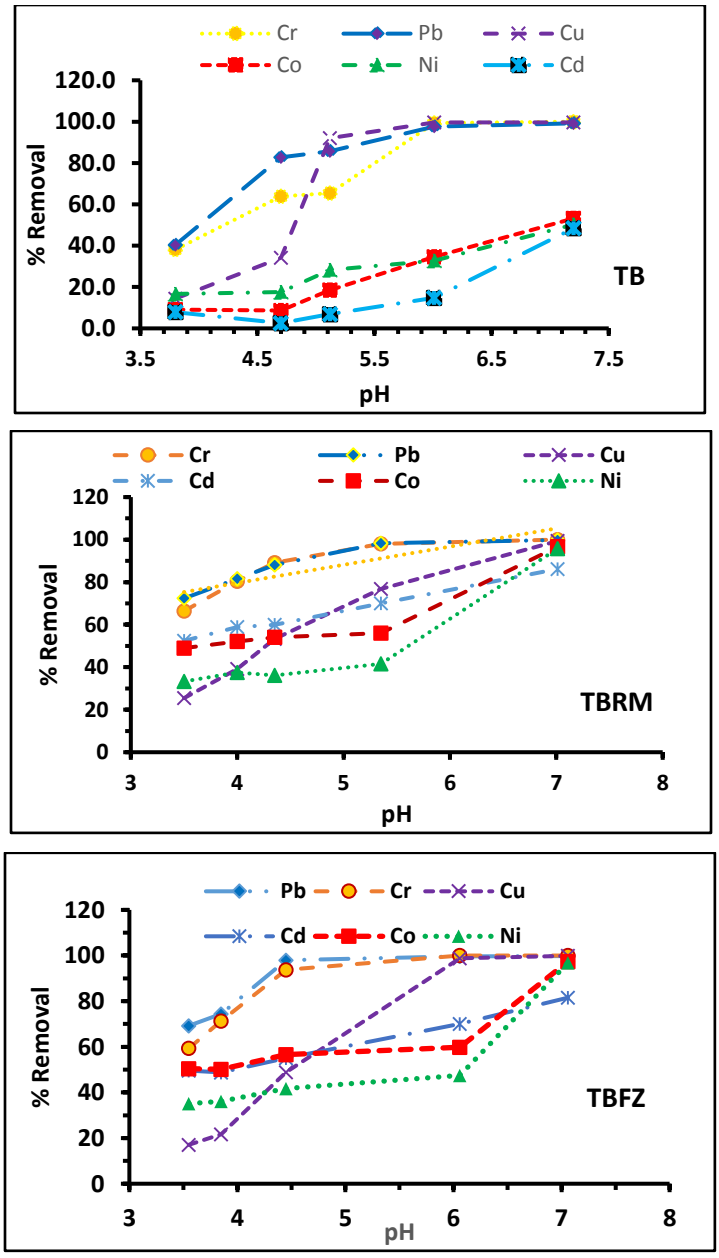


**Figure 3.11. pH effect on adsorption of metal ions by different fly ash materials. adsorbent :0.50 g, concentration of metal ions in SCS: 50.0 mg/L each : Volume of metal ions solution: 50.0 mL; time: 2 h, shaking: 120 rpm at 22 $^{0}$C**

### 3.3.4 Effect of adsorbent dosage on removal

The effect of adsorbent dossage on the adsorption of $Pb^{2+}$, $Cu^{2+}$, $Cr^{3+}$, $Co^{2+}$, $Cd^{2+}$ and $Ni^{2+}$ ions was studied on HTB(OH)150/4 with different dosages of adsorbent in solutions at pH 4.45-7.06. As shown in **Figure 3.12**, the removal percentage of $Pb^{2+}$, $Cu^{2+}$, $Cr^{3+}$, $Co^{2+}$, $Cd^{2+}$ and $Ni^{2+}$ ions increased as the dosage increased from 2.0 to 10.0 g/L.This may be explained by the metal ions competing for insufficient adsorption sites at lower HTB(OH)150/4 dosage. The increase in the removal percentage with increase in adsorbent dosage was due to an increase in active sites on the adsorbent, therefore enhancing the contact of metal ions with sorption sites **[50]**. At adsorbent dosage of 10.0 g/L or 0.5 g in 50.0 mL , the removal percentage of $Cu^{2+}$, $Ni^{2+}$, $Pb^{2+}$, $Cr^{3+}$, $Cd^{2+}$ and $Co^{2+}$ were 100, 100, 100, 100, 98 and 92 %, respectively.The adsorbent dosage was therefore fixed at 10.0 g/L for further equilibrium and kinetic studies.

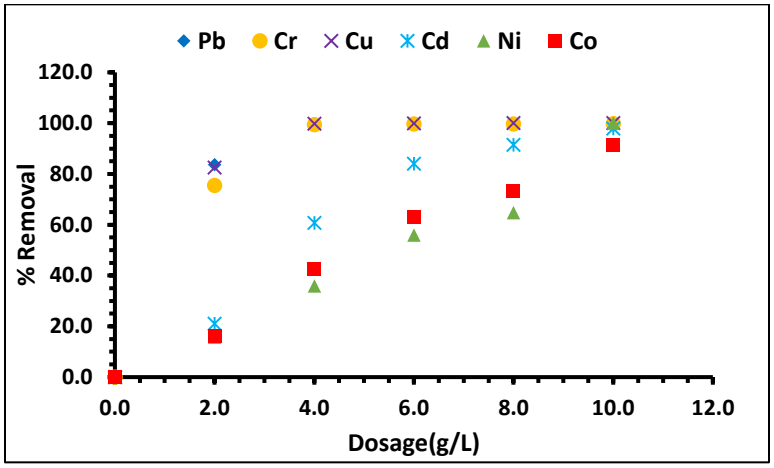


**Figure 3.12 Effect of adsorbent dosage on HTB(OH)15/4: concentration of SCS: 50.0 mg/Leach; dosage: 2.0 -10.0 g/L; pH of adsorption system from initial 4.45 to final 7.06; temperature: 22 ºC; shaking: 120 rpm; time: 2 h.**

## 3.4 The studies on adsorption kinetic mechanics

### 3.4.1 Adsorption kinetic studies

Kinetic studies were conducted initially on pristine fly ash TB and modified fly ash TBMW(OH)150/1/so, HTB(OH)150/4**,** TBMW($CO_3$)150/1. However, later on most of the studied were conducted with TBFZ, TBRM and TB in a synthesized cocktail solution (SCS) and spiked

tailing pond water (TPW). The contact time is an important factor in evaluating the adsorption efficiency, which helps to determine the minimum time needed in adsorption capacity measurement. Metal ion uptake percentages were determined as a funtion of time to determine an optimum contact time for the adsorption of metal ions on pristine fly ash TB and modified fly ash samples: TBRM, TBFZ, HTB(OH)150/4, TBMW(OH)150/1 and TBMW($CO_3$)150/1. The amount of each metal ion removed from the solution was calculated as explained in equation [2.8] with a consideration of volume change due to pH adjustment during the experiment.

The variation of percentage removal with respect to time is shown in **Figures 3.13** to **3.15. Figure 3.13**. compares the percentage removal of metals with time by TB and the hydrothermally modified adsorbents. Although at this point the pH control was not considered, it could be observed that the percentage removal was better for the modified samples, comparatively.

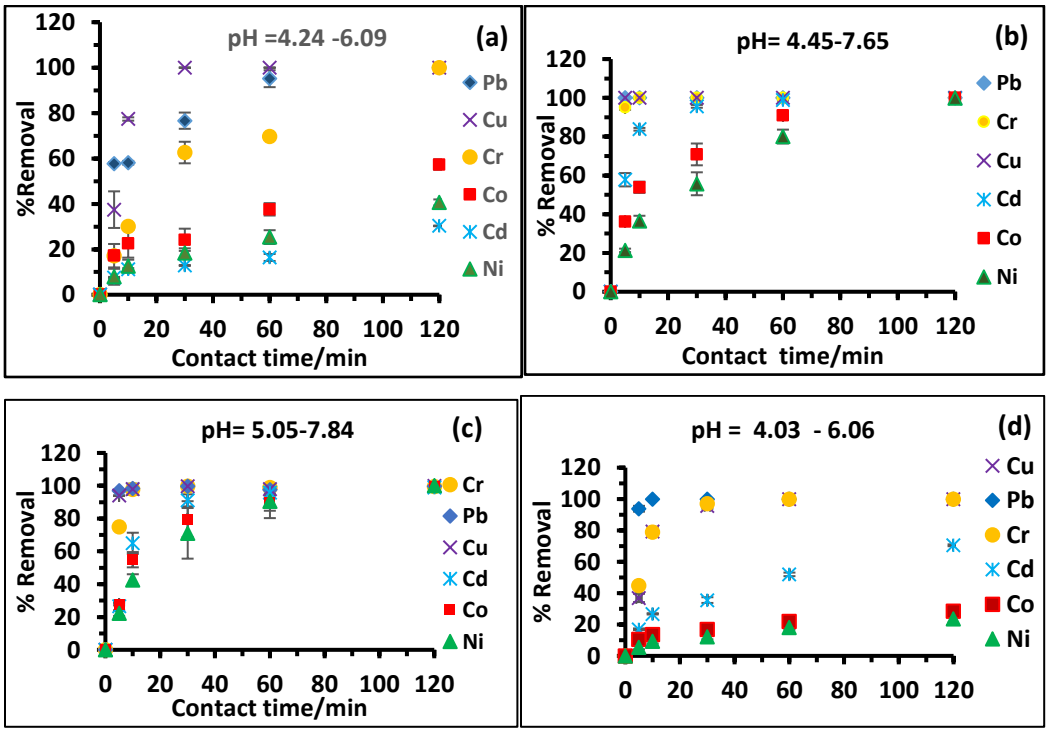


**Figure 3.13 Comparison of adsorption efficiency between different fly ash. Adsorbents: 0.50 g, concentration of metal ions 50.0 mg/L each; metal ions solution: 50.0 mL; time: 2 h; shaking speed: 120 rpm at 22 ºC (a) TB; (b) TBMW(OH)150/1/so; (c) HTB(OH)150/4; (d) TBMW($CO_3$)150/1.**

This group of data confirmed also the observation earlier that the metal ions Cr, Pb and Cu are easily adsorbed by all materials even the non-modified TB. The TBMW($CO_3$)150/1 did not show significant improvement in adsorption of Co, Ni and Cd compared to TB. This may indicate the importance of alkalinity of the solution in the modification process. Thus the sodium hydroxide is a better reagent in modification than sodium carbonate.

Higher efficiency in metal removal by the modified samples could be attributed to higher surface area, higher pore volume (**Table 3.2**) and higher cation exchange capacity (**Figure 3.9**), all obtained after modification. These parameters are the main factors which characterize a good adsorbent. The six metal ions can be classified into two groups: Cd, Ni and Co and Cr, Pb and Cu. The latter group of metals was easily removed from aqueous solution irrespective of the pH whereas the former group mostly required higher pH before very effective removal could be achieved.

The fast removal of Cr group could be attributed to their low solubility products. For $Cr(OH)_3$, $Cu(OH)_2$ and $Pb(OH)_2$, $K_p$ values are $1.0 \times 10^{-31}$, $4.8 \times 10^{-20}$ and $8.0 \times 10^{-16}$, whereas for the slow removal group, their hydroxides $Co(OH)_2$, $Ni(OH)_2$ and $Cd(OH)_2$ have $K_{sp}$ of $1.3 \times 10^{-15}$, $6.0 \times 10^{-16}$ and $4.5 \times 10^{-15}$, respectively. In other words, it is highly possible that the capture of these metal ions by the surface of adsorbents is due to formation of some kind of primary hydroxide complex which is always favorable to the metal ions with a lower $K_{sp}$ value. Apart from the possible formation of precipitate on the surface, adsorption process is probably co-existing. It is noticed that the removal of $Pb^{2+}$, $Ni^{2+}$, $Co^{2+}$ and $Cd^{2+}$ from the solution occurred at a pH much lower than their critical pH of hydroxide formation. It needs to be mentioned that even the pH of the solution of a studied system is below the critical pH of a metal, one cannot exclude a formation of hydroxide has not occur on the surface of a fly ash adsorbent due to its alkaline property.

Although these hydrothermally modified adsorbents has been proved efficient in removing metal ions, further production and investigation was abandoned due to the disadvanges associated with them. These include (1) high energy consumption; (2) risk of explosions of a heavy duty PTFE reactor under high temperature and pressure, (3) only a small amount of material (5.0 g) could be produced at a time.

A new modification protocol at low temperature was persued. This could yield higher amount produced ( approximately 50.0 g) at a time, no explosion was experienced and it did require much less energy consumption, which was more in line with the objectives of the study to develop low-cost adsorbent from waste materials at low cost. This led to the preparation of the adsorbents TBRM and TBFZ whose method of preparation has been outlined earlier on.

From this point, all tests conducted were based on TB, TBRM and TBFZ in either SCS or Vale tailing pond water -TPW. The pH of the liquid phase of studied adsorption systems was carefully adjusted and controlled to avoid the formation of hydroxides of metal ions in aqueous phase at a given time for a given metal. For instance, at 50.0 mg/L, $Cr^{3+}$ will form $Cr(OH)_3$ at pH 4.67 theoretically. An effort was made to control the pH in an aqueous phase below or at least not significantly higher than this value. It is noticed that Cr can be removed very quickly, after 30 min in TB and 10 min in TBRM and TBFZ. Although the pH of a fly ash systen is inevitably increased, in a short time of 10 – 30 min the pH in a testing system was usually below or around the critical pH of $Cr^{3+}$. Similarly, pH in the aqueous phase was controlled based on this consideration for all metals during the kinetic studies.

**Figure 3.14** compares the removal behavior for TB, TBRM and TBFZ in a SCS medium. As could be seen, Cr, Cu and Pb were quickly removed by all three adsorbents within the studied pH range by TB, TBRM and TBFZ. However, the removal was faster in TBRM and TBFZ compared to TB. Within a 30 min time interval the percentage removal of Cu by TBRM and TBFZ were 83.4 and 85.6 %, respectively whereas only 18.1 % had been removed by TB. For Pb, 83.4 % was removed by TB while 95.5 and 81.5 % were adsorbed by TBRM and TBFZ, respectively. A similar trend was observed for Cr removal. Whereas TBRM and TBFZ removed 95.6 and 96.4 %, respectively,TB recovered only 85.6 % within the same time. The differences in the removal efficiency of the adsorbents appeared more significantly when comparing adsorption percentages of Co, Ni and Cd. For Ni, the adsorption percentage by TB, TBRM and TBFZ were 49.7, 64.5 and 100.0 %, respectively after 360 min of contact time. A similar pattern was observed for Co for which the order of uptake by TB, TBRM and TBFZ were 36.2, 68.4 and 100 %, respectively. For Cd the removal order was also TB < TBRM < TBFZ with corresponding percentages as 58.0, 80.2 and 95.4 %. This can be attributed to the high surface area, improved pore volume and high cation

exchange capacities of both TBFZ and TBRM relative to TB. These ions were removed *via* adsorption since the pH (4.23 ± 0.06 - 7.52 ± 0.05) at which they were removed is less than the critical pH for precipitation of Co - pH 8.14, Cd- pH 8.90 and Ni-pH 8.19.

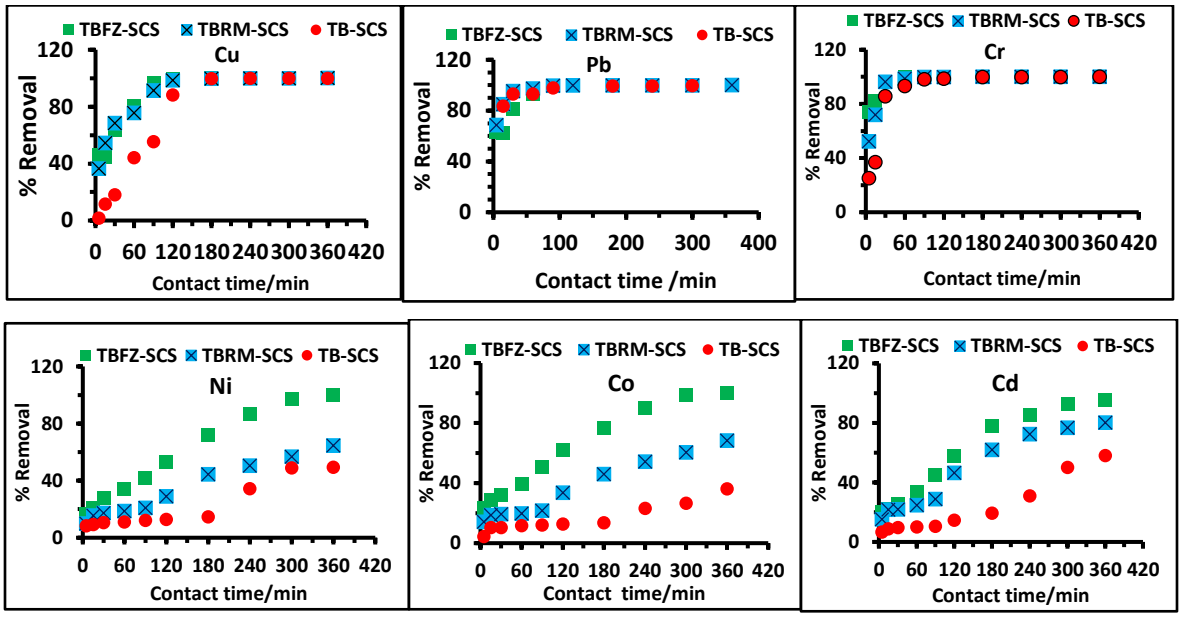


**Figure 3.14. Comparison of removal kinetics between adsorbents and metal ions.: Adsorbent: 1.50 g, concentration of metal ions: 50.0 mg/L each; volume of metal ions solution: 150.0 mL; time: 6 h at 22 ±1 ºC; shorizontal shaking:120 rpm; TB, TBRM and TBFZ in SCS; pH (TB): 4.15 -7.47 pH(TBRM): 4.40 -7.51 pH(TBFZ): 4.45-7.53.**

A comparison of metal removal rate by TB, TBRM and TBFZ in a tailing pond water (TPW) is presented in **Figure 3.15**. To facilitate a comparison with the results in a SCS medium, in this set of test, a cocktail solution of 50.0 mg/L for each metal was prepared in TPW. Although similar trends were observed for all metal ions, the removal rate was much higher for all metal ions in a TPW medium than they were in a SCS medium, and particularly remarkable for group Ni, Co and Cd. With TB and in SCS, 49.7 % of Ni, 36.2 % of Co and 58.0 % of Cd were removed at 360 min. However, in TPW these values increased to 79.9 % for Ni, 82.5 % for Co and 65.7 % for Cd, respectively. Similarly, with TBRM and in SCS, 64.5 % of Ni, 68.4 % of Co and 80.2 % of Cd was removed whereas in TPW these values increased to 80 % for Ni, 80.1 % for Co and

88.5 % for Cd at 360 min. For TBFZ, the same removal was observed for Ni and Co in both SCS and TPW whereas an increment from 95.4 to 100 % was recorded for Cd. These marked improvement in the removal efficiency of TB, TBRM and TBFZ in the presence of TPW could probably be due to the presence of high amount of anions ($SO_4^{2-}$; 664.2 mg/L and $Cl^-$ ;127 mg/L) that were contained in the TPW as shown in **Table 3.5.**

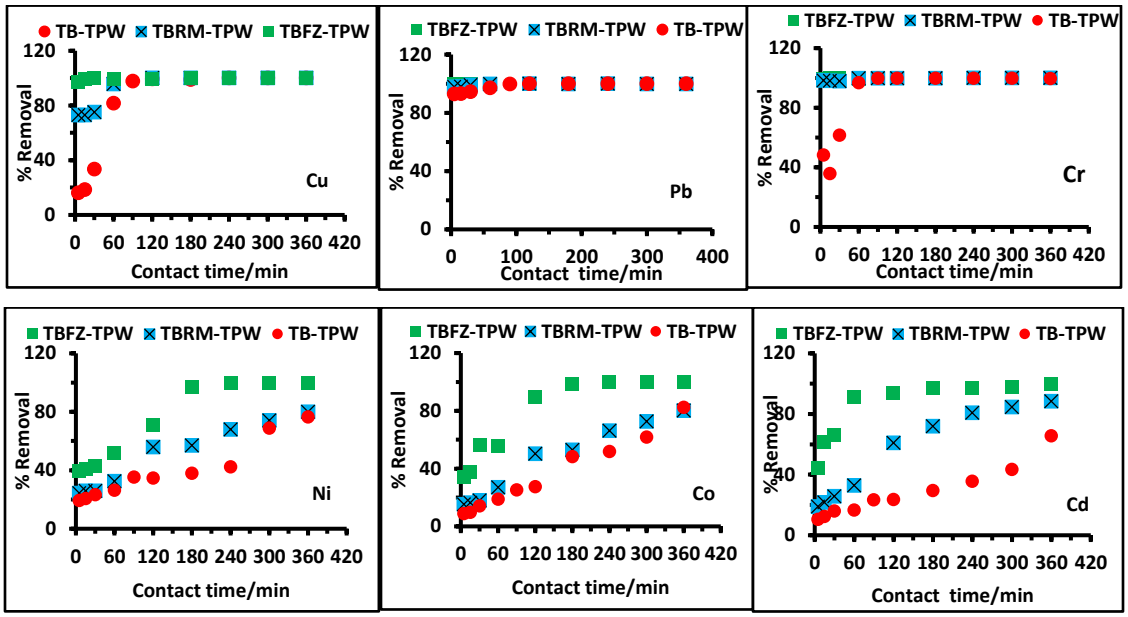


**Figure 3.15 Comparison of adsorption efficiency: adsorbent: 1.50 g, concentration of metal ions: 50.0 mg/L each; volume of metal ions solution: 150 mL; time: 6 h; shaking: 120 rpm at 22 $^0$C; ; TB, TBRM and TBFZ in TPW; pH (TB): 4.33 -7.45 pH (TBRM): 4.20 -7.53 pH (TBFZ): 4.35-7.57.**

According to Mckay **[52]**, three stages are essentially involved in the adsorption of metal ions by porous adsorbents **[51]**: (1) transfer of a solute from a bulk solution to the external surface of a adsorbent through a liquid boundary layer (film resistance); (2) transport of the solute from the external surface to the intraparticle active sites (intraparticle resistance); and (3) the interaction of the solutes with available sites on both the internal and external surfaces of the adsorbent (reaction resistance). The rate at which the solute is adsorbed by the adsorbent may be controlled by one or more of these stages above.

The adsorption rates of the metal ions with TB,TBRM and TBFZ were investigated by the Lagergren pseudo-first order equation [3.2] and pseudo- second order equatioin [3.3] models **[52]:**

$$\ln(q_e - q_t) = \ln(q_e) - k_1 t \qquad [3.2]$$

$$\frac{t}{q_e} = \left(\frac{1}{q_e} t\right) + \frac{1}{k_2 q_e^2} \qquad [3.3]$$

where $q_t$ ($mg \cdot g^{-1}$) is the adsorption at time t (min); $q_e$ ($mg \cdot g^{-1}$) is the adsorption capacity at adsorption equilibrium and $k_1$ ($min^{-1}$) and $k_2$ ($g \cdot mg^{-1} \cdot min^{-1}$) are the kinetic rate constants for the pseudo-first order and pseudo-second order models, respectively. The Largergren equation is based on the assumption that the sorbate uptake with time is directly proportional to the difference between the saturation concentration and the amount of adsorbate uptaken with time. The pseudo-second order kinetic equation is based on the assumption that the rate limiting step may be involved a chemical adsorption where valence forces through sharing or exchange of electrons between the adsorbent and adsorbate play a role **[53]**.

The kinetic adsorption data were fitted to both equations [3.2] and [3.3]., The outcome of the fitting showed that the results do not fit with Lagergren pseudo first–order model. However, the results seem to fit better to equation [3.3], for most of the cases. The fiting results are given **Tables 3.7** to **3.10**. A look at **Figures 3.14 and 3.15** suggest a two-step equilibrium removal mechanism exist, and it is more obvious for Co, Ni and Cd with TB and TBRM as adsorbents. Thus, in the model fitting a two – step fitting was conducted from t 5'-90' and t' 90'-360 tep. The fitting data in Table 3.7 – 3.10 showed that with TBFZ, the removal rate of all metal ions fit well the pseudo second order model in both SCS and TPW media and in both steps, their fitting correlation coefficients $R^2$ are between 0.91 – 1.0.

With TBRM, the fittings are less consistent, even though they are acceptable in most cases. In SCS medium and in the first 5 – 30 min, the fittings $R^2$ = 0.984 – 1.00 for all metals, and in a second step, for the fast removal group $R^2 \approx 1.0$, but for a slow removal group $R^2$ = 0.802 – 0.826. In a TPW medium, at the first 5 – 30 min, the fast removal group have $R^2$ = 0.990 – 1.000, but the

slow removal group the $R^2$ is 0.70, 0.80 and 0.85 for Co, Cd and Ni respectively; at the second 30 – 360 min, the $R^2$ s are all quite high at 0.942 – 1.00 for all 6 metal ions. In the pseudo-second order kinetic model fitting with TB, appeared a very clear pattern. In the first 5 – 30 min, the fittings are very good with $R^2$ = 0.90 – 0.998 in both SCS and TPW medium for all metal ions, except Cu in SCS which could be caused by a poor analytical error. In the second step of 30 – 360 min, the fittings for the fast removal group of Cr, Cu and Pb the $R^2$ are very high, mostly around 1.00, whereas the fitting for the slow removal group of Co, Ni and Cd are extremely poor at round 0.4 or lower. It suggests that to the slow removal group, in the first part of test, the removal of the metals is likely dominant by the chemical interaction occurred between adsorbate and adsorbent. The removal mechanism in first stage of 5 – 30 min seems different from the second stage of 30 – 360 min. The latter stage appears to relate with diffusion of alkali species from the inner fly ash particles to their outer surface.

A single step fitting with the pseudo secondary order kinetic model was also made for the fast removal group of Cr, Cu and Pb with TB, TBRM and TBFZ in SCS and TPW media. Their fitting coefficients of correlation $R^2$ were very similar to those fit with 2-time period. Therefore, the data are not presented here. From **Figure 3.14 and Figure 3.15**, some conclusion can be drawn. (1) The removal rate by modified fly ash is greatly increased comparing the non – modified one. This could be due to the low activated surface of TB adsorbent; (2) TBFZ is a better preparation than TBRM; (3) the metal removal is accelerated in tailing pond water; (4) the removal of Co, Ni and Cd on non – modified fly ash appeared subjected to different stages. At the beginning the removal is based on the surface interaction between the adsorbate and the adsorbent, and later the removal rate is possible dependent on the diffusion of alkali species.

The results regarding the pseudo-second order rate constants $k_2$ (g/mg·min) do not reveal any relationship or trend either among the metal ions or between the adsorbents confirming the differences that exist between the pristine fly ash TB and the modified fly ash TBRM and TBFZ. The results regarding the pseudo-second order rate constants $k_2$ do not reveal any relationship or trend either among the metal ions or between the adsorbents confirming the differences that exist bewtween the pristine fly ash TB and the modified fly ash TBRM and TBFZ.

**Table 3.7 Kinetic parameters of Cu(II), Pb(II), Cr(III), Co(II), Ni(II) and Cd(II), in SCS medium t'5-90**

| TB | Co(II) | Ni(II) | Cd(II) | Pb(II) | (Cr(III) | Cu(II) |
|---|---|---|---|---|---|---|
| $\frac{1}{(k_2\, q_e^2)}$ | 10.029 | 7.2629 | 6.7392 | 0.2334 | 3.5694 | 18.076 |
| $K_2$ (g/ mg min) | 0.1918 | 0.3381 | 0.5743 | 0.1476 | 0.0062 | 0.0019 |
| $q_e$ Calc.(mg/g) | 0.7209 | 0.6381 | 0.5083 | 5.387 | 6.720 | 5.3706 |
| $q_e$ Expt.(mg/g) | 0.665 | 0.662 | 0.4926 | 4.870 | 5.180 | 2.757 |
| $R^2$ | 0.9966 | 0.9955 | 0.9998 | 0.9984 | 0.9471 | 0.4060 |
| **TBRM** | **Co(II)** | **Ni(II)** | **Cd(II)** | **Pb(II)** | **(Cr(III)** | **Cu(II)** |
| $\frac{1}{(k_2\, q_e^2)}$ | 2.9241 | 6.286 | 5.2537 | 0.4896 | 0.9363 | 2.4222 |
| $K_2$ (g/ mg min) | 0.2325 | 0.1254 | 0.0968 | 0.071 | 0.0338 | 0.017 |
| $q_e$ Calc.(mg/g) | 1.2129 | 1.1263 | 1.4025 | 5.362 | 5.624 | 4.9213 |
| $q_e$ Expt.(mg/g) | 1.149 | 1.0708 | 1.3510 | 5.218 | 5.270 | 4.551 |
| $R^2$ | 0.9966 | 0.9957 | 0.9878 | 0.9999 | 0.9882 | 0.9844 |
| **TBFZ** | **Co(II)** | **Ni(II)** | **Cd(II)** | **Pb(II)** | **(Cr(III)** | **Cu(II)** |
| $\frac{1}{(k_2\, q_e^2)}$ | 4.5762 | 6.67 | 7.8392 | 1.3489 | 0.4742 | 3.0001 |
| $K_2$ (g/ mg min) | 0.0247 | 0.0258 | 0.0236 | 0.024 | 0.0712 | 0.0114 |
| $q_e$ Calc.(mg/g) | 2.977 | 2.409 | 2.325 | 5.555 | 5.444 | 5.417 |
| $q_e$ Expt.(mg/g) | 2.740 | 2.158 | 2.120 | 5.205 | 5.272 | 4.815 |
| $R^2$ | 0.9546 | 0.9705 | 0.9203 | 0.9936 | 0.9995 | 0.9629 |

**Table 3.8 Kinetic parameters of Cu(II), Pb(II), Cr(III), Co(II), Ni(II) and Cd(II), in SCS medium t' 90-360'**

| TB | Co(II) | Ni(II) | Cd(II) | Pb(II) | Cr(III) | Cu(II) |
|---|---|---|---|---|---|---|
| $\frac{1}{(k_2\, q_e^2)}$ | 160.26 | 199.05 | 211.23 | 0.0092 | 0.3866 | 11.359 |
| $K_2$ (g/ mg min) | 0.0001 | 0.005 | 0.000 | 5.107 | 0.092 | 0.002 |
| $q_e$ Calc. (mg/g) | 8.110 | -5.6306 | -4.2753 | 4.6135 | 5.3000 | 6.1843 |
| $q_e$ Expt.(mg/g) | 1.9900 | 2.5380 | 2.7000 | 5.2187 | 5.2800 | 4.9830 |
| $R^2$ | 0.133 | 0.172 | 0.691 | 0.994 | 1.000 | 0.943 |
| TBRM | Co(II) | Ni(II) | Cd(II) | Pb(II) | Cr(III) | Cu(II) |
| $\frac{1}{(k_2\, q_e^2)}$ | 58.1070 | 68.4100 | 44.7530 | 0.0580 | 0.0183 | 1.4063 |
| $K_2$ (g/ mg min) | 0.0002 | 0.0002 | 0.0004 | 0.6267 | 1.9676 | 0.0272 |
| $q_e$ Calc. (mg/g) | 10.0503 | 9.4697 | 7.8802 | 5.2450 | 5.2700 | 5.1099 |
| $q_e$ Expt.(mg/g) | 3.7700 | 3.3800 | 3.7720 | 5.2395 | 5.2800 | 4.9960 |
| $R^2$ | 0.8051 | 0.8258 | 0.8019 | 1.0000 | 1.0000 | 0.9995 |
| TBFZ | Co(II) | Ni(II) | Cd(II) | Pb(II) | Cr(III) | Cu(II) |
| $\frac{1}{(k_2\, q_e^2)}$ | 20.7260 | 31.6600 | 26.9760 | 0.0939 | -0.0037 | 0.4375 |
| $K_2$ (g/ mg min) | 0.0007 | 0.0003 | 0.0007 | 0.3868 | -9.7263 | 0.0907 |
| $q_e$ Calc. (mg/g) | 8.3542 | 10.0908 | 7.0721 | 5.2470 | 5.2714 | 5.0201 |
| $q_e$ Expt.(mg/g) | 5.5088 | 5.1640 | 4.4890 | 5.2370 | 5.2720 | 4.9826 |
| $R^2$ | 0.9927 | 0.9757 | 0.9765 | 1.0000 | 1.0000 | 0.9999 |

**Table 3.9 Kinetic parameters for Cu(II), Pb(II), Cr(III), Co(II), Ni(II) and Cd(II), in TPW medium ` t' 5'-90'**

| TB | Co(II) | Ni(II) | Cd(II) | Pb(II) | Cr(III) | Cu(II) |
|---|---|---|---|---|---|---|
| $\frac{1}{(k_2\, q_e^2)}$ | 15.28 | 4.8041 | 11.933 | 0.2162 | 3.5768 | 1.4286 |
| $K_2$ (g/ mg min) | 0.024 | 0.0341 | 0.0639 | 0.7587 | 0.0064 | 0.0202 |
| $q_e$ Calc.(mg/g) | 1.6507 | 2.4691 | 1.1453 | 5.249 | 6.635 | 5.8893 |
| $q_e$ Expt.(mg/g) | 1.397 | 2.387 | 1.199 | 5.225 | 5.257 | 5.431 |
| $R^2$ | 0.9189 | 0.9442 | 0.9517 | 0.9996 | 0.9012 | 0.9781 |
| **TBRM** | **Co(II)** | **Ni(II)** | **Cd(II)** | **Pb(II)** | **Cr(III)** | **Cu(II)** |
| $\frac{1}{(k_2\, q_e^2)}$ | 13.603 | 6.415 | 11.434 | 0.044 | 0.0592 | 1.5072 |
| $K_2$ (g/ mg min) | 0.0063 | 0.0015 | 0.0077 | 0.8274 | 0.6053 | 0.0199 |
| $q_e$ Calc.(mg/g) | 3.4141 | 10.2413 | 3.3602 | 5.241 | 5.2826 | 5.7803 |
| $q_e$ Expt.(mg/g) | 2.759 | 3.78 | 2.874 | 5.231 | 5.27 | 5.4316 |
| $R^2$ | 0.7423 | 0.8489 | 0.7963 | 0.999 | 1.000 | 0.9896 |
| **TBFZ** | **Co(II)** | **Ni(II)** | **Cd(II)** | **Pb(II)** | **Cr(III)** | **Cu(II)** |
| $\frac{1}{(k_2\, q_e^2)}$ | 4.1699 | 2.9122 | 3.7156 | 0.0014 | 20.03 | 0.0042 |
| $K_2$ (g/ mg min) | 0.0081 | 0.0132 | 0.0122 | 26.0141 | 0.0018 | 8.1136 |
| $q_e$ Calc.(mg/g) | 5.4555 | 5.0942 | 4.6882 | 5.24 | 5.26 | 5.4171 |
| $q_e$ Expt.(mg/g) | 4.981 | 4.789 | 4.303 | 5.241 | 5.268 | 5.111 |
| $R^2$ | 0.9086 | 0.959 | 0.9661 | 1.0000 | 1.0000 | 1.0000 |

**Table 3.10 Kinetic parameters for Cu(II), Pb(II), Cr(III), Co(II), Ni(II) and Cd(II), TPW t' 90'-360'**

| TB | Co(II) | Ni(II) | Cd(II) | Pb(II) | Cr(III) | Cu(II) |
|---|---|---|---|---|---|---|
| $\frac{1}{(k_2\ q_e^2)}$ | 64.72 | 40.612 | 90.079 | 0.0111 | -0.0552 | 0.0139 |
| $K_2$ (g/ mg min) | 0 | 0.0003 | 0.0002 | 3.2861 | -0.6568 | 2.4172 |
| $q_e$ Calc.(mg/g) | 17.9856 | 9.6993 | 6.9444 | 5.236 | 5.252 | 5.4555 |
| $q_e$ Expt.(mg/g) | 4.573 | 5.17 | 3.093 | 5.232 | 5.25 | 5.431 |
| $R^2$ | 0.4082 | 0.4421 | 0.3849 | 1.0000 | 1.0000 | 0.9999 |
| TBRM | Co(II) | Ni(II) | Cd(II) | Pb(II) | Cr(III) | Cu(II) |
| $\frac{1}{(k_2\ q_e^2)}$ | 29.408 | 18.236 | 19.37 | -0.0193 | 0.0722 | 1.0898 |
| $K_2$ (g/ mg min) | 0.0007 | 0.001 | 0.0018 | -1.8964 | 0.4968 | 0.1639 |
| $q_e$ Calc.(mg/g) | 6.734 | 7.2307 | 5.3821 | 5.227 | 5.28 | 5.5991 |
| $q_e$ Expt.(mg/g) | 4.442 | 5.406 | 4.1639 | 5.229 | 5.28 | 5.4316 |
| $R^2$ | 0.9422 | 0.9655 | 0.9992 | 1.0000 | 1.0000 | 0.9997 |
| TBFZ | Co(II) | Ni(II) | Cd(II) | Pb(II) | Cr(III) | Cu(II) |
| $\frac{1}{(k_2\ q_e^2)}$ | 2.7525 | 7.8623 | 2.5461 | -0.0092 | -0.0172 | 0.0271 |
| $K_2$ (g/ mg min) | 0.0107 | 0.0019 | 0.0174 | -3.9617 | -2.0974 | 1.252 |
| $q_e$ Calc.(mg/g) | 5.8343 | 8.2034 | 4.7529 | 5.238 | 5.265 | 5.4289 |
| $q_e$ Expt.(mg/g) | 5.5440 | 6.7600 | 4.5029 | 5.239 | 5.266 | 5.427 |
| $R^2$ | 0.9985 | 0.9700 | 0.9997 | 1.0000 | 1.0000 | 1.0000 |

### 3.4.2 Adsorption isotherm studies and maximum adsorption determination

In adsorption studies, the modeling of equilibrium data is very essential for the purpose of industrial applications since critical information could be obtained to evaluate different adsorbents under different conditions and to be able to optimize experimental procedures **[54].** The Langmuir and Freundlcih models are the most employed isotherms models to evaluate the relationship between the isotherm parameters. The Langmuir model is based on the monolayer sorption onto a sorbent surface containing a limited number of adsorptive sites with uniform energies. On the other hand, the Freundlich model is used to determine sorption on heterogeneous surfaces and multilayer sorption with different energies. The linear forms of Langmuir and Freundlich equations are shown in equations 3.4 and 3.5, respectively:

$$\frac{C_e}{q_e} = \frac{1}{q_m} C_e + \frac{1}{b.q_m} \quad [3.4]$$

$$log\ q_e = log\ k_f + \frac{1}{n} log\ C_e \quad [3.5]$$

where $C_e$ is the equilibrium concentration of metal ions (mg/L), $q_e$ is the amount of metal ions adsorbed per gram of adsorbent at equilibrium at a given concentration, $q_m$ is the theoretical maximum adsorption capacity (mg/g), and b represents the Langmuir equilibrium constant related to energy of adsorption (L/mg). $K_f$ (mg/g) is the Freundlich constant, an approximate indicator of the adsorption intensity and the value of 1/n gives an indication on the favorability of an adsorption.

The results shown in **Figures 3.16 – 3.21** represent the effect of concentration on adsorption. From these Figures, the experimental adsorption capacities were extrapolated at the plateau and compared as shown in Tables 3.12- 3.13. As one could be seen from **Figures 3.17-3.22**, it is obvious that the equilibrium capacities ($q_e$) of the metal ions increased with increasing initial concentration until reaching equilibrium as indicated by the presence of plateau in the graphs. At low concentrations, there are significant numbers of adsorbing sites available for removal of the metal ions Cr, Cu, Cd, Co, Pb and Ni and thus there is sharp increase in $q_e$ (mg/g) at low concentrations. As the concentration increases the adsorbing site become saturated and unless capable to absorb any further ions. Secondly, the increase in adsorption capacity with increasing initial concentration of metal ions may be due to a high driving force for a mass transfer. Similar results were reported in the removal of $Pb^{2+}$ and $Cd^{2+}$ by sawdust. **[55]**.

The experimental adsorption capacities varied markedly with regards to the adsorbents in both SCS and TPW. To prevent precipitation, the experiment was conducted below the critical pH of each of the metal ions and this was done with single ions. From **Tables 3.11 and 3.12**, $Pb^{2+}$ had the highest adsorption capacities in all the adsorbents and in both SCS and TPW except Ni in SCS by TBFZ and in TPW by TB. The maximum adsorption capacity for Pb was estimated to 0.385, 0.681 and 0.678 mmol/g with TB, TBRM and TBFZ, respectively in SCS, whereas in TPW, the

capacities recorded were 0.386, 0.681 and 0.717 mmol/g, respectively. The high adsorption capacities for Pb may be attributed to its behavior as a soft acid since soft acids strongly interact with hard base to form complexes than hard and borderline acids. Also, it could be observed that the capacities of $Pb^{2+}$ have improved when TPW was spiked with $Pb^{2+}$. This improvement may be due to the high content of $SO_4^{2-}$ ions which combines with $Pb^{2+}$ ions to form insoluble sparingly $PbSO_4$ ($K_{sp} = 1.06 \times 10^{-8}$ ).

When comparing the adsorption capacities recorded as obtained in SCS and TPW media, it generally revealed a general remarkable improvement augmentation in adsorption capacities. For instance, with reference to Cu, the adsorption capacity increased by 14 % with TB, 51% with TBRM and 102% with TBFZ. The large increase in maximum adsorption capacity in TPW was also observed for Cd and Co. It is also noticed that this remarkable increase in adsorption capacity occurred only with the modified fly ash samples. With non – modified fly ash, the changes in different media were insignificant, except for Ni.

When the comparison is made between the pristine fly ash TB and modified fly ash TBRM and TBFZ, it is easy to conclude that the modified fly ash adsorbents have much improved adsorption capacity, especially for Pb, Ni, Cd, Cu, Cr. There is no indication that the TBFZ possesses a clear advantage over TBRM, sometime, one is better than the other and vice versa.

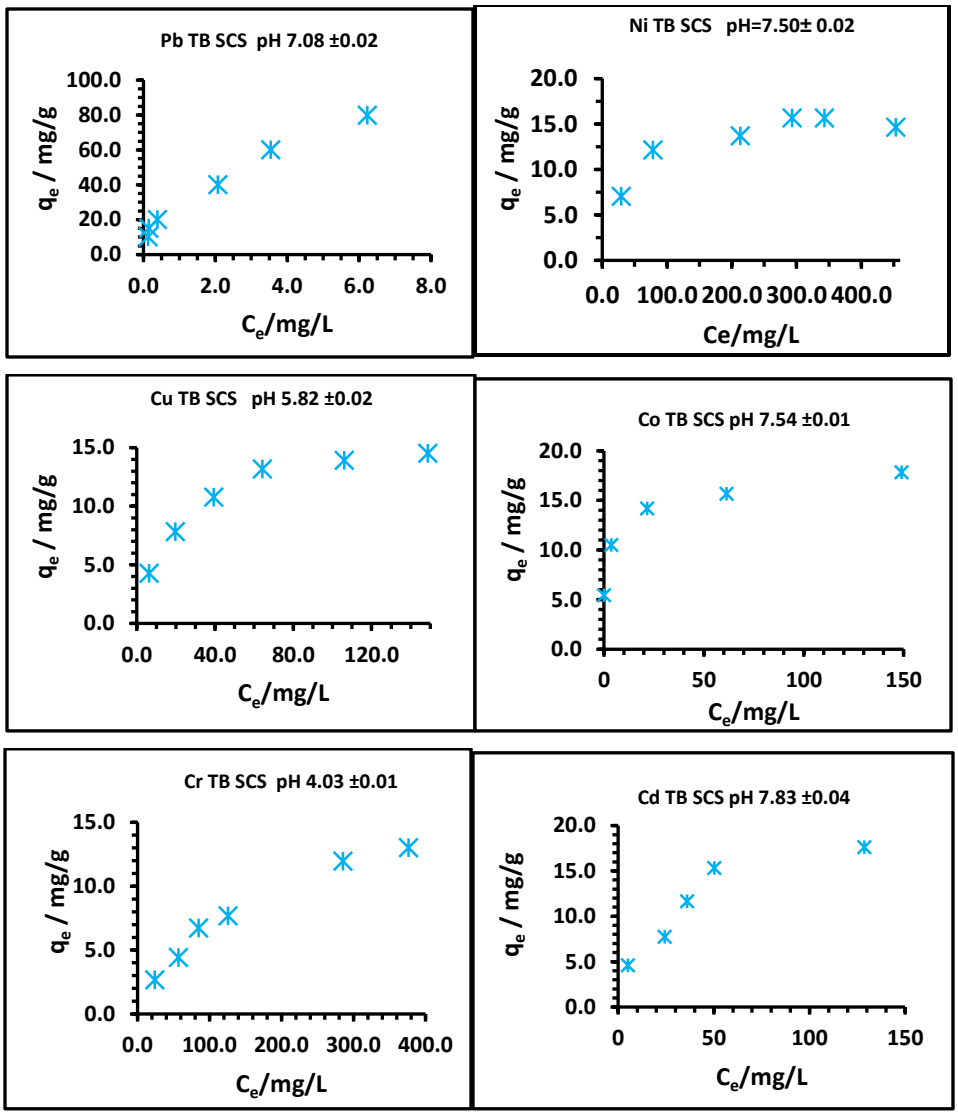


**Figure 3.16 Equilibrium isotherms of metal ions with TB performed with single element in batch mode: adsorbent: 0.50 g; initial concentration of metal ion: 50.0-300 mg/L; volume of aqueous solution: 50.0 mL; time: 2 h, shaking speed 120 rpm at 22 $^{0}$C.**

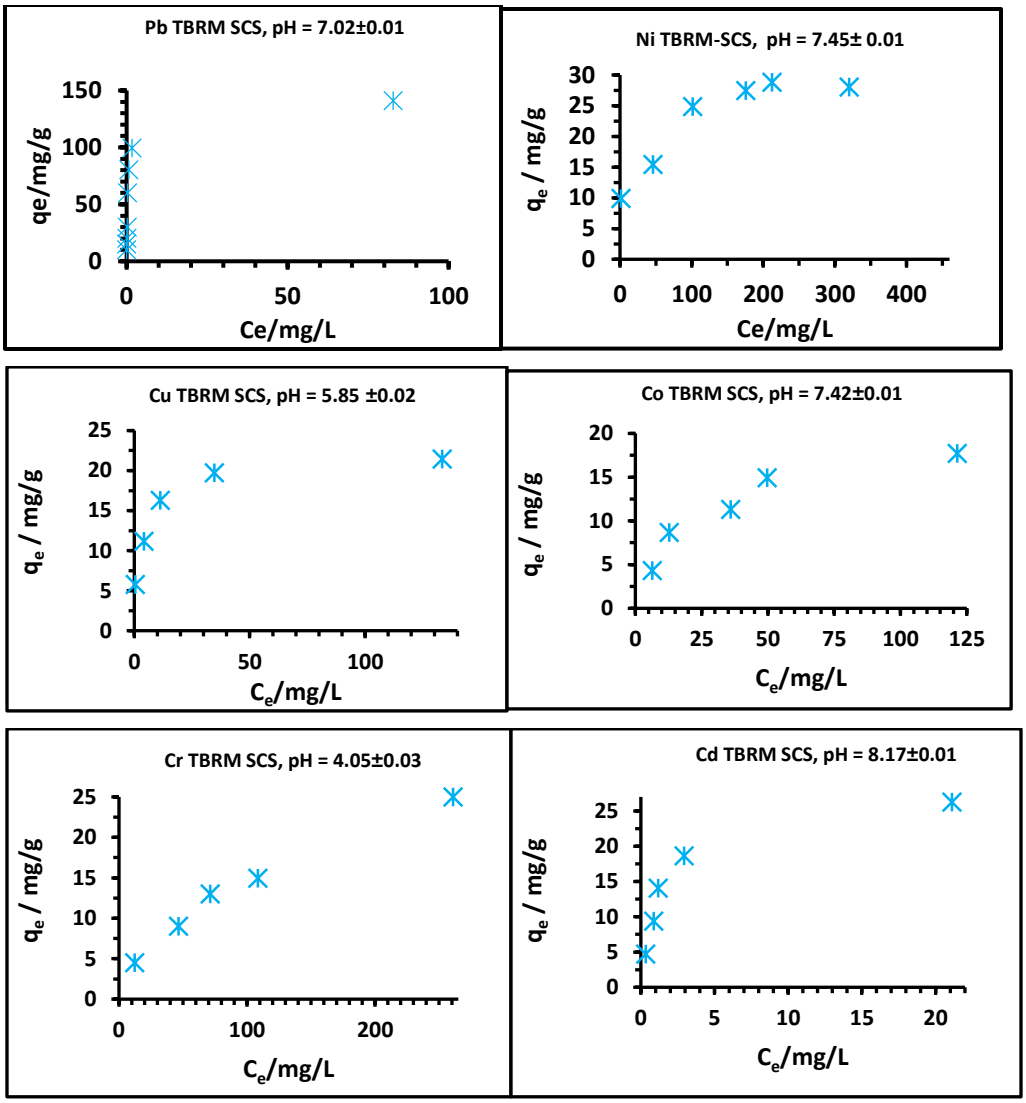


**Figure 3.17. Equilibrium isotherms of metal ions with TBRM performed with single element in batch mode: adsorbent: 0.50 g; initial concentration of metal ions: 50.0-300 mg/L; volume of aqueous solution: 50.0 mL; time: 2 h, shaking speed 120 rpm at 22 $^{0}$C.**

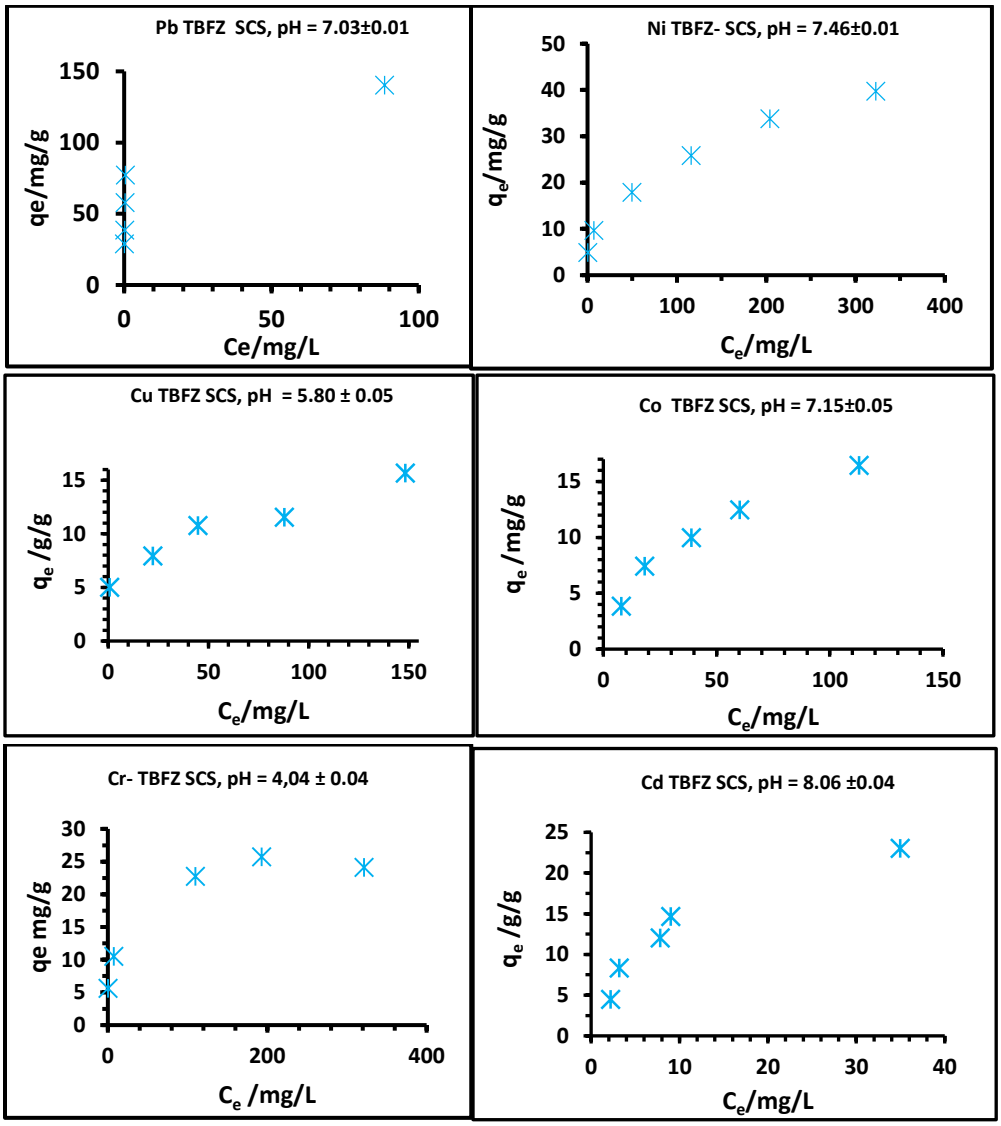


**Figure. 3.18. Equilibrium isotherms of metal ions by TBFZ performed with single element in batch mode: adsorbent: 0.50 g; initial concentration of metal ions: 50.0-400 mg/L each; volume of aqueous solution: 50.0 mL; time: 2 h; shaking speed: 120 rpm at 22 $^0$C.**

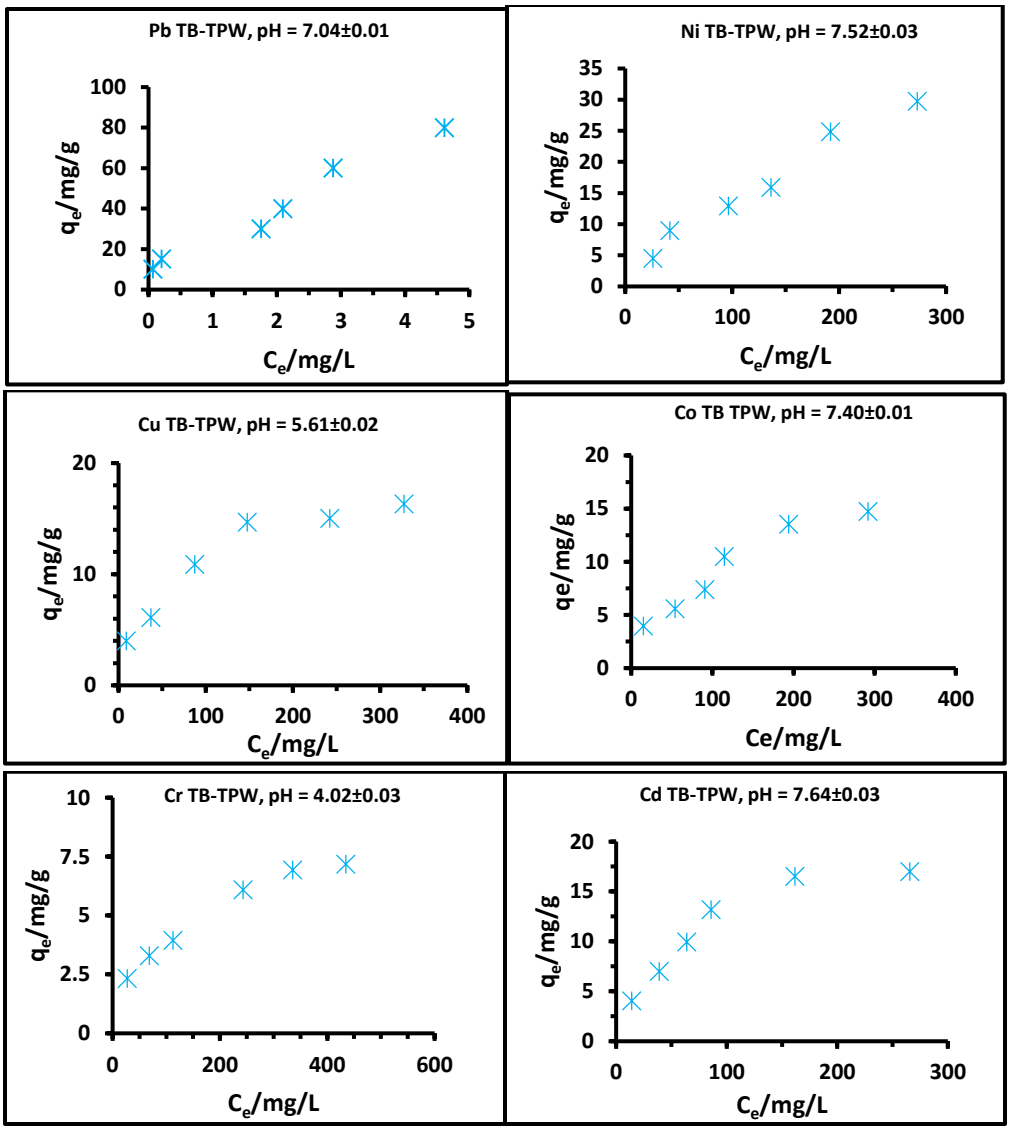


**Figure 3.19 Equilibrium isotherms of metal ions by TB performed with single element in batch mode: adsorbent: 0.50 g; initial concentration of metal ions: 50.0-800 mg/L; volume of aqueous solution: 50.0 mL; time: 2 h; shaking speed: 120 rpm at 22 $^{0}$C in TPW medium.**

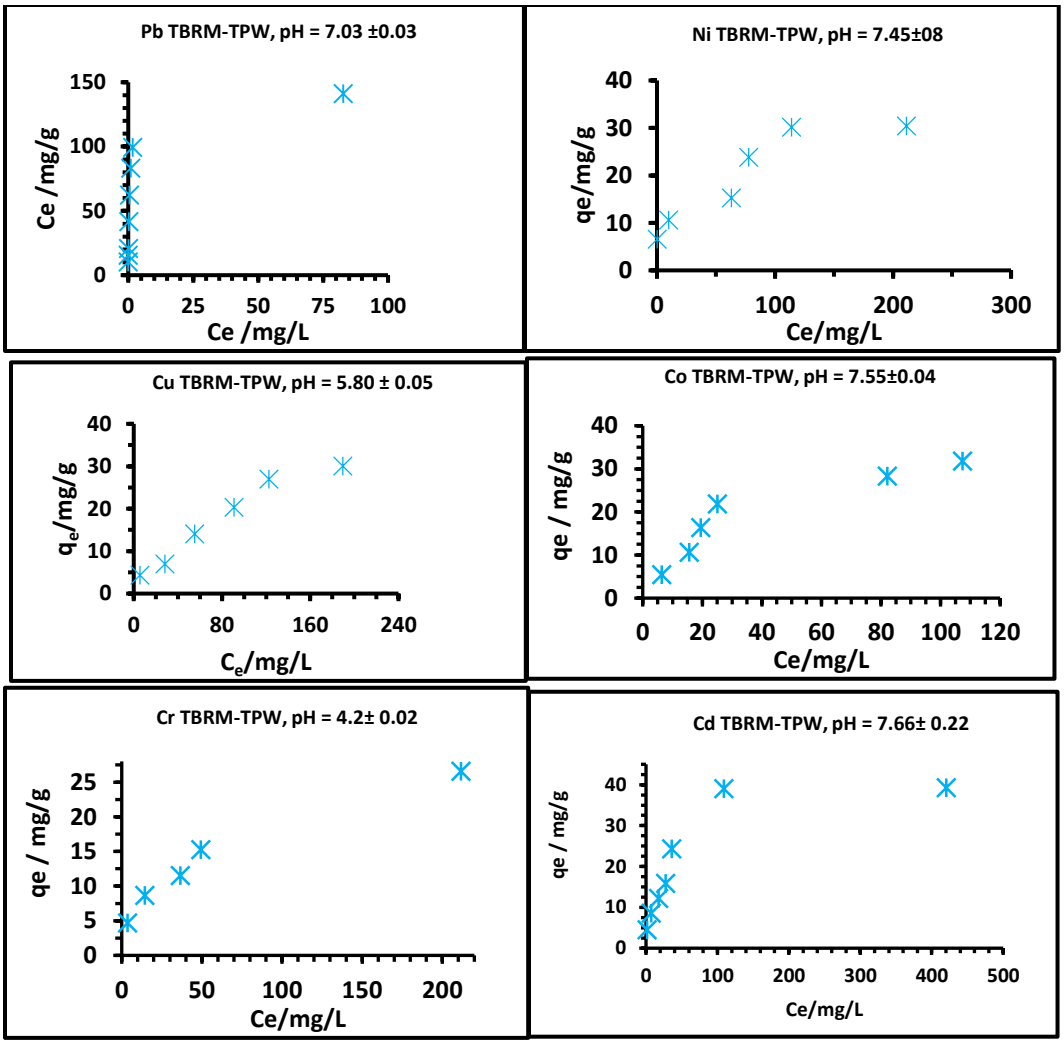


**Figure 3.20. Equilibrium isotherms of metal ions with TBRM performed with single element in batch mode: adsorbent: 0.50 g; initial concentration of metal ions: 50.0-400 mg/L: volume of aqueous solution: 50.0 mL; time: 2 h; shaking speed: 120 rpm at 22 $^0$C in TPW medium.**

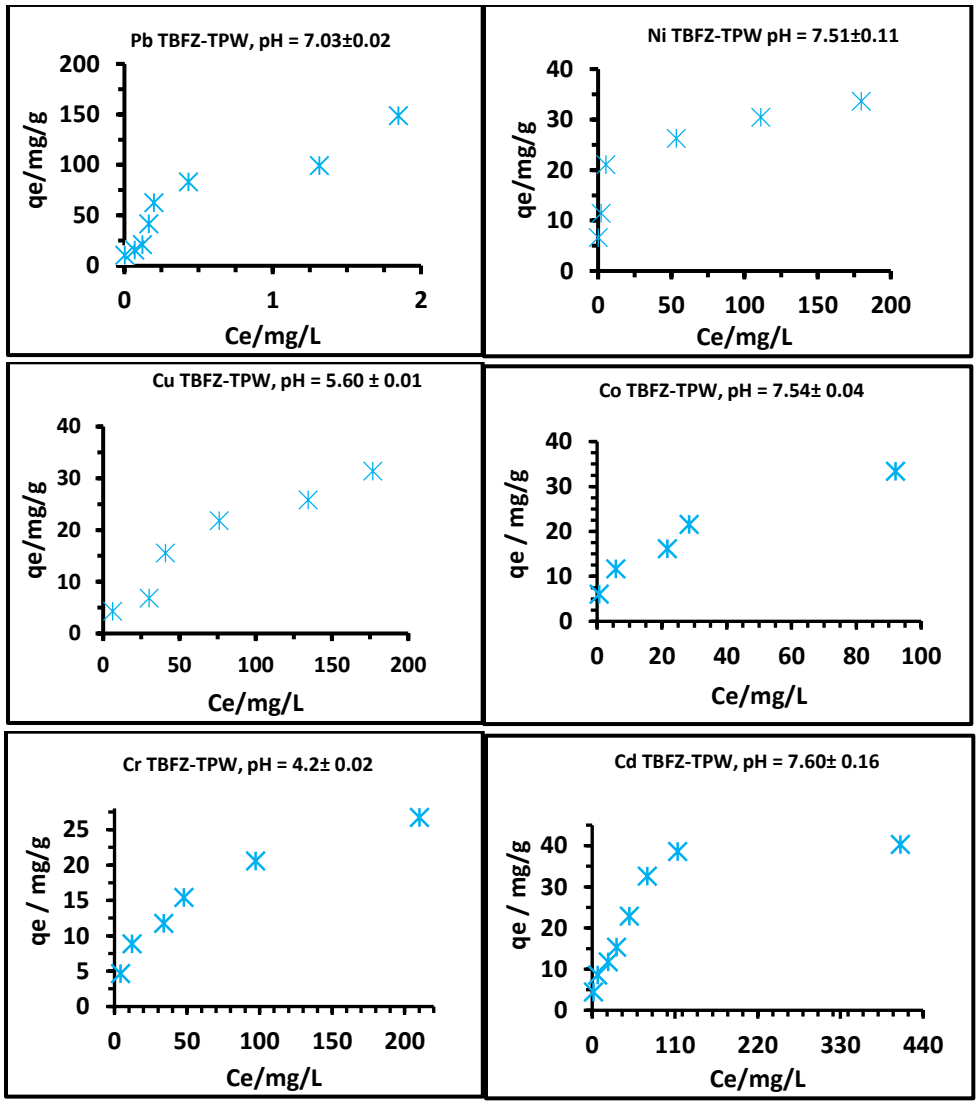


**Figure 3.21. Equilibrium isotherms of metal ions with TBFZ performed with single element in batch mode: Adsorbent: 0.50 g; initial concentration of metal ions: 50.0-800 mg/L; volume of metal ions solution: 50.0 mL; time: 2 h; shaking speed: 120 rpm at 22 $^{0}$C in TPW medium.**

**Table 3.11. Experimental maximum adsorption capacities in synthesized cocktail solution (SCS) medium**

| Sample ID | unit | Pb | Ni | Co | Cd | Cu | Cr |
|---|---|---|---|---|---|---|---|
| **TB** | pH | 7.08±0.02 | 7.40±0.02 | 7.42±0.01 | 7.83±0.04 | 5.82±0.02 | 4.03±0.01 |
| | mg/g | 79.7 | 15.2 | 17.8 | 17.6 | 14.52 | 13.02 |
| | mmol/g | 0.385 | 0.259 | 0.302 | 0.157 | 0.228 | 0.198 |
| **TBRM** | pH | 7.02±0.01 | 7.45±0.01 | 7.42±0.01 | 8.17±0.05 | 5.85±0.02 | 4.05±0.03 |
| | mg/g | 141 | 28.42 | 17.73 | 26.27 | 21.46 | 25.00 |
| | mmol/g | 0.681 | 0.484 | 0.301 | 0.234 | 0.31 | 0.481 |
| **TBFZ** | pH | 7.03±0.01 | 7.46±0.01 | 7.15±0.05 | 8.06±0.04 | 5.80±0.05 | 4.09±0.05 |
| | mg/g | 140.5 | 39.8 | 16.4 | 23.0 | 15.7 | 25.7 |
| | mmol/g | 0.678 | 0.678 | 0.278 | 0.205 | 0.247 | 0.494 |

**Table 3.12 Experimental maximum adsorption capacities in tailing pond water (TPW) medium**

| Sample ID | unit | Pb | Ni | Co | Cd | Cu | Cr |
|---|---|---|---|---|---|---|---|
| **TB** | pH | 7.08±0.02 | 7.52±0.03 | 7.40±0.01 | 7.83±0.04 | 5.61±0.02 | 4.02±0.03 |
| | mg/L | 79.9 | 29.7 | 14.7 | 17.0 | 16.3 | 7.2 |
| | mmol/L | 0.386 | 0.506 | 0.249 | 0.151 | 0.257 | 0.138 |
| **TBRM** | pH | 7.03±0.03 | 7.45±0.08 | 7.55±0.04 | 7.66±0.22 | 5.60±0.01 | 4.02±0.03 |
| | mg/L | 141 | 30.4 | 31.8 | 39.3 | 30.1 | 26.6 |
| | mmol/L | 0.681 | 0.518 | 0.54 | 0.35 | 0.468 | 0.512 |
| **TBFZ** | pH | 7.03±0.02 | 7.51±0.11 | 7.54±0.04 | 7.60±0.16 | 5.61±0.01 | 4.16±0.08 |
| | mg/L | 148 | 33.6 | 33.4 | 40.3 | 31.3 | 26.7 |
| | mmol/L | 0.717 | 0.572 | 0.567 | 0.359 | 0.50 | 0.514 |

The comparison of adsorption capacities among TB, TBRM and TBFZ in **Tables 3.11 and 3.12** generally shows improvement from the pristine TB to the modified adsorbents TBRM and TBFZ in both SCS and TPW solutions. When TB, TBRM and TBFZ were applied to remove Pb from SCS, the experimental adsorption capacity increased from 79.70 mg/g in TB to 141.0 and 140.5 mg/g, respectively for TBRM and TBFZ, respectively constituting about 77 and 76 % improvement. For Ni, the adsorption capacity improved from 15.2 mg/g to 28.42 and 39.80 mg/g for TBRM and TBFZ, respectively which is about 87% and 162%, respectively. Similar trends

were observed for all the metal ions in the TPW except for $Co^{2+}$ and $Cr^{3+}$ which revealed decreases in adsorption capacity regarding the application of TB as adsorbent; the reduction in adsorption capacity for $Co^{2+}$ was 17 % and that of $Cr^{3+}$ was 45 % for TB. The reason in the improved capacities could be attributed to the increase in surface area, pore volume and enhanced cation exchange capacities in TBRM and TBFZ, respectively.

Langmuir and Freundlich models' equations 3.6 and 3.7 respectively were applied to the data to determine the calculated adsorption capacities and other parameters. The values of $q_m$ calculated ($mg \cdot g^{-1}$) and b ($mg^{-1}$) can be determined from the linear plot of $C_e/q_e$ versus $C_e$. Additionally, by plotting log $q_e$ versus log $C_e$, values of $K_f$ and n can be determined from the slope.

The calculated and experimental adsorption capacities were also compared as shown in **Tables 3.13 – 3.18**. The adsorption parameters were calculated considering the Langmuir's equation (3.6) and Freundlich equation (3.7). Both models provide good fit for the adsorption process with good correlation coefficients in either the Langmuir or Freundlich model. Similar results were reported by Visa and Chelaru. **[35].** these results support the assumption that electrostatic attractions govern the monolayer adsorption on substrates that are very heterogeneous in nature. Observations from **Tables 3.13 - 3.18** revealed that most of the calculated maximum adsorption capacities from the isotherm investigation agree well with the experimental values or are slightly higher. However, an exceptionally higher difference in the calculated and experimental adsorption capacity (34 mg/g) was observed in **Table 3.16** for Ni in TPW with TB as adsorbent. Other higher values were recorded for Co, Pb and Cd in TPW with TB being the adsorbent.

Similar discrepancies were recorded for both TBRM and TBFZ all in TPW. This discrepancy may be due to the high anion and cation content of the TPW. Also, the discrepancies in the values regarding TPW may be due to the complex nature of TPW.

**Table 3.13 Adsorption isotherm parameters, TB – SCS**

| | Langmuir | | | | | | Freundlich | | |
|---|---|---|---|---|---|---|---|---|---|
| | | $1/q_m$ | $q_m$ exp. | $q_m$ calc. | $1/q_i$ b | b | $R^2$ | $K_f$ | |
| | | g $(mg)^{-1}$ | mg $g^{-1}$ | mg $g^{-1}$ | | $L(mg)^{-1}$ | | mg $g^{-1}$ | |
| **Co(II)** | 0.997 | 0.06 | 17.80 | 18.02 | 0.213 | 0.261 | 0.998 | 0.94 | 6.8 |
| **Ni(II)** | 0.991 | 0.06 | 15.20 | 16.29 | 1.854 | 0.033 | 0.87 | 0.50 | 3.7 |
| **Cu(II)** | 0.999 | 0.06 | 14.52 | 16.47 | 1.174 | 0.052 | 0.953 | 0.36 | 2.5 |
| **Pb(II)** | 0.924 | 0.01 | 79.69 | 89.29 | 0.015 | 0.737 | 0.979 | 1.50 | 2.1 |
| **Cd(II)** | 0.960 | 0.05 | 17.60 | 21.41 | 1.301 | 0.036 | 0.936 | 0.35 | 1.7 |
| **Cr(III)** | 0.987 | 0.05 | 13.02 | 18.52 | 8.655 | 0.006 | 0.983 | 0.35 | 1.7 |

$q_m$ exp. – the max. adsorption capacity obtained experimentally

$q_m$ cal. - the max. adsorption capacity obtained Langmuir model fitting

**Table 3.14 Adsorption isotherm parameters, TBRM - SCS**

| **Metal Ion** | Langmuir | | | | | | Freundlich | | |
|---|---|---|---|---|---|---|---|---|---|
| | | $1/q_m$ | $q_m$ exp. | $q_m$ calc. | $1/q_m$ b | b | $R^2$ | $K_f$ | n, 1/slope |
| | | g $(mg)^{-1}$ | mg $g^{-1}$ | mg $g^{-1}$ | | $L(mg)^{-1}$ | | mg $g^{-1}$ | |
| **Co(II)** | 0.989 | 0.047 | 17.73 | 21.14 | 1.122 | 0.053 | 0.919 | 0.356 | 1.5 |
| **Ni(II)** | 0.985 | 0.033 | 28.35 | 30.12 | 0.665 | 0.050 | 0.912 | 0.941 | 4.7 |
| **Cu(II)** | 1.00 | 0.046 | 21.46 | 21.93 | 0.148 | 0.308 | 0.937 | 0.884 | 4.4 |
| **Pb(II)** | 1.00 | 0.007 | 141 | 142.86 | 0.005 | 1.373 | 0.923 | 1.916 | 1.5 |
| **Cd(II)** | 0.999 | 0.036 | 26.27 | 28.17 | 0.045 | 0.787 | 0.845 | 1.018 | 2.6 |
| **Cr(III)** | 0.94 | 0.029 | 25.00 | 34.84 | 3.338 | 0.009 | 0.995 | 0.039 | 1.8 |

$q_m$ exp. – the max. adsorption capacity obtained experimentally

$q_m$ cal. - the max. adsorption capacity obtained Langmuir model fitting

**Table 3.15 Adsorption isotherm parameters, TBFZ -SCS**

| **Metal Ion** | Langmuir | | | | | | Freundlich | | |
|---|---|---|---|---|---|---|---|---|---|
| | | $1/q_m$ | $q_m$ exp. | $q_m$ calc. | $1/q_m$b | b | $R^2$ | $K_f$ | n,1/slope |
| | | g $(mg)^{-1}$ | mg $g^{-1}$ | mg $g^{-1}$ | | L $(mg)^{-1}$ | | mg $g^{-1}$ | |
| **Co(II)** | 0.986 | 0.046 | 16.4 | 21.69 | 0.88 | 0.052 | 0.936 | 0.92 | 4.2 |
| **Ni(II)** | 0.952 | 0.024 | 39.8 | 41.49 | 0.408 | 0.059 | 0.961 | 0.82 | 4.3 |
| **Cu(II)** | 0.946 | 0.062 | 15.7 | 16.13 | 1.073 | 0.058 | 0.93 | 0.7 | 5.0 |
| **Pb(II)** | 1.00 | 0.007 | 140.5 | 140.85 | 0.005 | 1.365 | 0.973 | 2.12 | 1.1 |
| **Cd(II)** | 0.984 | 0.033 | 23.0 | 30.12 | 0.352 | 0.094 | 0.91 | 0.57 | 1.8 |
| **Cr(III)** | 0.96 | 0.039 | 25.7 | 25.97 | 7.184 | 0.005 | 0.882 | 0.88 | 5.1 |

$q_m$ exp. – the max. adsorption capacity obtained experimentally

$q_m$ cal. - the max. adsorption capacity obtained Langmuir model fitting

**Table 3.16. Adsorption isotherm parameters, TB -TPW**

| Metal Ion | Langmuir | | | | | | Freundlich | | |
|---|---|---|---|---|---|---|---|---|---|
| | $R^2$ | $1/q_m$ g $(mg)^{-1}$ | $q_m$ exp. mg $g^{-1}$ | $q_m$ Cal. mg $g^{-1}$ | $1/q_m$ b | b $L(mg)^{-1}$ | $R^2$ | $K_f$ mg $g^{-1}$ | n, (1/slope) |
| **Co(II)** | 0.915 | 0.041 | 14.7 | 24.27 | 4.038 | 0.017 | 0.943 | 0.02 | 2.1 |
| **Ni(II)** | 0.735 | 0.016 | 29.7 | 63.69 | 5.229 | 0.006 | 0.966 | 0.36 | 1.3 |
| **Cu(II)** | 0.983 | 0.053 | 16.3 | 18.9 | 2.93 | 0.021 | 0.965 | 0.19 | 2.4 |
| **Pb(II)** | 0.67 | 0.011 | 79.9 | 87.72 | 0.017 | 0.745 | 0.916 | 1.52 | 2.3 |
| **Cd(II)** | 0.983 | 0.046 | 17.0 | 21.93 | 3.111 | 0.019 | 1.00 | 0.04 | 1.9 |
| **Cr(III)** | 0.982 | 0.114 | 7.2 | 8.77 | 12.312 | 0.011 | 0.991 | 0.26 | 2.3 |

**Table 3.17 Adsorption isotherm parameters, TBRM -TPW**

| Metal Ion | Langmuir | | | | | | Freundlich | | |
|---|---|---|---|---|---|---|---|---|---|
| | $R^2$ | $1/q_m$ g $(mg)^{-1}$ | $q_m$ exp. mg $g^{-1}$ | $q_m$ Cal. mg $g^{-1}$ | $1/q_m$ b | b $L(mg)^{-1}$ | $R^2$ | $K_f$ mg $g^{1}$ | n, 1/slope |
| **Co(II)** | 0.96 | 0.02 | 31.8 | 42.55 | 0.87 | 0.027 | 0.886 | 0.37 | 1.7 |
| **Ni(II)** | 0.903 | 0.03 | 30.4 | 33.00 | 0.781 | 0.039 | 0.87 | 0.91 | 4.4 |
| **Cu(II)** | 0.837 | 0.02 | 30.19 | 42.37 | 2.138 | 0.011 | 0.92 | 0.88 | 4.4 |
| **Pb(II)** | 1.00 | 0.01 | 141.05 | 142.86 | 0.004 | 1.842 | 0.938 | 1.87 | 2.4 |
| **Cd(II)** | 0.992 | 0.02 | 39.3 | 42.37 | 0.678 | 0.035 | 0.93 | 0.59 | 2.3 |
| **Cr(III)** | 0.921 | 0.02 | 26.66 | 40.16 | 0.769 | 0.032 | 0.979 | 0.45 | 2.5 |

**Table 3.18. Adsorption isotherm parameters, TBFZ -TPW**

| Metal Ion | Langmuir | | | | | | Freundlich | | |
|---|---|---|---|---|---|---|---|---|---|
| | $R^2$ | $1/q_m$ g $(mg)^{-1}$ | $q_m$ exp. mg $g^{-1}$ | $q_m$ Cal. mg $g^{-1}$ | $1/q_m$ b | b $L(mg)^{-1}$ | $R^2$ | $K_f$ mg $g^{-1}$ | |
| **Co(II)** | 0.952 | 0.029 | 33.4 | 34.48 | 0.379 | 0.077 | 0.979 | 0.84 | 3.1 |
| **Ni(II)** | 0.993 | 0.03 | 33.6 | 33.44 | 0.159 | 0.188 | 0.952 | 1.09 | 5.2 |
| **Cu(II)** | 0.980 | 0.025 | 31.78 | 39.84 | 1.43 | 0.018 | 0.99 | 0.25 | 1.8 |
| **Pb(II)** | 0.842 | 0.006 | 148.64 | 166.67 | 0.003 | 2.069 | 0.843 | 1.96 | 0.7 |
| **Cd(II)** | 0.983 | 0.023 | 40.32 | 44.44 | 0.847 | 0.027 | 0.935 | 0.54 | 0.7 |
| **Cr(III)** | 0.975 | 0.033 | 26.7 | 30.77 | 1.283 | 0.025 | 0.986 | 0.4 | 2.5 |

$q_m$ exp. – the max. adsorption capacity obtained experimentally

$q_m$ cal. - the max. adsorption capacity obtained Langmuir model fitting

The values of n in all **Tables 3.13 - 3.18** are between 0.7- 6.8 which indicates the favourability of the adsorption process on all the adsorbents: TB, TBRM and TBFZ in both SCS and TPW.

The elemental composition of TB and TBFZ before and after adsorption isotherm analysis was obtained with SEM–EDS for qualitative purposes. The SEM images with the qualitative spectra are shown in **Figures 3.4(a) and 3.5(b)**. It was observed that no peak of the given metal ion $Cu^{2+}$, $Cr^{3+}$, $Pb^{2+}$, $Co^{2+}$, $Cd^{2+}$ and $Ni^{2+}$ was identified on the surface of the adsorbents before adsorption. However, peaks of each of the metal ions were identified on the surface of the adsorbents after adsorption has occurred. The presence of the ions in the spectra is a confirmation of adsorption of the metal ions on the surface of TB and TBFZ since SEM-EDS analyzes samples in the top few µm of the material. Also, a comparison of SEM images before and after adsorption reveals morphological changes in the samples after adsorption. It was observed that the irregular shaped particles are partially covered by precipitates and complexes formed by the metal ions.

### 3.4.3 Adsorption mechanisms and XPS results

The functional oxidized groups present on the surface of fly ash are $SiO_2$, $Al_2O_3$, $Fe_2O_3$ and other oxides as presented in **Table 3.3**. The surface of silica always has the tendency to attract metal ions **[56]**. The central ion found in silicates ($Si^{4+}$) has very significant affinity for electrons: thus, the oxygen atoms that surround the silicon ions have low basicity, rendering the silica surface to behave as a weak acid. The oxygen atoms attached to the silica surface are free to react with $H_2O$ leading to the formation of silanol (Si-OH groups). These silanol groups influence the charge on the surface of silica with respect to pH. In very acidic medium or low pH, positively charged silica surface is generated, and at high pH values, there is prevalence of negatively charged silica surface.

The surface charge of iron and aluminum oxides behave similarly as silica depending on the pH of the solution. The aqueous solutions of a synthesized cocktail solution used in the adsorption experiments were normally very acidic and with pH around 2.8, whereas the adsorbents were alkaline in nature. When mixing the two, the pH of the aqueous phase in an adsorption system will increase with time. As a result of that silica, alumina and iron were likely to produce negative charges at an active sites on the surface of the fly ash as shown in equations [3.6] and [3.7], which then allow metals ($M^{n+}$) and metal hydroxides (($M(OH)_2$) to form complexes at the surface as demonstrated in equations [3.8], [3.9] and [3.10] as indicated in **[57-58]**.

$$\equiv SiOH + OH^- \rightarrow \equiv SiO^- + H_2O \quad [3.6]$$

$$\equiv AlOH + OH^- \rightarrow \equiv AlO^- + H_2O \quad [3.7]$$

$$2(\equiv SiO^-) + M^{2+} \rightarrow (\equiv Si\text{-}O)_2M \quad [3.8]$$

$$2(\equiv AlO^-) + M^{2+} \rightarrow (\equiv Al\text{-}O)_2M \quad [3.9]$$

$$XO^- + M(OH)_2 \rightarrow \quad XO\text{-}M(OH)_2^- \quad [3.10]$$

where $XO^-$ are the free surface sites on fly ash with X being Si, Al, Fe, etc.

Figure 3.22 represents the XPS spectra of TBFZ after the adsorption of three selected metal cations namely $Cu^{2+}$, $Ni^{2+}$ and $Pb^{2+}$ in single element adsorption. Binding energy peaks for $Cu_{2p}$, $Ni_{2p}$ and $Pb_{4f}$ appeared at 935.48, 856.46 and 138.80 eV respectively whereas none of the selected metal ions were observed in the control TBFZ. This results further confirms the adsorption of these metal ions on the surface of the adsorbents since XPS techniques are employed to detect elements that are present within the top 1-12nm of the surface of the sample. The XPS data also revealed high concentrations of Si and Al also confirming the abundance of these atoms as proven in **Table 3.3**.

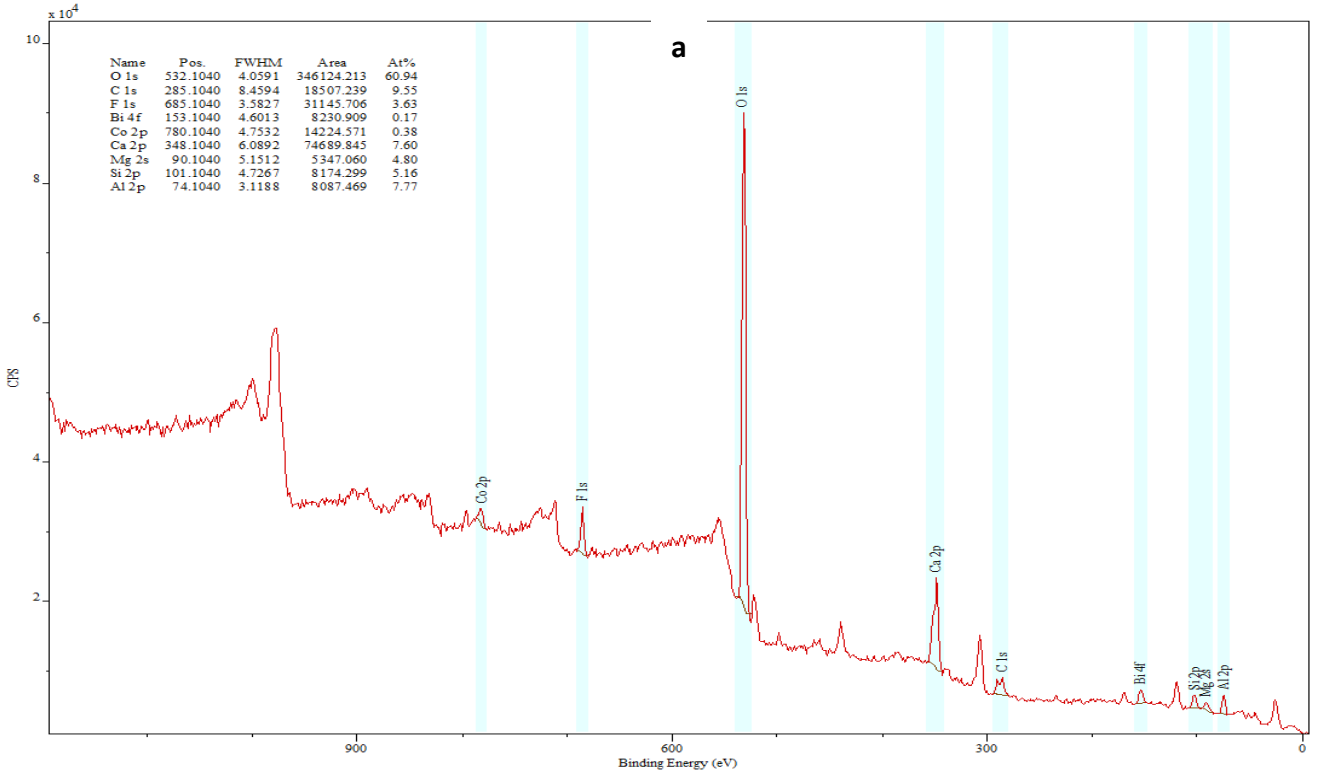
a
x 10^4
CPS
Binding Energy (eV)
Name Pos. FWHM Area At%
O 1s 532.1040 4.0591 346124.213 60.94
C 1s 285.1040 8.4594 18507.239 9.55
F 1s 685.1040 3.5827 31145.706 3.63
Bi 4f 153.1040 4.6013 8230.909 0.17
Co 2p 780.1040 4.7532 14224.571 0.38
Ca 2p 348.1040 6.0892 74689.845 7.60
Mg 2s 90.1040 5.1512 5347.060 4.80
Si 2p 101.1040 4.7267 8174.299 5.16
Al 2p 74.1040 3.1188 8087.469 7.77
O 1s
Co 2p
F 1s
Ca 2p
C 1s
Bi 4f
Si 2p
Mg 2s
Al 2p

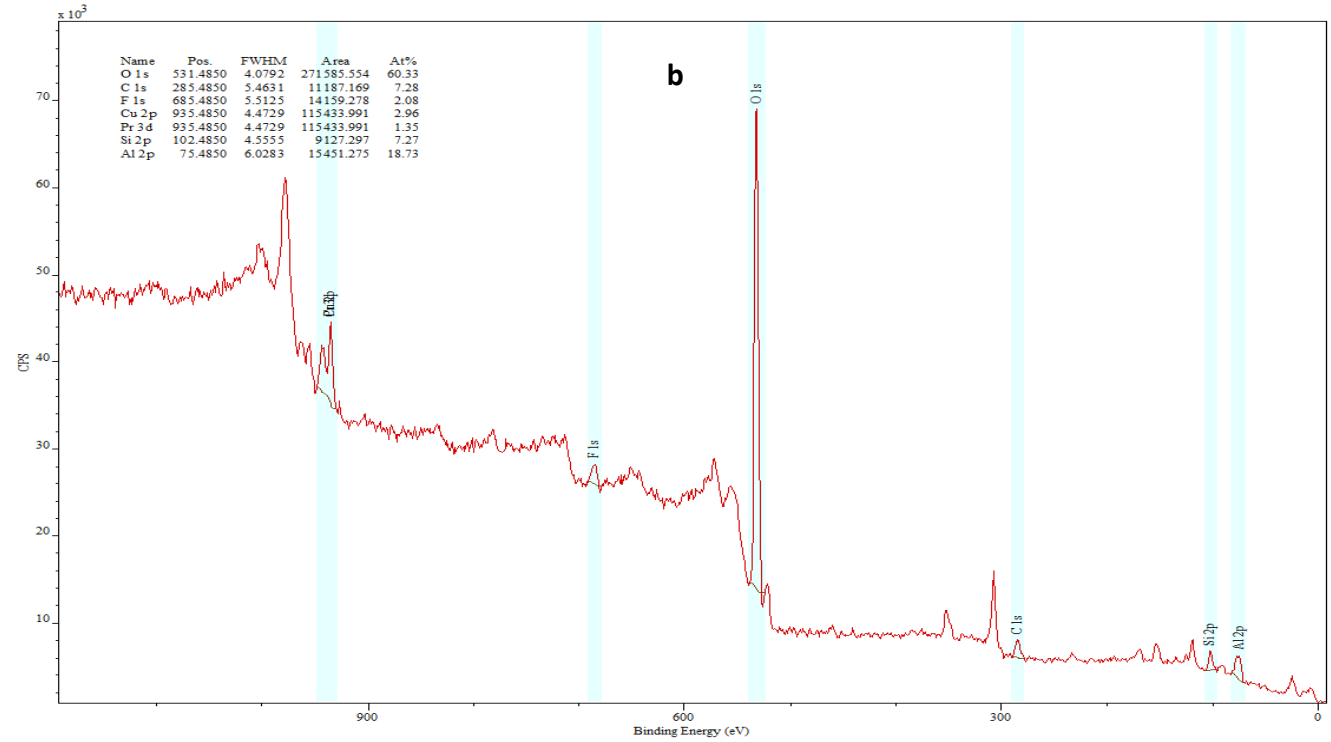
b
x 10^3
CPS
Binding Energy (eV)
Name Pos. FWHM Area At%
O 1s 531.4850 4.0792 271585.554 60.33
C 1s 285.4850 5.4631 11187.169 7.28
F 1s 685.4850 5.5125 14159.278 2.08
Cu 2p 935.4850 4.4729 115433.991 2.96
Pr 3d 935.4850 4.4729 115433.991 1.35
Si 2p 102.4850 4.5555 9127.297 7.27
Al 2p 75.4850 6.0283 15451.275 18.73
O 1s
F 1s
C 1s
Si 2p
Al 2p

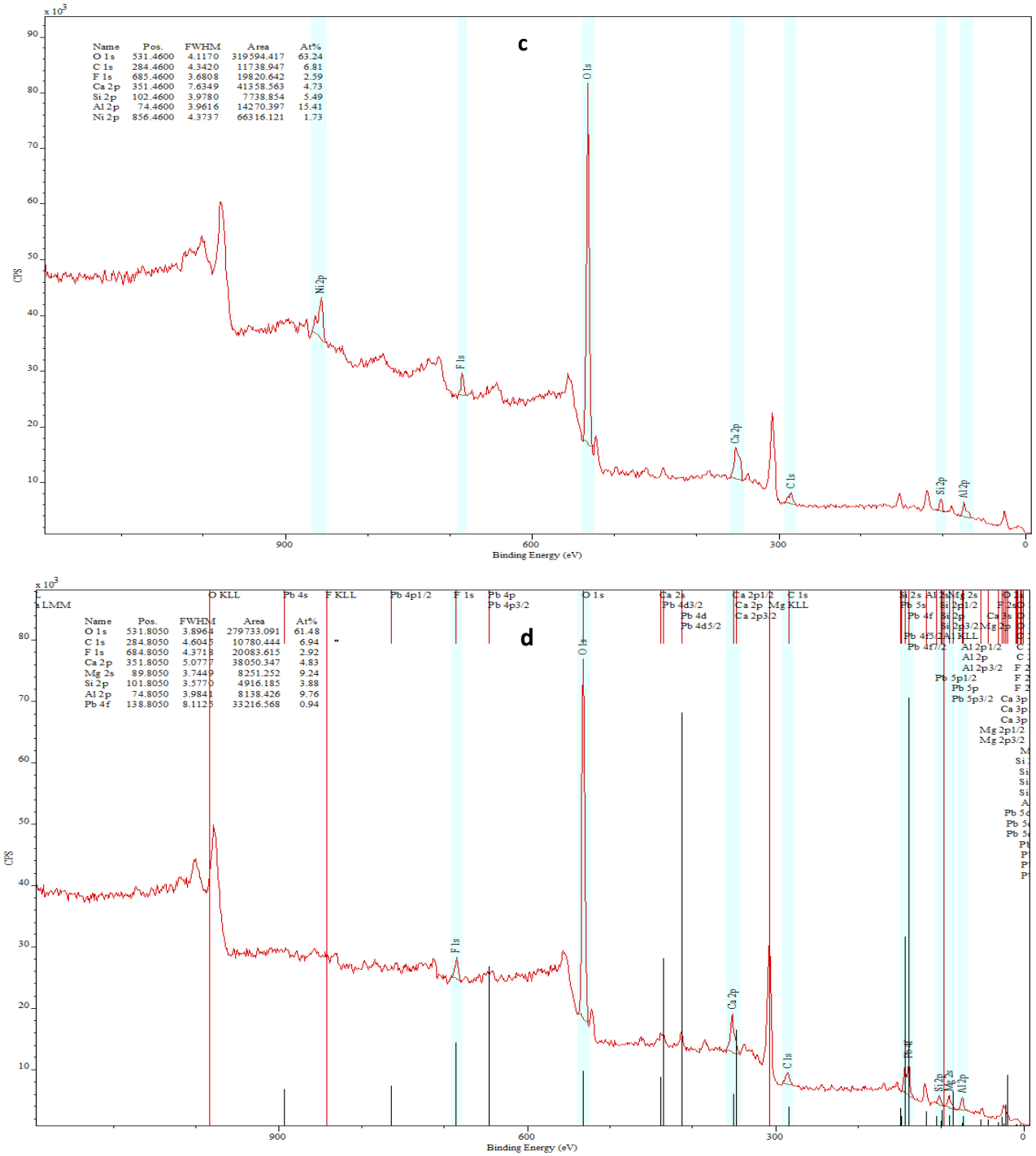


**Figure 3.22. XPS spectra of metal ions with TBFZ performed in batch mode: Adsorbent: 0.50 g; volume of metal ions solution: 50.0 mL; time: 2h; shaking speed: 120 rpm at 22 $^{0}$C in TPW medium**

(a) **TBFZ; (b) TBFZ with 500 mg/L Cu; (b) TBFZ with 400 mg/L Ni and (d) TBFZ with 600mg/L Pb (for experimental details see 2.6.6)**

### 3.4.4 Studies on adsorption thermodynamic properties of Cu and Ni on TBFZ

Adsorption studies were performed at four different temperatures in an initial concentration range of 50.0-500 mg/L for Ni and Cu (2.6.7). Cu and Ni were selected because these two ions are present at a much larger concentration in the Vale tailing pond water than any other metals, and also because they have demonstrated different removal behaviour - one represents the fast removal and another the slow removal group. Experimental results are shown in **Figures 3.23 and 3.24**. The results indicate a general increase in adsorption capacity with temperature with an exception for Ni at T=295.15K which could be due to an experimental error. The results suggest the adsorption of Ni and Cu onto TBFZ is endothermic.

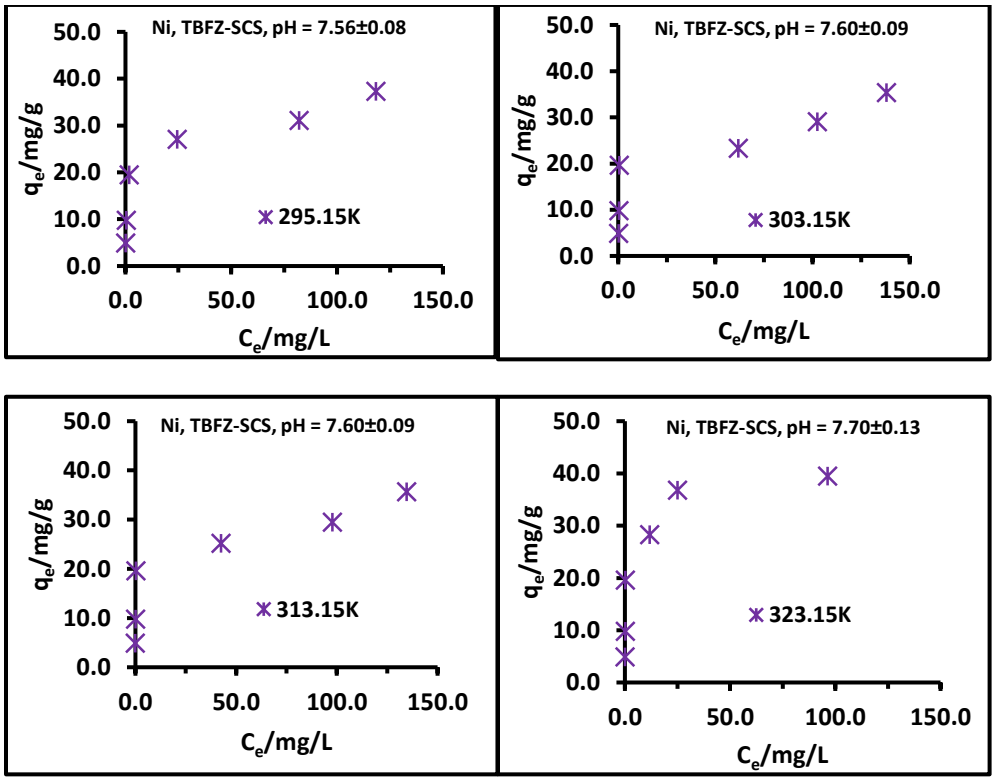


**Figure 3.23. Adsorption isotherms of Ni ion on TBFZ at different temperature performed in batch mode: adsorbent: 0.50 g; initial concentration: 50.0-500 mg/L; volume of aqueous solution: 50.0 mL; time: 2 h, shaking speed 120 rpm.**

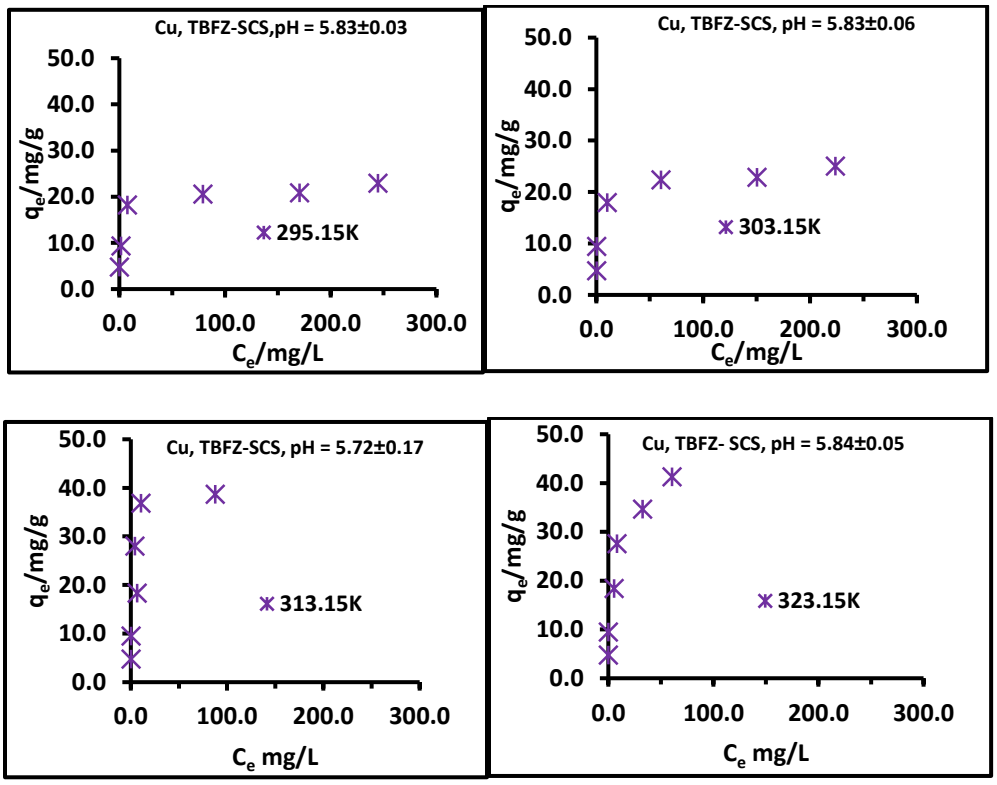


**Figure 3.24. Adsorption isotherms of Ni ion on TBFZ at different temperature performed in batch mode. Adsorbent: 0.50 g; initial concentration: 50.0-500 mg/L; volume of aqueous solution: 50.0 mL; time: 2 h, shaking speed 120 rpm.**

**Table 3.19** presents the experimental maximum adsorption capacity and the value calculated based on the Langmuir model. The two sets of data are close to each other. At high temperature, there is increase in kinetic energy of the ions and this facilitate the movement of metal ions from aqueous phase to the solid phase leading to an increase in adsorption capacity.

**Table 3.19 Calculated and experimental adsorption capacities on TBFZ at different temperatures.**

| | Ni | | Cu | |
|---|---|---|---|---|
| T | $q_m$ exp. | $q_m$ calc. | $q_m$ exp. | $q_m$calc. |
| K | mg/g | mg/g | mg/g | mg/g |
| 295.15 | 37.283 | 37.28 | 22.905 | 22.47 |
| 303.15 | 35.315 | 32.79 | 25.031 | 24.69 |
| 313.15 | 35.663 | 33.78 | 38.639 | 39.53 |
| 323.15 | 39.497 | 39.84 | 41.300 | 41.84 |

### 3.4.5 Thermodynamic parameters

The adsorption thermodynamic properties, such as Gibbs free energy change (ΔG°), change in entropy (ΔS°) and enthalpy (ΔH°), were determined based the following equations for nickel and copper with TBFZ as adsorbent:

$$\Delta G = - RT \ln q_m \quad [3.11]$$

$$\Delta G° = \Delta H° - T\Delta S° \quad [3.12]$$

where R is the gas constant (8.314 $J \cdot mol^{-1} \cdot K^{-1}$), T is the absolute temperature in Kelvin, $q_m$ is calculated from the Langmuir model (**Figures 3.23 and 3.24**). The ΔG at different temperature can be calculated from the $q_m$ in equation [3.11]. Once the ΔG is found, the adsorption standard entropy ΔS° and enthalpy ΔH° can be obtained from the slope and intercept of plot of ΔG° versus T as shown in **Figure 3.25**. Similar results was reported by Yuem Bing et al. **[59]**. The results are presented in **Table 3.20**. The higher the temperature, the more negative the standard Gibbs free energy (ΔG°) from -7.64 to -10.03. kJ/mol, indicating that the adsorption process was feasible as well as spontaneous with increase in temperature.

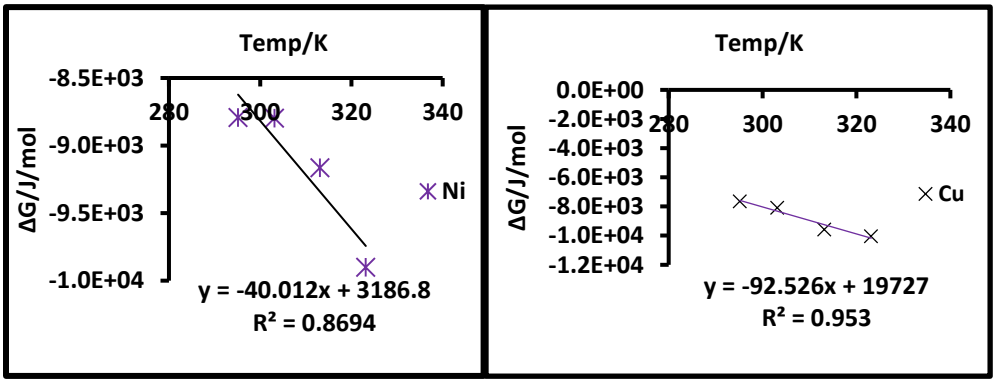


**Figure 3.25. The plots of ΔG° versus T for nickel and copper on TBFZ. The adsorption medium is deionized water with an adjusted pH as indicated in Figure 3.22 and 3.23.**

**Table 3.20. Thermodynamic parameters of nickel and copper on TBFZ in deionized water**

| Metal | $q_m$ | | | | ΔH° kJ/mol | ΔS° kJ/mol | ΔG° kJ/mol | | | |
|---|---|---|---|---|---|---|---|---|---|---|
| Temp/K | 295.15 | 303.15 | 313.15 | 323.15 | | | 295.15 | 303.15 | 313.15 | 323.15 |
| Ni | 35.97 | 32.79 | 33.78 | 39.84 | 3.186 | -0.040 | -8.79 | -8.80 | -9.20 | -9.90 |
| Cu | 22.47 | 24.69 | 39.53 | 41.84 | 19.727 | -0.001 | -7.64 | -8.08 | -9.57 | -10.03 |

The positive values of ΔH° of 3.186 and 19.727 kJ/mol for Ni and Cu, indicate that the adsorption process is endothermic in nature. It would be expected that an increase in temperature would result in increase in adsorption capacity which is supported by increase in adsorption capacity as confirmed in **Table 3.19**. The magnitude of the enthalpy can be used to distinct physisorption and chemisorption to a certain extent. A bonding strength of < 84 kJ/mol is considered physisorption, while bond strength between 84–420 kJ/mol can be classified as chemisorption**[60]**. Also Nollet et al. **[27]** demonstrated that the physical adsorption process normally had activation energy of 5-40 kJ/mol while chemical adsorption had a relatively higher activation energy from 40 to 800 kJ/mol. Accoding to these critera, the adsorption of the Ni and Cu should be considered as physisorption.

The negative ΔS° values for both Ni and Cu suggest decreasing randomness at the solid-liquid inter-phase during the adsorption process as the temperature increased. In solution, the metal ions can move more randomly as temperature increased. However, at the surface of the adsorbent their movement are restricted leading to a decrease in randomness. Therefore, the negative values confirm the restricted movement.

**Table 3.21** compares the experimental maximum adsorption capacities of the modified TBFZ and TBRM with those of reported previously. As observed in **Table 3.21**, both TBRM and TBFZ possess significant improvements over other existing adsorbents. Although hydrothermally modified fly ash **[34]** and surfactants modified titanate nanotubes **[64]** have higher adsorption capacity for $Pb^{2+}$ than TBFZ and TBRM, their method of preparation involved application of expensive materials and complex method of preparation. For the hydrothermally modified fly ash the modification included the addition of analytical grade $Al_2O_3$ to augment the aluminium oxide

content of the fly ash. Also modification was carried out at elevated temperature at 150 $^{o}$C for 6h which required a special rector made of Ni metal. For surfactant modified titanate nanotubes, the process of producing such materials is time consuming as well as being an expensive material. Whereas most previous adsorbents have been applied in the removal of few ions, TBRM and TBFZ have been applied in the simultaneous removal of six metal ions and they all show remarkable adsorption capacity especially regarding the removal of $Pb^{2+}$ by both TBFZ and TBRM. Both have shown good characteristics such as high CEC, high surface area, high pore volume, reusability, easy to produce with less energy consumption. Therefore, this low cost and easy to produce material could be a highly suitable alternative for the removal of metal ions.

**Table 3.21. Comparison of maximum adsorption capacities of different adsorbents for removal of metal ions**

| | Maximum adsorption capacities (mg /g) | | | | | | |
|---|---|---|---|---|---|---|---|
| Adsorbent type | $Pb^{2+}$ | $Cu^{2+}$ | $Cr^{3+}$ | $Co^{2+}$ | $Cd^{2+}$ | $Ni^{2+}$ | **Ref.** |
| NaOH-Methyl orange modified FA (room temp.) | 31.65 | - | - | - | - | - | **[61]** |
| Thiol grafted fly ash | | | | | 72.3 | | **[31]** |
| Modified fly ash (zeolite 4A) | - | 50.45 | 41.6 | 13.7 | - | 8.9 | **[46]** |
| Hydrothermal modified fly ash | 194.7 | 76.9 | - | - | - | - | **[34]** |
| Amino functionalized $Fe_2O_3$ nanoparticles | - | 12.4 | - | - | - | - | **[62]** |
| Surfactant modified titanate nanotubes | 145.8 | 41.7 | - | - | - | - | **[63]** |
| $TiO_2$ nano particles | - | - | - | - | 7.9 | - | **[64]** |
| Fly ash zeolite | 70.6 | - | - | - | 95.6 | - | **[65]** |
| TBRM (expt.) | 141.0 | 21.5 | 25.0 | 17.7 | 26.3 | 28.4 | This work in SCS |
| TBFZ (expt.) | 140.5 | 15.70 | 25.7 | 16.4 | 23.0 | 39.9 | This work in SCS |

FA: Fly ash

### 3.5 Studies on the reusability of TBFZ powder

An efficient adsorbent should not only possess good adsorption capacity but also have an acceptable regeneration capacity. Hence, the regeneration capabilities of TBFZ was investigated with 0.5 M $HNO_3$ (2.6.8). It was observed during the adsorption experiment that at lower pH, the

adsorption was unfavorable due to competition between the metal ions and $H^+$ ions. It was therefore assumed that the adsorbed metal ions could be leached or desorbed in acidic medium. The results are presented in **Figure 3.26**.

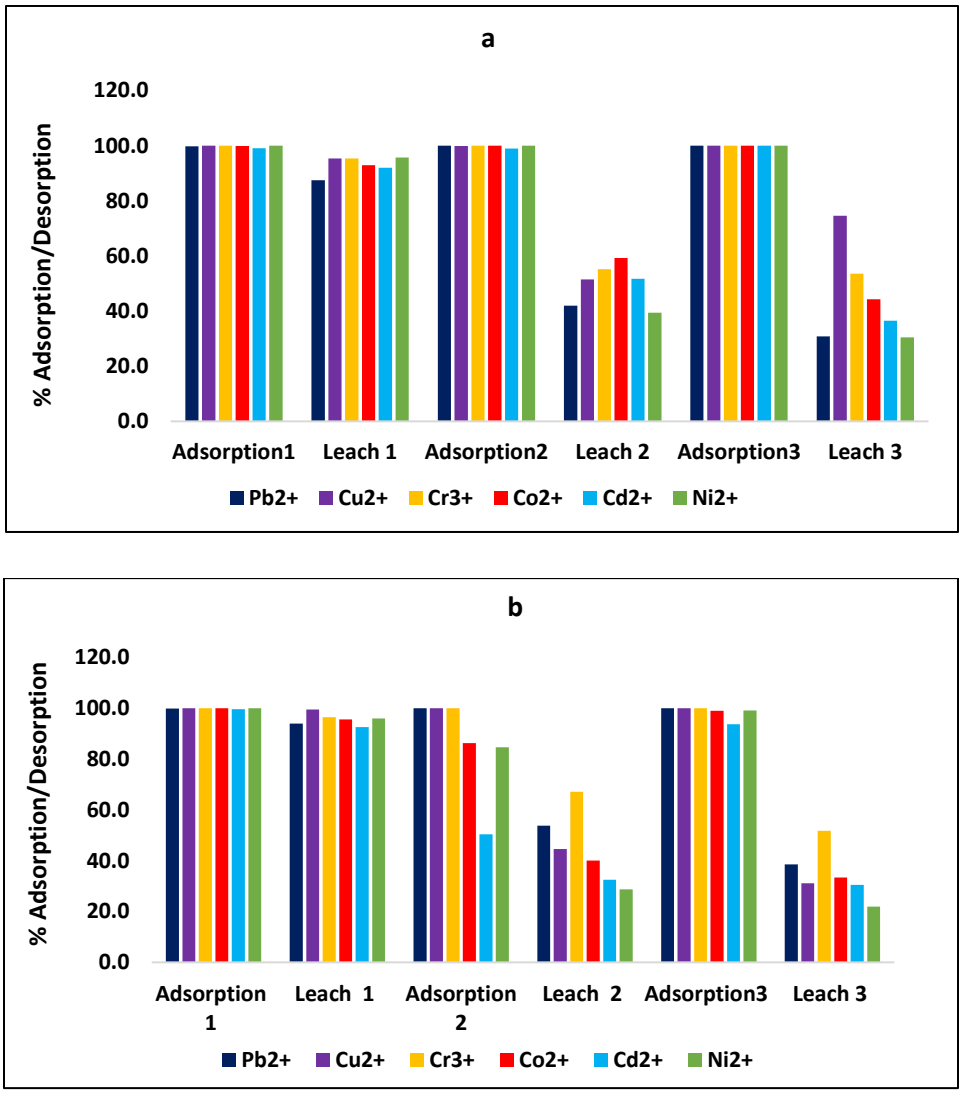


**Figure 3.26 Adsorption – leach cycles with mass:solution 1.0g:100mL metal concentrations: 50.0 mg/L each; adsorption time: 6 h; leaching solution : 0.5 M $HNO_3$; leaching time: 1 h; shaking speed: 120 rpm. Temperature 21±1 $^oC$. (a) TBFZ ; (b) TBFZ regenerated after each adsorption – desorption cycle. Regeneration condition: 10.0 mL of 2.0 M NaOH; regeneration time: 14 h stagant, followed by washing.**

It was observed that the sample was able to adsorb more than 90% in the 3 cycles in both TBFZ and TBRM. The leaching was very effective in the first cycle with a leachbility of 86, 95, 95, 93, 92 and 96% for $Pb^{2+}$, $Cu^{2+}$, $Cr^{3+}$, $Co^{2+}$, $Cd^{2+}$ and $Ni^{2+}$, respectively. However, there was significant decrease with a leaching value of in the second leaching (42, 52, 55, 59, 52 and 39%) and in the third leaching respectively. (31, 74, 54, 44, 36 and 31%. The problem encountered during the leaching process was a continuous loss of mass in each adsorption – desorption cycle. Although a calculation strategy was applied, the decreasing mass made the experimental error relatively high which might affect the accuracy of results. An effort was made to recondition the adsorbent with 2.0M NaOH overnight after each leaching. But the result as presented did not demonstrate marked differences (**Figure 3.26b**).

### 3.6 Studies on metal removal with a column system

Fixed bed column studies were done to determine the removal precentage of adsorbate at two flow rates with same mass of bed in function of time. The pH profile of the elute with time was monitored during the adsorption procedure.The results are presented in **Figure 3.27.**

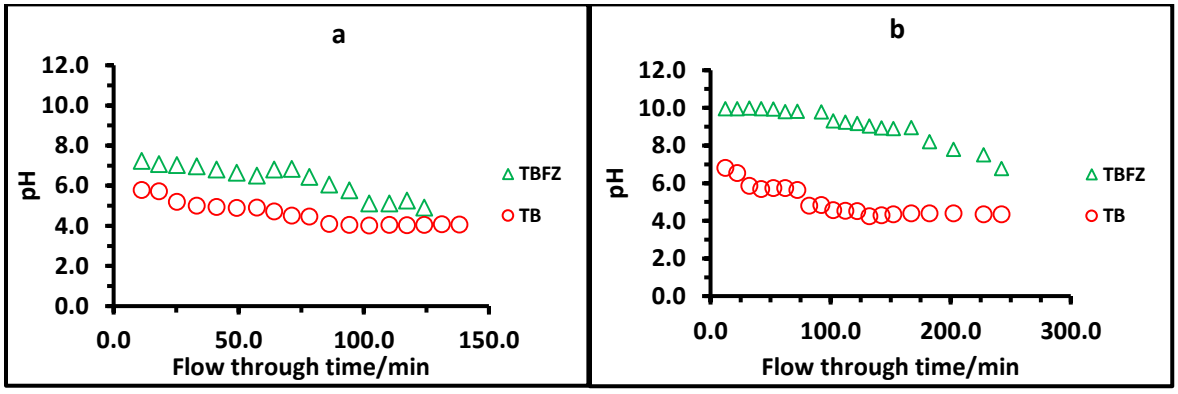


**Figure 3.27. pH evolution of the elute in column study; adsorbent: 5.0 g; concentration of SCS : 50.0 mg/L each; volume of initial loaded solution: 500 mL; flowrate: (a) 4.2 mL/min ; (b) 2.1 mL/min.**

As could be seen from **Figure 3.27**, both TBFZ and TB had steeper drop in pH during the faster flow rate compared to the slower one. At faster flow rates there is very little interaction between the adsorbent and the solutions therefore insufficient $OH^-$ ions are released from the

adsorbent leading to a more acidic pH in the elutes. On the other hand, a slower flow rate implies better interaction beween adsorbent and solution leading to increase in the release of $OH^-$ ions with corresponding increase in pH during the elution of eluent as observed in **Figure 3.26(b)**. The pH of eluent after the passage of 500 mL of cocktail solution for TBFZ and TB were 4.90 and 4.06, respectively for the faster flow rates whereas for the slower flow rate, the pH were 6.77 and 4.34 for TBFZ and TB, respectively. Both TB and TBFZ are alkaline in nature but TBFZ is more alkaline due to its modification with 2.0 M NaOH and, therefore will always produce a large amount of $OH^-$ ions comparatively. This is confirmed in both flow rates as evidenced on **Figures 3.26 (a) and (b).**

The design of the column for water treatment depends on the load of pollutant, the water matrix and the results from the batch investigation. During the passage of the contaminated water, a mass transfer zone is developed in the column. The thickness of this zone is affected by factors including the characteristics of the adsorbent, those of pollutants and hydraulic factors. With time the trasfer zone expands and reaches the bottom of the column where the effluent concentration get closer to the influent concentration. At this point a breakthrough point occurs **[66]**. It is this point at which the column get saturated.

The effluent concentrations (mg/L) were measured at different time intervals at a fixed bed mass and two different flow rates. The removal efficiency with respect to time is depicted in **Figures 3.28** and **3.29**. In **Figure 3.28**, the removal percentage of TB and TBFZ over a period of 12 - 242 min with a flow rate of 2.1 mL/min is compared. In TBFZ, the removal percentage is very high with values of ~100 % for Pb, Cr and Cu; whereas for Ni, Cd and Co the values were 100-94 % , 100-97 % and 99-92 %, respectively. For TB the removal percentages for Pb, Cr, Cu, Ni, Cd and Co were 99-46, 98-40, 99-46, 98-28, 89-42 and 95-37 %, respectively. A gradual drop of removal percentage with time was observed for all metals and with both adsorbents TBFZ and TB.

It could therefore be inferred that TB was easily saturated with metal load while TBFZ had better performance over the same period. A similar trend was observed when the flow rate was doubled to 4.2 mL/min, as shown in **Figure 3.29**. However, there was a decrease in the removal percentage of all the metal ions when the flow rate was doubled. With TB, when the flow rate was

doubled, the range of removal percentage of Pb, Cr, Cu, Ni, Cd and Co decreased from 99-46 to 79-34, 99-46 to 66-40, 99-46 to 91-35, 98-28 to 44-26, 89-42 to 49-39 and 95-37 to 51-44 %, respectively. The decrease in removal efficiencies with respect to increase in flow rate could be attributed to insufficient interaction between the adsorbate and adsorbent. During the faster flow rate, there is inadequate interaction or contact time to facilitate ion exchange, complexation or adsorption of metal ions to a greater extent leading to less removal percentages compared to slower flow rate.

With slow flow rate the residence time for the adsorbate is long enough for a better interaction and ion exchange leading to improved removal percentage for all metal ions. The increase in removal percentage of TBFZ relative to TB could be attributed to the higher surface area, increase in pore volume, better cation exchange capacity of TBFZ and a higher alkalinity of the treated material as demonstrated earlier . The removal of metal ions from the effluent could be either due to adsorption or precipitation considering the pH range since it was difficult to control the pH during the column studies.

The results obtained from the column studies are consistent with those obtained from the batch mode studies. In the batch mode, two groups of metals were identified: Cu, Cr and Pb were always removed with high removal percentages in the batch mode whereas Co, Cd and Ni were more difficultly removed and had normally less removal percentages. Similar observations were found in the column mode studies.

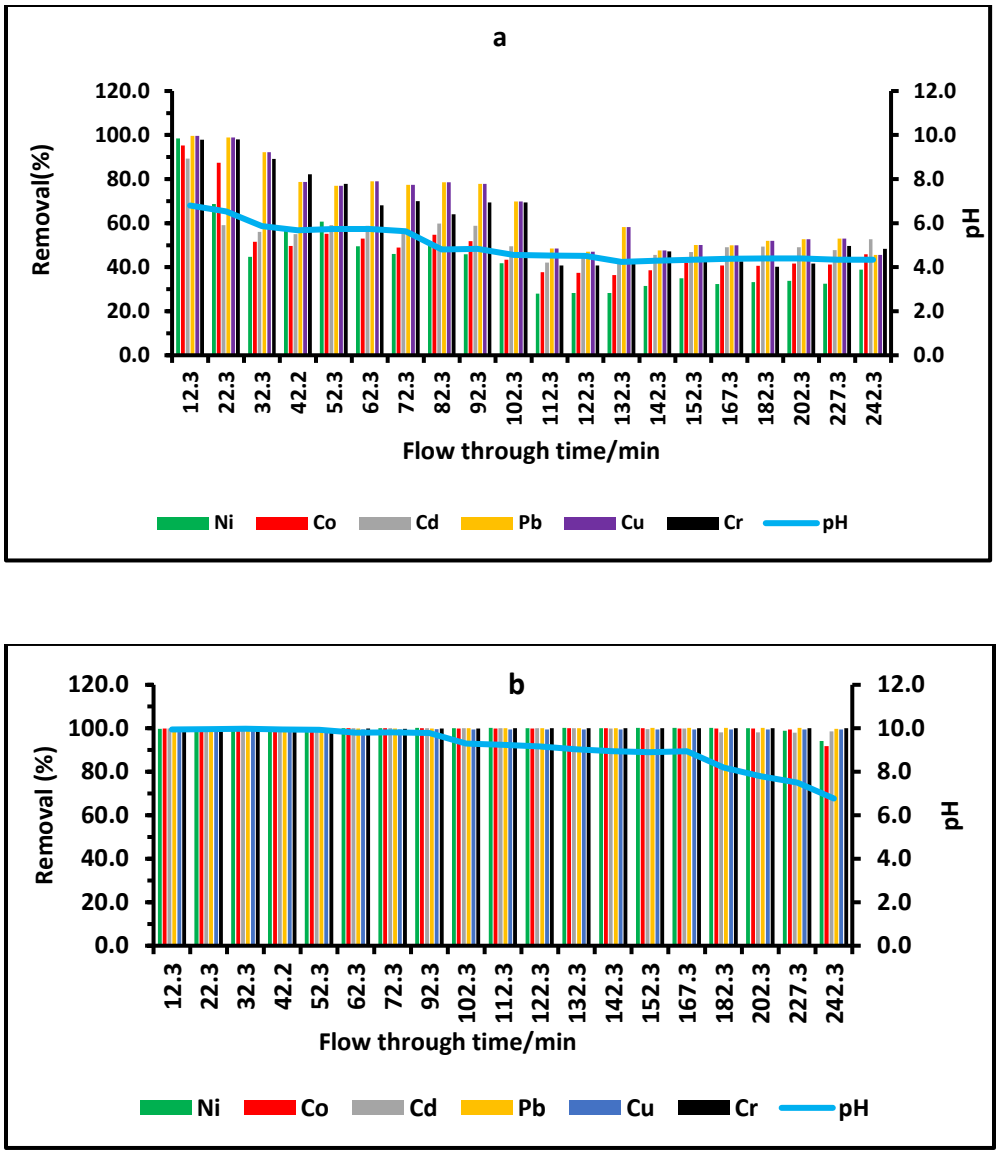


**Figure 3.28 Comparison of removal efficiency between adsorbents TB and TBFZ at a flow rate 2.1 mL/min. Adsorbent: 5.0 g; concentration of initial loaded SCS : 50.0 mg/L each; loaded SCS solution: 500 mL. (a) TB pH 6.80- 4.34 ; (b) TBFZ pH 9.95-6.77**

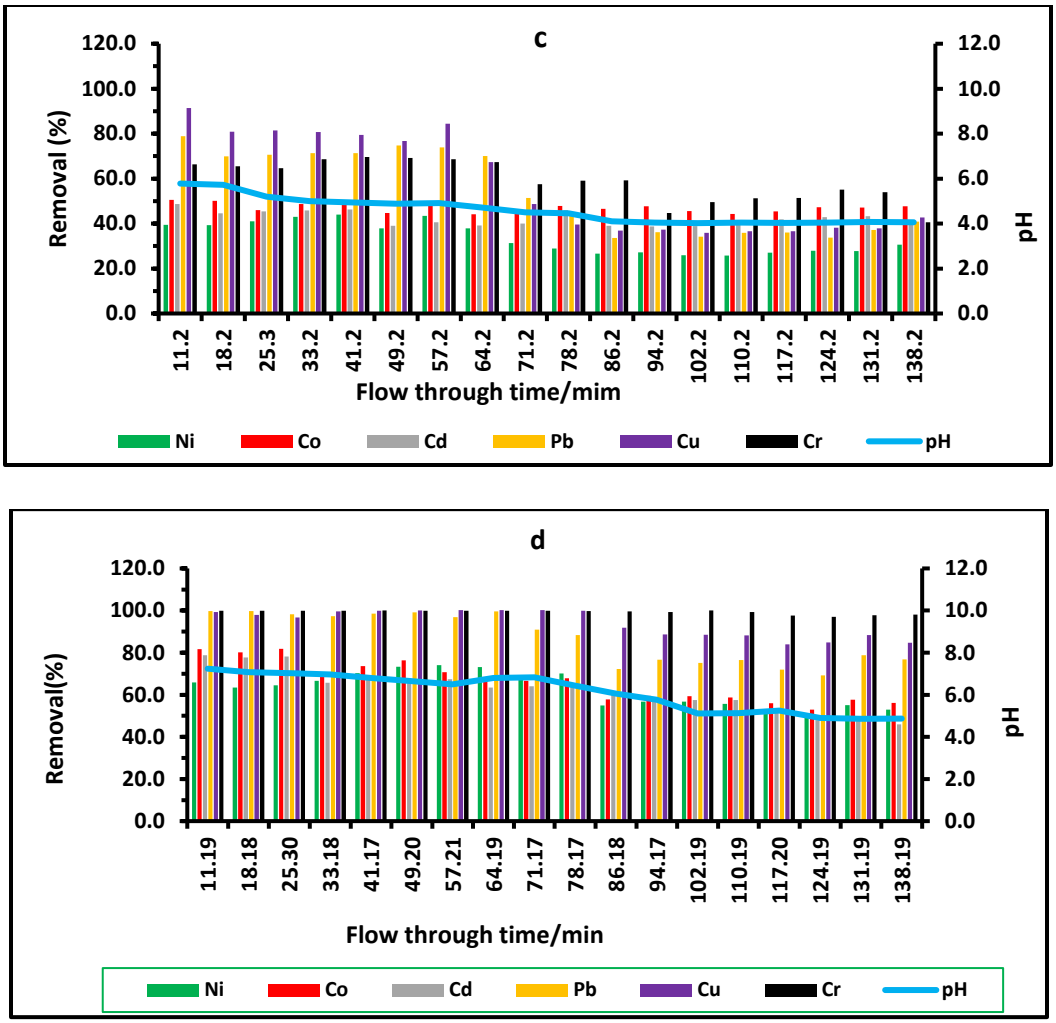


**Figure 3.29 Comparison of removal efficiency between adsorbents TB and TBFZ at a flow rate 4.2 mL/min. Adsorbent: 5.0 g; concentration of initial loaded SCS : 50.0 mg/L each; loaded SCS solution: 500 mL. (a) TB pH 5.78-4.06 ; (b) TBFZ pH 7.24-4.87**

### 3.7 TBFZ formulation, characterization and preliminary testing

Adsorption of metal ions from aqueous solutions have been studied by applying powdered adsorbents over the years. In this research, an innovative material in the form of a formulated foam composite has been developed from TBFZ and applied in the removal of metal ions from SCS and tailing pond water (TPW). Two different formulations that included fly ash TBFZ, bonding agent (BA) and foaming agent (FA) were tested, with ratios of TBFZ:FA:BA = 0.22:0.33:0.45 and TBFZ:FA:BA = 0.17:0.50:0.33. However, the latter was unstable during shaking with sorbates in solution. The physical and mechanical properties of TBFZ:FA:BA = 0.22:0.33:0.45 has been

determined. The adsorption properties and regeneration potential of the foamed adsorbent were also investigated.

### 3.7.1 Physical and mechanical properties of TBFZ:FA:BA = 0.22:0.33:0.45

The formulated foam is a composite material composed of cement (commonly Portland cement) and other cememtitious materials such as fly ash and slag cement. A foaming agent was first dissolved in water to create the foam, then it was added to a cement based slurry. The foamy cement was generated and the slurry set around the foam bubbles. Once the water dried, the slurry had enough strength to maintain its shape around the voids **[67]**.

With all real foams, each closed cavity represents a bubble independent of neighboring gas bubbles. Within the foam, the gas exist as intermittent or dispersive phase whereas the continuous phase is present as matrix or liquid **[68]**. A foaming agent (FA), mastercell 25 and a bonding bonding agent (BA) were added to make TBFZ a foamy material. The physical and mechanical properties were determined.

#### 3.7.1.1 Studies on absorption of water

The formulated foamy material was soaked in DW for 24 h, and then dried at room temperature untill its mass became constant. The absorption of water percentage was calculated from the formula below:

$$\text{Water absorption (\%)} = \frac{(wet\ mass - dry\ mass)}{dry\ mass} * 100 \qquad [3.13]$$

Water absorption is a parameter used for indicates the porosity of a foamy material. Water absorption by complete immersion was found to be 70.63% in mass as shown in **Table 3.22**. The 70.63 % water absorption could be attributed to the voids created by the foaming agent as they get filled with water indicating the highly porous nature of the formulated foam. The presence of voids lead to increase in porosity but this may also decrease the strength of the foamy concrete. In comparison with other foamy materials such as waste clay brick with clay percentages of 25, 50, 75 and 100 %, the corresponding percentages of water absorption were: 15.98, 16.02, 16.33, 17.38 and 19.29 %, respectively **[69]**.

**Table 3.22 Physical and mechanical properties of the formulated composite material**

| | |
|---|---|
| Compressive strength (kPa) | 1361.7 |
| Density (g/cm$^3$) | 0.72 |
| Water absorption (%) | 70.63 |
| BET Surface Area (m$^2$/g) | 19.48 |
| BJH Cumulative Pore Vol.(cm$^3$/g) | 0.004 |

### 3.7.1.2 Determination of Density

The density of foamy material is important because it can provide information regarding material strength, durability and permeability. The density of TBFZ:FA:BA = 0.22:0.33:0.45 was found to be 0.72 g/cm$^3$ as shown in **Table 3.22**. Comparatively, it is less than that of water and this could be attributed to the voids that were formed throughout the structure, which could also be observed on the surface of the foamy material of TBFZ:FA:BA = 0.22:0.33:0.45 as observed in **Figure 3.30( a).** Its low density allows it to floating in an aqueous phase for some time, either it was in an acidic, basic or neutral solution **(Figure 3.30 b)**.

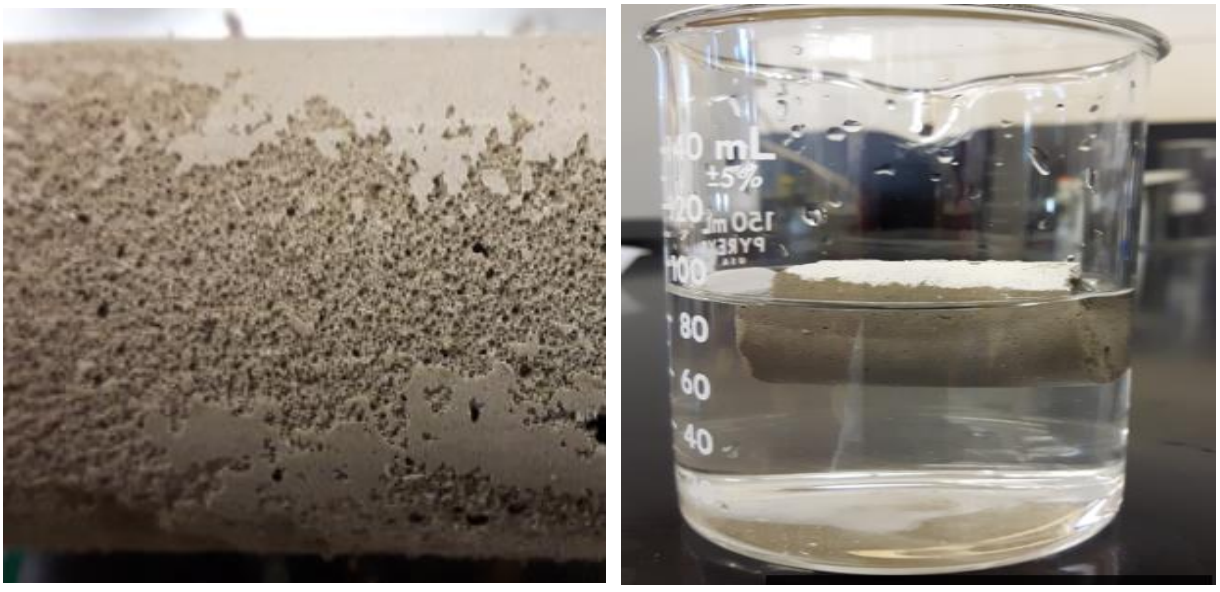


**Figure 3.30 (a) (left) TBFZ:FA:BA = 0.22:0.33:0.45 showing voids and (b) (right) TBFZ:FA:BA = 0.22:0.33:0.45 floating in DW.**

The advantage of this lightweight formulated material is that as it sinks from the top of the solution due to absorption, metal ions present in the solution will be absorbed into the material and also adsorbed onto the surface. Therefore, the removal efficiency will be enhanced significantly.

### 3.7.1.3 Determination of the compressive strength of TBFZ:FA:BA = 0.22:0.33:0.45

The compressive strength of a material is the maximum stress that it can withstand when loaded axially. It is one of the most important properties of a materials that indicates the maximum strength this material can endure. All other mechanical parameters such as flexural strength, splitting tensile strength and modulus of elasticity directly depend on the compressive strength of the material. The load - deflection profiles for the sample are displayed in **Figure 3.31**. The compressive strength calculated after applying a maximum average axial load was 1361.7 kPa as shown in **Table 3.5**. Normally conpressive strength is quoted in MegaPascal (MPa) for constructional materials. However, considering the purpose for which this particular formulated material is being used, the value of 1361.7 kPa ( 1000 $N/m^2$ = 1 KPa) is very significant. The maximum load was extrapolated from the load - deflection profiles and the average was calculated. The average maximum load that the material could withstand was 1094.26 N and at the maximum load the formulated foam fractured.

During a compressive test, different types of fracture can be encountered. These are: cone, cone and split, cone and shear, shear and columnar. The images obtained during the compression and colapse are displayed in **Figure 3.32** indicating that the fracture of TBFZ:FA:BA = 0.22:0.33:0.45 was columnar. The lateral sides get spalled and there was a dense columnar cracking in the bulk of the material. The material was found to be resistant to disintegration, attrition and mechanical wear during the dynamic contact of the adsorption medium.

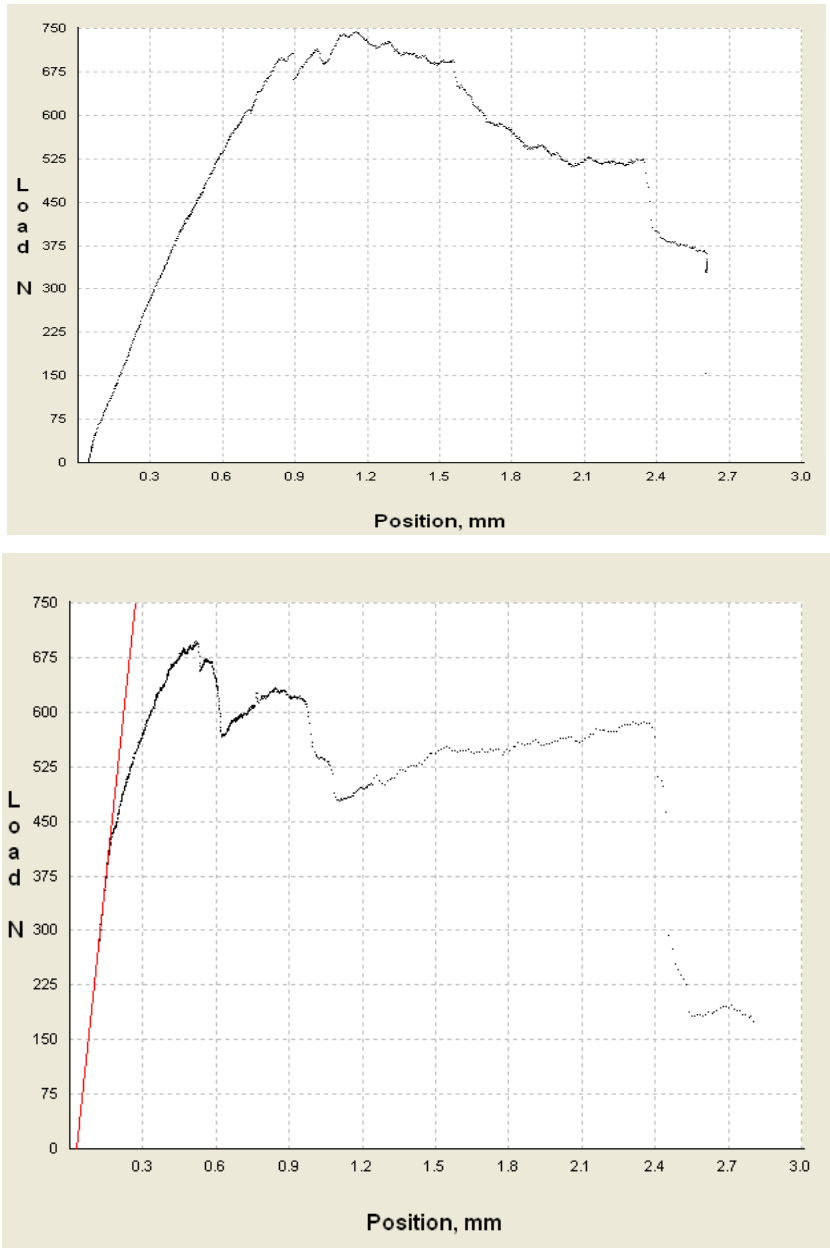


**Figure 3.31 Load - deflection profiles of TBFZ:FA:BA = 0.22:0.33:0.45 during compression.**

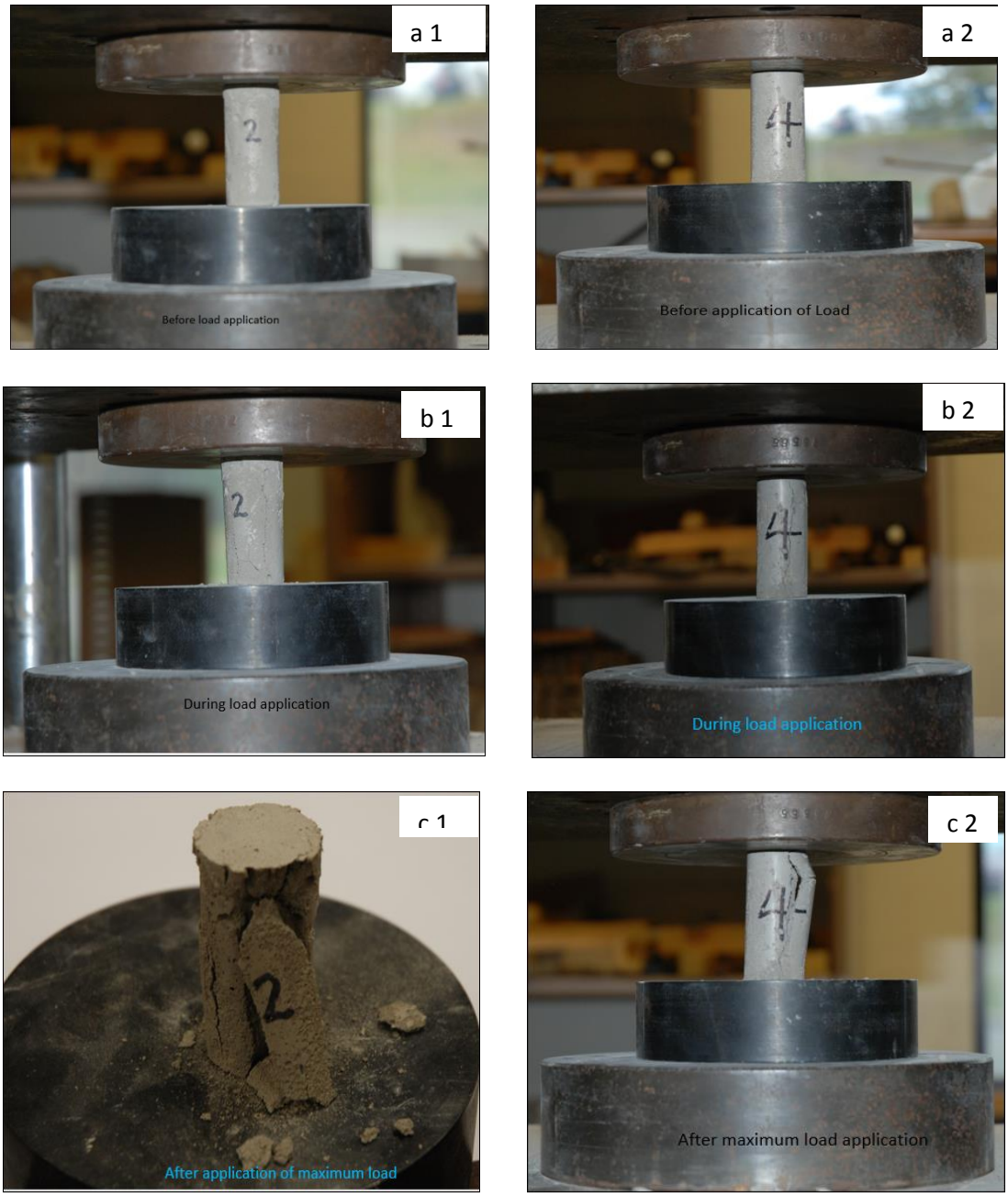


**Figure 3.32 Images of TBFZ:FA:BA = 0.22:0.33:0.45 (a1, a2) Test set up, (b1, b2) during fracture and (c1, c2) after fracture.**

### 3.7.2 The determination of leachability of dissolved organic carbon (DOC)

The foaming agent incorporated into the formulated foam is a surfactant and therefore it is likely to be gradually released in solution. The composition of the foaming agent includes benzensulfonic acids, C14-C16 alkenes, C14-C16 alkanes hydroxy, sodium salts and dimethyl sodium salts. These chemicals make the foaming agents soluble in water. In order to ascertain their solubility, a leaching test was conducted over a period of 21 days using tailing pond water and Millipore water. The pH evolution during this period was also monitored .The results are presented in **Figure 3.33.**

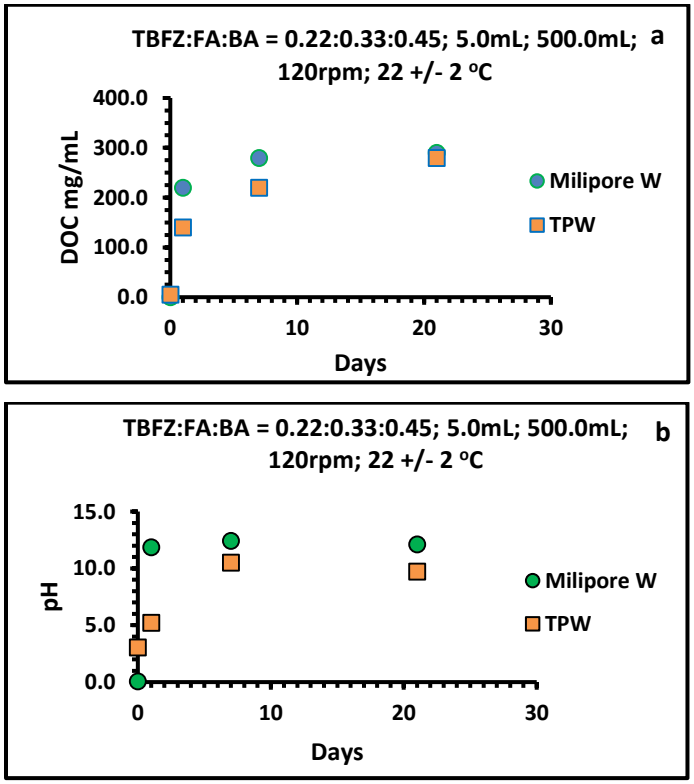


**Figure 3.33 Comparison of (a) DOC release in TPW and Millipore water and (b) pH profile of TBFZ:FA:BA = 0.22:0.33:0.45 in TPW and Millipore water**.

**Adsorbent: 5.0 g; Volume of TPW : 500.0 mL; Volume of Millipore : 500 mL; shaking speed: 120 rpm;Temperature: 22± 2 °C .**

The results indicate that there was a rapid increase in DOC within the first seven days, which seems to stabilize thereafter until a point of saturation is attained as represented by the plateau for both Millipore water and TPW. The increase in DOC is a confirmation of the solubility or biodegradability of the foaming agent in water therefore removing any doubt of bioaccumulation. It is also observed that TPW had a lower DOC content throughout the experimental period relatively to Millipore water.

A similar trend is observed for the changes in pH . Both TPW and Millipore water showed marked increase in pH with respect to increase in the number of days. However, TPW shows a lower pH values probably due to the presence of high concentrations of anions such as sulphate, nitrate, chloride and iron(III) hydroxide. In other words, TPW tends to have a better buffering capacity than Millipore water. The increase in pH is due to the alkaline nature of the formulated foam which is also advantageous for the removal of metal ions from solution by adsorption or as the result of formation of hydroxides of metal ions in the material.

### 3.7.3 Application of formulated foam composite for the removal of metal ions

The formulated foams as well as the foaming agent were applied to remove metal ions from aqueous solutions to evaluate their efficiencies.

#### 3.7.3.1. pH profile of formulated materials in kinetic studies

**Figure 3.34** illustrates the pH evolution of the solution during the kinetics investigation. The pH of the solution when the formulated material was used as adsorbent was low and had to be adjusted with 0.1 M NaOH. The pH was adjusted and monitored between 2.95 to 7.85 within a time frame of 6 h as the adsorption proceeded. As could be observed in **Figure 3.34**, the pH seemed to stabilize after 180 min for both DW and TPW at a pH close to 8.0. This feature enhanced the adsorption removal by both formulated materials compared to the foaming agent alone (FA).

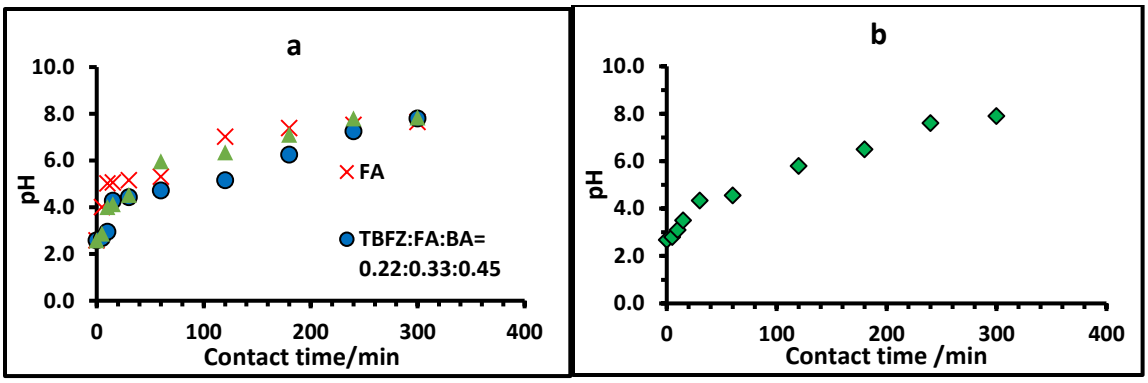


**Figure 3.34 pH profile of formulated material during adsorption (a) in SCS and (b) TBFZ:FA:BA = 0.22:0.33:0.45 in TPW.**

### 3.7.3.2 pH Effect on adsorption by TBFZ: FA:BA = 0.22:0.33:0.45

The adsorption in mg/g ($q_e$) increased as pH increased in TBFZ:FA:BA = 0.22:0.33:0.45 as displayed in **Figure 3.35.** This behavior is consistent with that of TBFZ from which the formulated foam was developed. The mechanism or mode of removal could be two-fold: first is the adsorption on the surface and second with the absorption within the material. As the solution is absorbed by the material, the metal ions will the trapped in the pores or voids of the formulated foam leading to the decrease of ions in the solution. At low pH, there is competition between metal ions and $H^+$ ions resulting in low $q_e$ (mg/g) values. However, as the pH increased the surface of the material is deprotonated creating sufficient anionic sites to improve the $q_e$ values. The order of selectivity at pH 6.35 was: $Cr^{2+} > Pb^{2+} > Cu^{2+} > Ni^{2+} > Co^{2+} > Cd^{2+}$.

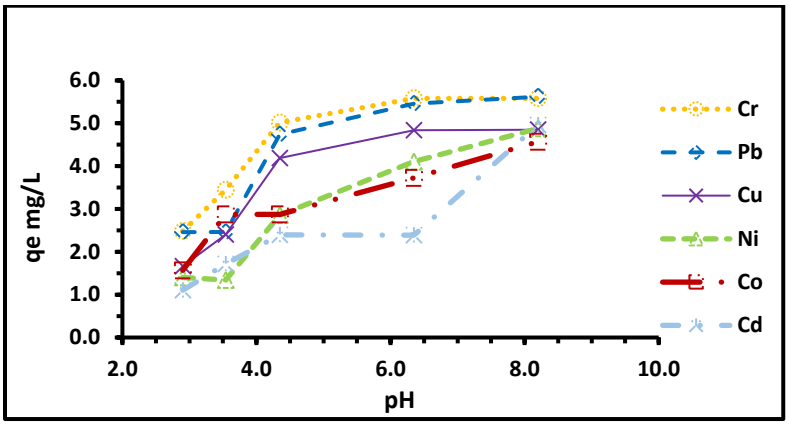


**Figure 3.35 pH effect on adsorption of metal ions; adsorbent: 0.50 g; concentration of metal ions: 50.0 mg/L each; volume of metal ions solution: 50.0 mL; time: 6 h; shaking speed: 120 rpm at 22 $^0$C TBFZ:FA:BA = 0.22:0.33 :0.45.**

### 3.7.3.3 Adsorption kinetics on formulated material

The adsorption kinetic study on TBFZ:FA:BA = 0.22:0.33:0.45, TBFZ:FA:BA = 0.17:0.50:0.33 and FA was investigated in SCS. Additionally, a kinetic study on TBFZ:FA:BA = 0.22:0.33:0.45 in TPW was also investigated. The results presented in **Figure 3.36** reveal that the removal percentage of metal ions by the foaming agent did not change significantly with time compared to the formulated materials as observed in **Figure 3.36(c).** With the exception of $Pb^{2+}$ which had 74.5% adsorbed after 5 min all the other ions had less than 50.0 % removed. Also it was observed that all the metal ions revealed desorption with time. For $Pb^{2+}$, the percentage removal decreased from 74.5 to 51.4% whereas for $Cu^{2+}$, it decreased from 48.2 to 9.9%. $Ni^{2+}$, $Co^{2+}$ and $Cd^{2+}$ decreased from 47.0, 39.5 and 41.0% to 10.0, 8.2 and 38.1%, respectively. $Cr^{3+}$ recorded the least percentage removal and did not show significant decrease during the period.

Although the foaming agent contains sulphonic groups, it is possible that such groups did not deprotonate sufficiently to create anionic sites which could enhance electrostatic attraction between the cations and the sulphonic groups. Also, it is possible that FA alone does not possess enough surface area and CEC capacity to facilitate adsorption. On the other hand, the presence of Al-OH, Si-OH, Ti-OH, Fe-OH, etc. present in the formulated materials could be deprotonated as pH increases to create sufficient anionic sites therefore improving removal efficiency as presented

in **Figures 3.36 (a) , (b) and (d).** The removal efficiency was more than 96% for all metal ions for both TBFZ:FA:BA = 0.17:0.50:0.33 and TBFZ:FA:BA = 0.22:0.33:0.45 after 300 min in SCS. Also due to the percentage absorption of water (70.6%) by TBFZ:FA:BA = 0.22:0.33:0.45, the removal efficiency was enhanced in TBFZ:FA:BA = 0.22:0.33:0.45 and TBFZ:FA:BA = 0.17:0.50:0.33, respecively.

It was observed during the adsorption process that TBFZ:FA:BA = 0.17:0.50:0.33 was undergoing erosion and deterioration probably due to the high content of FA. High FA proportions in formulated foams decreased the density and hence decreased the compressive strength **[70]**. In this regards, further test were conducted on only TBFZ:FA:BA 0.22:0.33:0.45.

The comparison of the removal percentage by TBFZ:FA:BA = 0.22:0.33:0.45 in SCS and TPW shows a better removal in TPW. By 180 min, the percentage removal by TBFZ:FA:BA = 0.22:0.33:0.45 for Cd, Ni, Co, Cr, Pb and Cu were 33, 81, 81, 100, 100 and 100 %, respectively. On the other hand, at a time of 180 min the removal percentage by TBFZ:FA:BA = 0.22:0.33:0.45 in TPW improved to 66, 100, 81, 100, 100, 100 %, in the same order. The result is consistent with earlier observation where adsorption by powdered materials of fly ash had demonstrated improved efficiency in TPW. Therefore, TBFZ:FA:BA = 0.22:0.33:0.45 was more efficient in the presence of TPW relative to SCS, likely due to the high ionic strenght and composition of TPW.

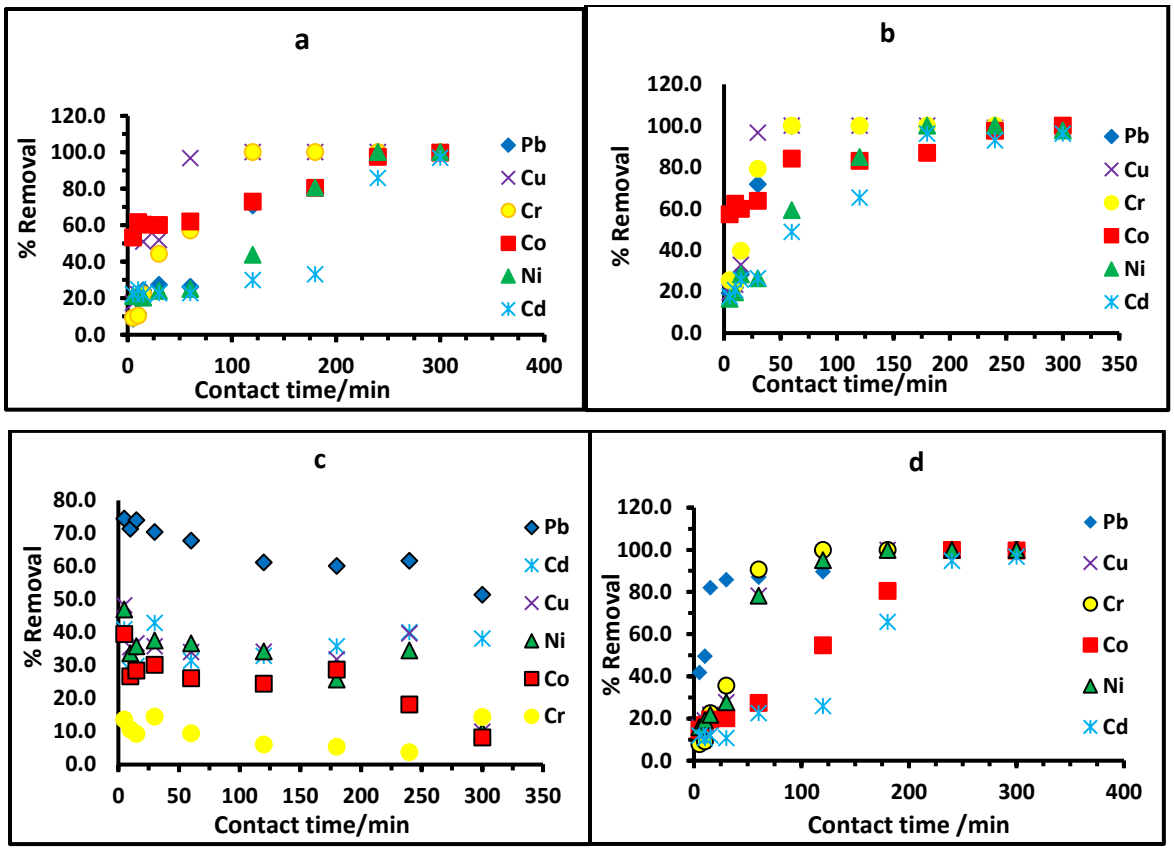


**Figure 3.36 Comparison of adsorption efficiency of adsorbents: adsorbent: 1.0 g; concentration of metal ions: 50.0 mg/L each; volume of metal ions solution: 100.0 mL; time: 6 h; shaking speed 120 rpm at 22 $^0$C in: (a) TBFZ:FA:BA = 0.22:0.33:0.45-SCS, pH: 2.56-7.80**
**(b) TBFZ:FA:BA = 0.17:0.50:0.33–SCS, pH ; 2.87-7.84**
**(c) FA–SCS, pH :4.0 - 7.65 and (d) TBFZ:FA:BA = 0.22:0.33:0.45–TPW, pH: 2.8-7.9.**

### 3.7.4 Studies on the reusability of TBFZ:FA:BA 0.22:0.33:0.45

The adsorption - leaching cycle of TBFZ:FA:BA = 0.22:0.33:0.45 with 1.0 M and 0.5 M $HNO_3$ were compared and are displayed in **Figure 3.37**. Both the first and second adsorption cycle was significant with adsorption percentages of more than 60 % for all metal ions in both (a) and (b). The leaching was very poor for both of 0.5 M and 1.0 M acid solution. However, among the two leachates, 1.0 M $HNO_3$ was better especially in the second cycle with percentage leaching of 32, 33 and 43 % for Co, Cd and Ni, respectively, whereas 0.5 M leached 28, 27 and 35 %, respectively. Pb and Cu were leached at almost equal percentages in both 1.0 M and 0.5 M $HNO_3$ while the most significant difference was observed with Cr with a decrease in leaching precentage from 16.8 to 1.0 % (94 % decrease). Both 0.5 M and 1.0 M were strong enough to cause attrition

of the adsorbent just after the second cycle, thus adsorption –leaching cycle was terminated after the second cycle. Although there was high percentage adsorption values of TBFZ:FA:BA = 0.22:0.33:0.45 after 2 cycles, the degree of leaching back the metal ions was very poor therefore making the reusability inefficient. The poor desorption nature of the formulated material requires that further work be done by applying other leaching solutions.

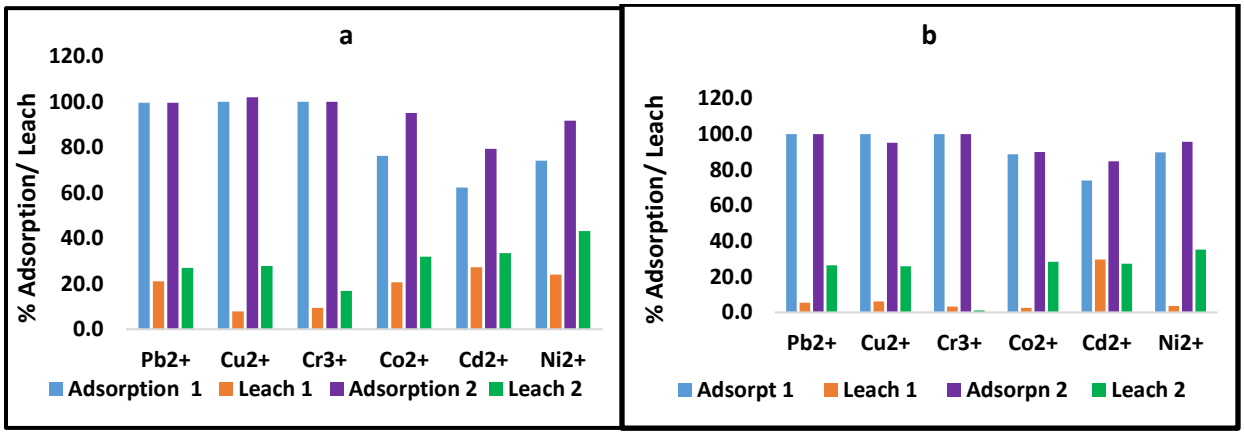


**3.37 Adsorption – leach cycles mass: solution, 1.0 g:100.0 mL; metal ion: 50.0 mg/L each; time: 6 h; shaking speed: 120 rpm; temperature; 22 ºC**
**(a) Leach with 1.0 M $HNO_3$; (b) Leach with 0.5 M $HNO_3$**

# Chapter 4

# 4. Results and discussion on grape waste material (GWM)

## 4.1 Characterization of adsorbents of grape waste material (GWM)

The particle sizes of the biosorbent ranged from 38 - 212 µm with 212 µm constituting the more abundant size with 40.81 % and 38 µm with the least amount of 3.95 %, as displayed in **Table 4.1**. This variation in sizes might be due to the blender that was used for crushing the grape fruits. Particle of sizes 38, 106, 150 and 212 µm were applied to study the effect of particle size distribution on adsorption.

The FTIR spectroscopy technique was applied for the chemical characterization of the biosorbent to probe the functional groups on the surface of the sorbent. **Figure 4.1** shows the FTIR spectra of GWM. The broad band stretching observed in the range 3600-3300 $cm^{-1}$ could be regarded as hydroxyl groups (OH) resulting from the sugars in the grapes and also OH compounds formed after fermentation of the grape juice.

**Table 4.1 Particle size distribution of GWM**

| Size/ µm | Mass Retained/g | Composition % in mass |
|---|---|---|
| < 38 | 0.3888 | 3.98 |
| 38 | 0.3858 | 3.95 |
| 45 | 0.4621 | 4.73 |
| 53 | 0.9552 | 9.78 |
| 75 | 1.5347 | 15.72 |
| 106 | 0.8655 | 8.86 |
| 150 | 1.1871 | 12.16 |
| 212 | 3.9845 | 40.81 |

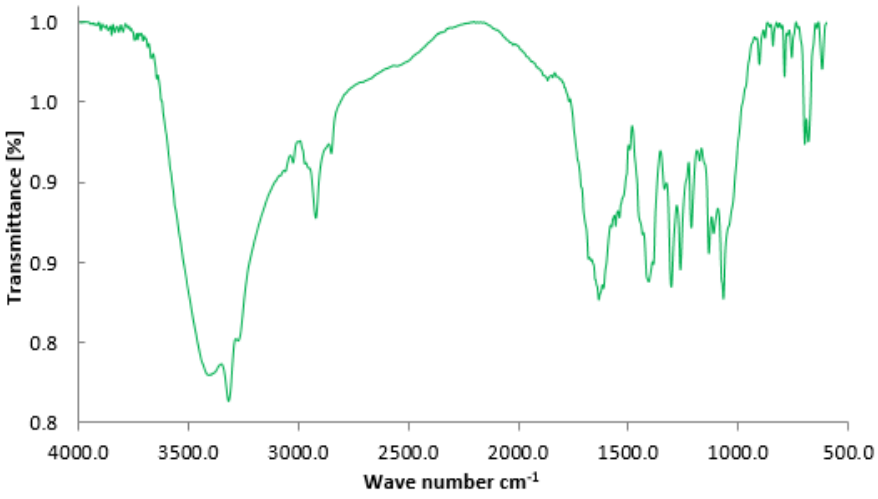


**Figure 4.1 FTIR of GWM**

Also, the C-H stretching band in the range 2901 - 2923 $cm^{-1}$ could be attributed to the organic nature of GWM. Most organic groups contain the C-H in their structure. Lastly, the stretching band of N-H identified in the range 3000 - 3200 $cm^{-1}$ could be due to amine groups in the material. The presence of hydroxyl and N-H groups could enhance the removal of metal ions from aqueous solutions.

## 4.2 The studies on adsorption of metal ions with GWM

Different adsorption test were conducted on GWM to investigate the properties which affect the removal of metal ions from aqueous solutions. The factors investigated include: pH, particle size and contact time.

### 4.2.1 Effect of pH on adsorption of metal ions by GWM

The pH of the solution is one of the critical paramaters controlling the adsorption process. The effect of pH on adsorption percentage (%) was investigated by increasing it from 2.60 to 6.80 under the following conditions: 50.0 mg/L of each metal ion (mixed); mass of adsorbent: 0.50 g; volume of solution; 50.0 mL, stirring: 120 rpm; temp: 22 $^{o}$C. As clearly observed in **Figure 4.2,** the increase in pH leads to improvement in the percentage removal. The results show that the adsorption of $Cr^{3+}$, $Pb^{2+}$, $Cu^{2+}$, $Co^{2+}$ and $Ni^{2+}$ were very low at pH below 4.0 but increased significantly at pH 6.8. However, the removal of $Cd^{2+}$ was high (56 %) even at pH 4.0

and further increased to 91 % at pH 6.8. $Pb^{2+}$and $Cd^{2+}$ were the most efficiently sorbed at pH 6.8 whereas Ni was the least removed at the same pH with a percentage removal of 48.7%.

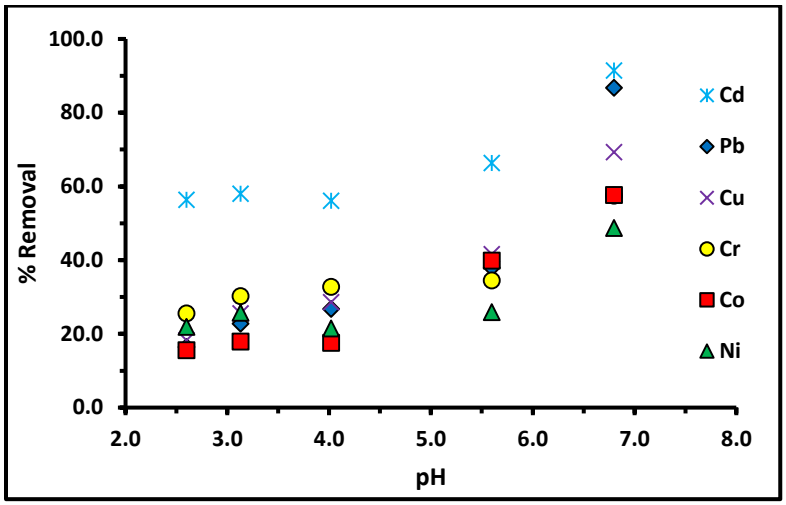


**Figure 4.2. Effect of pH on the sorption of $Cr^{3+}$, $Pb^{2+}$, $Cu^{2+}$, $Co^{2+}$, $Ni^{2+}$, $Cd^{2}$ onto GWM**

The adsorption (%) was lower at pH below 4.0 due to electrostatic repulsion between the metal cations and the protonated OH and N-H groups on the surface of the material. Under acidic conditions, there is reversal of charge and reduced metal - chelating ability for the metal ions, which enhance high numbers of hydrogen ($H^+$) ions to favor the protonation of the OH and amino sites. On the other hand, the increase in adsorption percentage at pH above 6.0 is due to deprotonation of OH and N-H groups leading to increased electrostatic attraction between metal ions and the deprotonated groups. The deprotonated hydroxyl groups could also be involved in complex coordination with metal ions **[71, 72]**.

### 4.2.2 Effect of particle size on adsorption

The effect of particle size was investigated with GWM selected sizes 38, 106, 150 and 212 µm. The results are displayed in **Figure 4.3**. As could be observed, as the particle sizes increased from 38 to 212 µm, the removal percentage decreased for all the metal ions. For Cu the removal percentage decreased from 74 to 69 % whereas Pb and Cd reduced from 96 to 92 %, each. Also in all the different sizes, the order of removal was Pb > Cd > Cr > Co > Cu > Ni, except in particle size 212 µm where Co was slightly higher than Cr with percentage removals of 82.6 and 80.8 %,

respectively. This observation could be attributed to the fact that as the sizes decrease there is increase in surface area, which is one of the most critical characteristics of a good adsorbent.

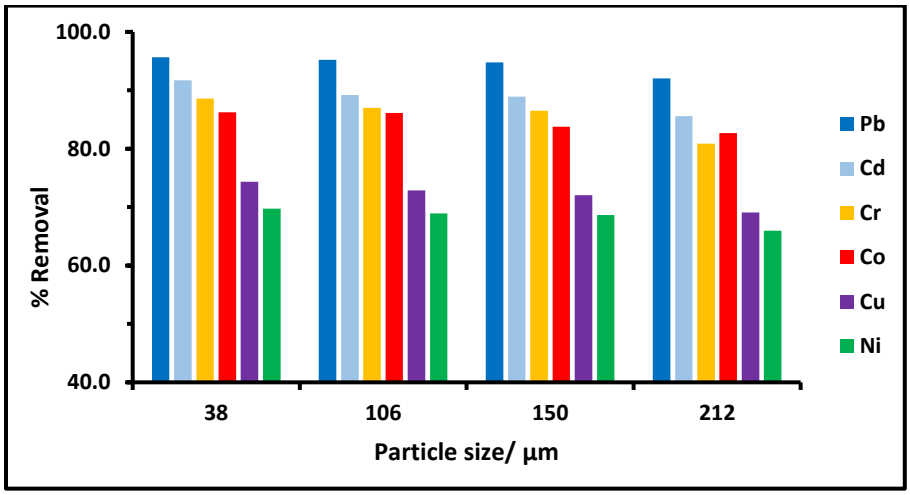


**Figure 4.3 Particle size effect on adsorption of metal ions; adsorbent: 0.50 g; concentration of metal ions: 50.0 mg/L each; volume of metal ions solution: 50.0 mL; time: 4 h, shaking speed: 120 rpm at 22 $^{0}$C.**

### 4.2.3 Effect of contact time

The influence of contact time on percentage removal was investigated with initial concentrations of 10.0 and 50.0 mg/L. The removal percentage were determined at varying time intervals. The results are shown for $Cu^{2+}$, $Cr^{3+}$, $Pb^{2+}$, $Co^{2+}$, $Cd^{2+}$ and $Ni^{2+}$ in **Figure 4.4**. As observed, the removal of the metal ions increased for all ions and for both 10.0 and 50.0 mg/L concentrations, respectively within the time interval. However, the 10.0 mg/L concentration showed better removal percentages. At 240 min, the removal percentage for Cu was 97.9 and 81.4 % for 10.0 and 50.0 mg/L, respectively. Similar results were obtained for $Pb^{2+}$ at 93.0 and 88.1 %, for $Cr^{3+}$ at 74.0 and 53.9 %, $Cd^{2+}$ at 86.1 and 82.0 %, $Co^{2+}$ at 98.1 and 50.1 % , and $Ni^{2+}$ at 93.2 and 50.1 %. The results indicate that the removal was dependent on the initial concentration. When the initial concentration was increased from 10.0 to 50.0 mg/L, the sorption of $Cu^{2+}$, $Cr^{3+}$, $Co^{2+}$ and $Ni^{2+}$ decreased after 240 min of contact.

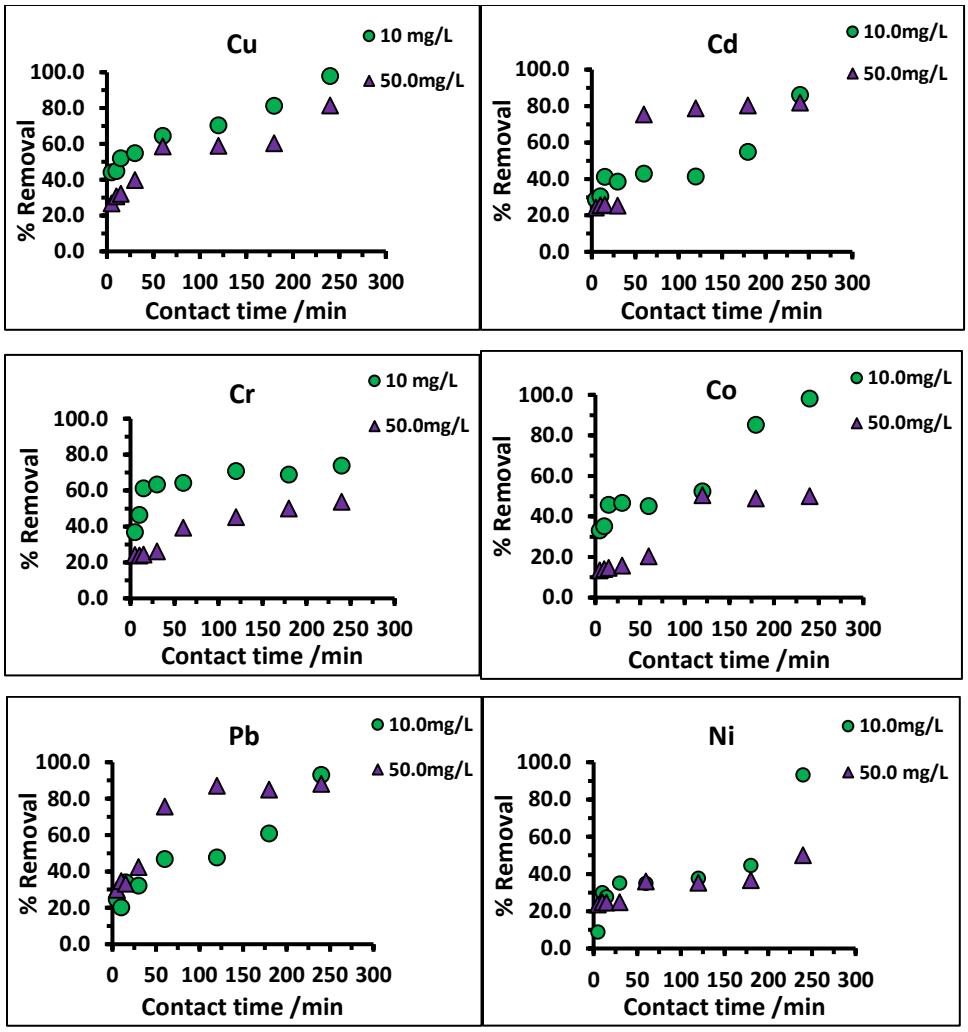


**Figure 4.4 Comparison between removal percentage and concentration for adsorption of mixed metal ions at: pH = 3.53-6.45; mass: 1:100; Speed: 120 rpm; Temp: 22±2 $^{0}$C.**

The decrease in the sorption was likely due to the competition for the adsorption sites on GWM in the presence of all metal ions. Similar results were reported by Panayotova and Velikov **[73]**. It should be noted that adsorption mechanism of multi-metal ions depend on many factors making it very complicated.The factors include: concentration and other competing ions present, chemical (functional groups) and physical properties (particle size, surface area, porosity) of both adsorbents and adsorbates, as well as pH and others.

It was observed that the pseudo-second order model fitted better than the pseudo-first order for all studied metals. The model selected for fitting the data was based on the tendency to estimate

the quantity of metal ions removed at the initial and final stages of adsorption. **Table 4.2** lists the results obtained from the pseudo-second order kinetics model. It reveals that both 10.0 and 50.0 mg/L concentrations have their calculated and experimental adsorption capacities, $q_e$ agreeing well. Also the correlation coefficients for metal ions are greater than 0.83 in both concentrations except for $Ni^{2+}$ at 10 mg/L. This suggests the applicability of this kinetic model to best fit the data. The pseudo-second order nature of the adsorption process also suggest that the metal ions have been removed through chemical reactions **[74]**.

**Table 4.2 Adsorption kinetic model rate constants for metal ions.**

| Initial conc. (mg/L) | Metal ions | $q_e$ exp. (mg/g) | $q_e$ cal. (mg/g | $k_2$ (g/mg/min) | $R^2$ $R^3$ |
|---|---|---|---|---|---|
| 10.0 | $Cu^{2+}$ | 1.14 | 1.12 | 0.047 | 0.9694 |
| | $Pb^{2+}$ | 0.92 | 0.86 | 0.028 | 0.8553 |
| | $Cr^{3+}$ | 0.79 | 0.79 | 0.219 | 0.9981 |
| | $Co^{2+}$ | 1.09 | 1.09 | 0.026 | 0.8636 |
| | $Cd^{2+}$ | 1.10 | 0.96 | 0.035 | 0.8363 |
| | $Ni^{2+}$ | 0.81 | 0.66 | 0.032 | 0.7143 |
| 50.0 | $Cu^{2+}$ | 4.03 | 3.88 | 0.011 | 0.9560 |
| | $Pb^{2+}$ | 4.86 | 5.32 | 0.009 | 0.9900 |
| | $Cr^{3+}$ | 2.81 | 2.94 | 0.017 | 0.9890 |
| | $Co^{2+}$ | 2.30 | 2.84 | 0.006 | 0.8672 |
| | $Cd^{2+}$ | 4.07 | 4.75 | 0.006 | 0.9430 |
| | $Ni^{2+}$ | 2.41 | 2.25 | 0.025 | 0.9492 |

## 4.3 Summary and Recommendations

In this study, grape waste from wine preparation was applied as a low cost adsorbent to remove mixed metal ions from aqueous solutions. Factors that were investigated include: pH effect, particle size and contact time. The investigation revealed that the material is very effective for the removal of $Cd^{2+}$ at even low pH, contrary to fly ash which required higher pH before it could effectively remove $Cd^{2+}$ from aqueous solutions. Although the investigation is inconclusive, it points to the facts that this material looks very promising for the remediation of $Cd^{2+}$ in particular but it looks also effective for $Cu^{2+}$, $Co^{2+}$, $Pb^{2+,}$ $Cr^{2+}$ and $Ni^{2+}$. The result obtained indicated that, the adsorption is influenced by pH, particle size, contact time and initial concentration.

There are extra investigations that need to be carried out on this material. Further characterizations need to be done to establish the actual chemical compounds of the material. SEM needs to be applied to ascertain the morphology of the material. Also, $N_2$ adsorption could be employed to determine the surface area, pore volume and pore size distribution of this material. Other adsorption tests that need to be investigated are adsorption isotherms to measure the adsorption capacities of the material for each metal ion as well as thermodynamic properties. Also XPS should be used to investigate the kind of adsorption mechanism which removes the metal ions from the solution.

# Chapter 5

# Conclusion and Further work on fly ash

In this research a formulated foam composite material has been produced from coal fly ash through alkaline modification followed by the incorporation of cement and a foaming agent. The objective of this study was to modify fly ash, characterize and apply the modified fly ash for adsorption of multicomponent elements from aqueous solutions and to apply the modified fly ash in the formulation of a foamed material. Two path of modifications were followed that used high and low temperature procedures. Both pathways yielded materials with improved surface area, pore volume, smaller particle sizes and increased cation exchange capacities. However, due to problems encountered during the high temperature modification and predictable increased cost, this pathway was terminated.

The low temperature modification involving either room temperature or freezing and thawing cycle yielded materials which possess characteristics of good adsorbents. These were denoted as TBRM and TBFZ. TBFZ was further modified by the incorporation of a foaming agent (FA) and a bonding agent (BA) into a formulated foam denoted as TBFZ:FA:BA = 0.22:0.33:0.45. The material was proven to be an effective adsorbent for the removal of mixed metal ions from aqueous solutions, cocktail solutions made by adding a mixture of metal ions in distilled and an industrial water sample collected from a mining effluent. The characterization employing different instrumentation was done and the comparison made among the materials including pristine fly ash TB and the modified samples TBRM, TBFZ and composite TBFZ:FA:BA = 0.22:0.33:0.45. The modified samples TBRM, TBFZ and TBFZ:FA:BA = 0.22:0.33:0.45 showed improved surface area in the order TBFZ > TBRM > TBFZ:FA:BA = 0.22:0.33:0.45 > TB, as well as increased pore volume and increased cation exchange capacity. The cation exchange capacity of the materials were in the order of TBFZ > TBRM > TB. XRD analysis revealed slight differences in the crystalline phases of TB, TBRM and TBFZ. Additionally, the formulated foam material had an efficient water absoption capability and a relatively high compressive strength capable of withstanding different levels of stress and strain.

The adsorption kinetics of a cocktail solution of $Cu^{2+}$, $Cr^{3+}$, $Co^{2+}$, $Cd^{2+}$, $Pb^{2+}$ and $Ni^{2+}$ with 50.0 mg/L each in SCS was investigated under controlled pH. It was observed that TB, TBRM and TBFZ removed 100 % of $Cu^{2+}$, $Pb^{2+}$ and $Cr^{3+}$ ions after 300 min. However, the 100 % removal was achieved by TBRM and TBFZ earlier than TB. Similarly, in the removal of Ni, Co and Cd ions from SCS, TBFZ and TBRM had faster removal compared to TB with percentage removal of 95, 80 and 58 % of $Cd^{2+}$ by TBFZ, TBRM and TB, respectively. For $Co^{2+}$ the removal percentage by were of 100, 68 and 36% and 100, 65 and 49 % of $Ni^{2+}$, respectively by TBFZ, TBRM and TB. The spiking of TPW with metal ions and subsequent removal by TB, TBRM and TBFZ showed improved removal percentages in the kinetic adsorption studies. For the metals $Cu^{2+}$, $Cr^{3+}$ and $Pb^{2+}$, a 100 % removal was attained at shorter times compared to the SCS. The adsorbents TB, TBRM and TBFZ had percentage removal of 77, 80 and 100 % of $Ni^{2+}$, 82, 80 and 100 % of $Co^{2+}$ and 66, 88 and 100 % of $Cd^{2+}$, respectively. The kinetic adsorption studies with composite TBFZ:FA:BA = 0.22:0.33:0.45 demonstrated similar results in both SCS and TPW. Two groups of metal ions were identified in this studies. The groups are $Cr^{3+}$, $Cu^{2+}$, $Pb^{2+}$ for higher removal rates and $Co^{2+}$, $Ni^{2+}$ and $Cd^{2+}$ for slightly lower efficiency. This identification was attributed to the differences in solubility products of the hydroxides and complexation constants with $OH^-$ of the metal ions.

In order to determine the adsorption capacities of TB, TBRM and TBFZ in both SCS and TPW, pH was controlled at 7.04 ± 0.03 for $Pb^{2+}$, 7.40 ± 0.03 for $Ni^{2+}$, 7.33 ± 0.16 for $Co^{2+}$, 8.02 ± 0.17 for $Cd^{2+}$, 5.8.2 ± 0.03 for $Cu^{2+}$ and 4.06 ± 0.03 for $Cr^{3+}$, respectively in SCS whereas in TPW the pH was controlled at 7.05 ± 0.03, 7.49 ± 0.04, 7.49 ± 0.08, 7.70 ± 0.12, 5.94 ± 0.59 and 4.07 ± 0.08 for the same order, respectively. The maximum adsorption capacities $q_m$ of TB, TBRM and TBFZ in SCS were estimated at 0.385, 0.681 and 0.678 mmol/g for Pb, respectively. For Ni, $q_m$ of TB, TBRM and TBFZ were 0.259, 0.484 and 0.678 mmol/g, resepctively. Co revealed values of 0.303, 0.301 and 0.278 mmol/g whereas those of Cd were 0.157, 0.234 and 0.205 mmol/g, respectively. Both TBRM and TBFZ adsorbed Cu and Cr more efficiently than TB. While TBRM and TBFZ showed values of 0.312 and 0.251 mmol/g, respectively for Cu, TB only had a $q_m$ of 0.23 mmol/g.

The adsorption of Cr was more significant in TBRM and TBFZ showing values of 0.48 and 0.49 mmol/g as compared to 0.20 mmol/g for TB. Similar trend with improved adsorption capacities was observed with regards to TPW. This enhanced adsorption capacities of the materials in TPW was atttributed to the high amount of cations and anions or high ionic strength in the TPW. Very significant improvement of adsorption capcities were observed for materials with outstanding high values for Pb in TBRM and TBFZ showing 0.68 and 0.72 mmol/g, respectively.

The regeneration of the material was more effective for TBFZ compared to TBFZ:FA:BA = 0.22:0.33:0.45 as the former went through three cycles of adsorption – leaching while the later went through only through two before starting to become eroded. The reason for the effective regeneration of TBFZ was attributed to the enhanced surface area of this modified fly ash compared to TBFZ: FA:BA = 0.22:0.33:0.45. It was also observed that both 0.5 M and 1.0 M $HNO_3$ leaching solutions were strong enough to cause attrition and deterioration of the formulated foam just after the first leaching.

The column studies supported the behavior of the adsorbents tested in the batch mode. Similar trends in terms of percentage removal with time were also demonstrated by the column studies. Removal percentages were very high for TBFZ for all metal ions when the flow rate was 2.1 mL/min compared to TB. A comparison between 4.2 and 2.1 mL/min flow rates showed better removal percentages by both TB and TBFZ when the slower flow rate was applied. The reason was attributed to sufficient interaction between the adsorbent and adsorbate due to longer residence time for the adsorbate. Also the same groups of metal ions identified in the batch mode was confirmed in the column studies.

The following conclusions can be made from this research work:

(i) The results indicate that Thunder Bay fly ash can be modified with an alkaline treatment at room, freezing and elevated temperatures

(ii) The alkaline modification induced higher porosity, increase in surface area and enhanced cation exchange capacity

(iii) Incorporation of cement and a foaming agent into fly ash improved the absorption of water thus increasing the adsorption properties of the new composite material.

(iv) The control of pH of the solution could significantly improve the sorption rate and sorption capacity of metal ions onto Thunder Bay fly ash, whether modified or not

(v) Kinetic data could be modeled by a pseudo-second order kinetics equation

(vi) Langmuir and Freundlich isotherms could be used to model the isothermal sorption of $Pb^{2+}$, $Cr^{3+}$, $Cu^{2+}$, $Co^{2+}$, $Ni^{2+}$ and $Cd^{2+}$ on modified fly ash materials

(vi) The results indicate a significant potential of the modified Thunder Bay fly ash (powder and formulated foam) as effective adsorbents for the removal of $Cd^{2+}$, $Pb^{2+}$, $Cu^{2+}$, $Cr^{3+}$, $Ni^{2+}$ and $Co^{2+}$ from the seepage water of mine tailings

## Suggestions for future work

This section proposes some of the further investigations that could be carried out to compliment this study :

(i) Further studies on the characterisation of metal loaded adsorbents by XPS or other surface techniques to confirm adsorption as a physical adsorption process.

(ii) Further tests on the influence of anions in the improvement of metal removal behavior with the adsorbents.

(iii) Tests with other organic and inorganic foaming agents could be explored in the conversion of powdered material to formulated foam.

(iv) Other physical and chemical properties of the formulated foam before and after soaking in water should be investigated.

(v) Develop a formulated composite that could be tested under real environmental conditions in mine sites.

# References


[1] Food and Agricultural Organization. The state of the World's land and water resources for food and agricultural (SOLAW). Managing sytems at risk, Earthscan, London, 2011.

[2] United Nations world water Development Report.(2015). Water for sustainable World - Facts and figures.

[3] Department, U. S. G. S. (2013). "Scientific Investigations Report 2013." **5079**.

[4] World Health Organisation (2015). "Key facts from joint and monitoring program (JPM) 2015 Report."

[5] Department, U. S. G. S. (2016). "Contaminants found in ground water." URL.

[6] http://www.health.gov.au (2010). "Water - its importance and source.".

[7] https://www.epa.gov/ground-water-and-drinking-wate.

[8] Rashed, M. N. (2013). "Adsorption technique for the removal of organic pollutants from water and waste water." Organic pollutants - Monitoring, Risk and Treatment : 167-194.

[9] Matilainen Anu, M. V., Mika sillanpää (2010). "Natural organic matter removal by coagulation during drinking water treatment: A review." Advances in Colloid and Interface Science **159**: 189-197.

[10] KU, Y., and JUNG, I.-L. (2001). "Photocatalytic reduction of Cr(VI) in aqueous solutions by UV irradiation with the presence of Titanium dioxide." Water Research **35**: 135-142.

[11] Fu, F. and Wang, Q. (2011). "Removal of heavy metal ions from wastewaters: A review." Journal of Environmental Management **92**: 407-418.

[12] Matlock, M. M., Howerton, B. S. and Atwood, D. A. (2002). "Chemical precipitation of heavy metals from acid mine drainage." Water Research **36**(19): 4757-4764.

[13] Kang, S. Y., Lee, J., Moon, S. H. and Kim, K. W. (2004). "Competitive adsorption of characteristics of Co2+, Ni2+ and Cr 3+ by IRN-77 cation exchange resin in synthesized waste water." Chemosphere **56**: 141-147.

[14] Rouquerol F., R. J., Sing K.,S., W., Llewellyn P. and Maurin G. (2014). "Adsorption by powders and porous solids: principles, methodology and applications." Academic Press, London.

[15] Gupta, V. K., Ali, I., Saleh, T. A., Nayak, A. and Agarwal, S. (2012). "Chemical treatment technologies for wastewater recycling- an overview." RSC Advances **2**: 6380-6388.

[16] Aziz, H. A., Aldan, M. N. and Ariffin, K. S. (1993). "Heavy metals ( Cd,Pb,Zn,Cu,Cr(III) removal from waster in Malaysia:post treatment by high quality lime stone." Bioresource Technology **99**: 1578-1583.

[17] Gupta, V. K., Carrott, P. J. M., Carott, M. M. L. R. and Suhas (2009). "Low-Cost Adsorbents : Growing Approach to Wastewater Treatment- a Review." Critical Reviews in Environmental Science and Technology **39**: 783- 842.

[18] Ahmaruzzaman, M. (2011). "Industrial waste as low- cost potential adsorbents for the treatment of wastewater laden with heavy metals." Advances in Colloid and Interface Science **166**: 38-39.

[19] Wang, S. and Wu, H. (2006). "Environmental -benign utilization of fly ash as low-cost adsorbents." Journal of Hazardous Materials **B 136**: 482-501.

[20] Natural Resources,Canada (2006). "Mineral and Commodity Reviews,"." Canadian Minerals Yearbook.

[21] Heidrich, C., Hans-Joachim, Feuerborn and Weir, A. (2013). "Coal Combustion production-A golbal perspective." VGB Power Tech **12**.

[22] Feuerborn, H. J.-. Coal ash utilization over the world and in Europe, Workshop on Envionmental and Health Aspects of Coal Ash Utilization, Europian coal Combustion Products Association, Tel-Aviv, Israel 2005.

[23] Lyer, R. S. and Scott, J. A. (2001). "Power Station fly ash- A review of value-added utilization outside of construction industry." Resource Conservative Recycle **31**: 217-228.

[24] Subhajit, D., Haribandhu, C., G, U. and Ashis, S. (2016). "Fabrication of inexpensive polyethylemine-functionalized fly ash for highly enhanced adsorption of both cationic and anionic toxic dyes from water." Energy and Fuel **30**: 6646-6653.

[25] Singh, N. (2009). "Adsorption of herbicides on fly ash from aqueous solutions." Journal of Hazardous Materials **168**: 233-237.

[26] Duta, A. and Visa, M. (2015). "Simultaneous removal of two industrial dyes by adsorption and photocatalysis on fly -as-$TiO_2$ composite." Journal of Photochemistry and Photobiology A: Chemistry **306**: 21-30.

[27] Nollet, H., Roels, M., Lutgen, P., Meeren, P. v. d. and Vertraete, W. (2003). "Removal of PCBs from wastewater using fly ash." Chemosphere **53**: 655-665.

[28] Deokar, K.S., Mandavgane, A.S. and Kulkarni, B. D. (2016). "Adsorptive removal of 2,4-dichlorophenoxyacetic acid from aqueous solution using bagasse fly ash as adsorbent in batch and packed-bed techniques." Clean Technical Environmental Policy **18**: 1971-1983.

[29] Gupta, V. K. and Ali, I. (2001). "Removal of DDD and DDE from wastewater using bagasse fly ash,s sugar industry waste." Water Research **35**(1): 33-40.

[30] Banerjee,S. S.  M. V. J., R.V. Jayaram. (2004). "Removal of Cr(VI) and Hg(II) from aqueous solutions using fly ash and impregnated fly ash." Separation Science Technology **39**: 1611-1629.
[31] Subhajit, D., Haribandhu, C., Udayabhanu, G., Gupta, R. and Ashis, S. (2017). "Fabrication and application of low -cost thiol functionalized coal fly ash for selective adsorption of heavy  toxic metal ions from water." Industrial and Engineering Chemistry Research: 1-32.
[32] Hui, K. S., Chao, C. Y. H. and Kot, S. C. (2005). "Removal of mixed heavy metal ions in wastewater by zeolite 4A and residual products from recycled coal fly ash." Journal of Hazardous Materials **B127**: 89-101.
[33] Ulatowska, J., Polowczyk, I., Sawinski, W., Bastrzyk, A., Kozlecki, T. and Sadowski, Z. (2014). "Use of fl y ash and fl y ash agglomerates for As(III) adsorption from aqueous solution." Polish Journal of Chemical Technology **16**(1): 21-27.
[34] Nascimento, M., Soares, P. S. M. and Sousa, V. p. d. (2009). "Adsorption of heavy metal cations using coal fly ash modified by hydrothermal method." Fuel **88**: 1714-1719.
[35] Pitsopoulos, K. P. (1999). "cation – exchange – Capacity (CEC) of zeolitic volcanic clastic materials: Application of ammonium acetate saturation (AMAS) method." Clay and Clay Minerals **47**(6): 688 – 696.
[36] Chelaru, A. and Visa M., (2014). "Hydrothermally modified fly ash for heavy metals and dyes removal in advanced wastewater treatment." Applied Surface Science **303**: 14-22.
[37] Case, S. C. and case, E. D. (1990). "Characterization of fly ash from coal fired power- plants." Journal of Material Science **25**: 5215-5219.
[38] Gatima, E., Mwinyihija M. and Killham K. (2006). "Determination of adsorption efficiency based on cation exchange capacity related to red earth, bone meal and pulverised fly ash as ameliorants to lead contaminated soils." International Journal of Environmental  Science  and Technology. **3**(3): 269-280,.
[39] Alvarez-Ayuso, E., Garcia-sanchez, A. and Querol, X. (2003). "Purifaction of metal electroplating waste waters using zeolites." Water Research **37**: 4855-4862.
[40] Steenbruggen, G. and Hollman, G. G. (1998). "The synthesis of zeolites from fly ash and the properties of  the zeolites products " Journal of Geochemical Exploration **62**: 305-309.
[41] Semmens, M. J. and Seyfarth., M. (1978). "The selectivity of  clinoptilolite for certain heavy metals in : L.B sand, F.A. mumpton (Eds), natural zeolites : Occurance, properties, use." Pergamon Press Ltd. Oxford.: 517-526.
[42] Inglezakis, V. J. and Grigoropoulou, H. P. (2001). "Applicabilty of simplified models for the estimation of ion exchange diffusion coefficients in zeolites." Journal of Colloidal and Interface Science. **234**: 434-441.

[43] Inglezakis, V. J., Loizidou, M. D. and Grigoropoulou, H. P. (2002). "Equilibrium and kinetic ion exchange studies of $Pb^{2+}$,$Cr^{3+}$,$Fe^{3+}$ and $Cu^{2+}$ on natural clinoptilolite." Water Research **36**: 2784-2792.

[44] Majdan, M., Pikus, S., Ternes, M. K.-., Gladysz-Plaska, Staszczuk, P., Fuks, L. and Skrzypek, H. (2003). "Equlibrium study of selected divalent d-electron metals adsorption on A -type zeolite." Journal of Colloid and Interface Science **262**: 321-330.

[45] Cho, H., Oh D. and . and Kim K. (2005). "A study on removal charecteristics of heavy metals from aqueous solution by fly ash." Journal of Hazardous Materials. **127**.

[46] Hui, K. S., Chao, C. Y. H., Kot, S. C. and (2005). "Removal of mixed heavy metal ions in wastewater by Zeolite 4A and residual products from recycled coal fly ash." Journal of Hazardous Materials **B 127**: 89-101.

[47] Eleonora Soco, J. K. (2013). "Adsorption of nickel (II) and copper(II) ions from aqueous solution by coal fly ash." Journal of Environmental Chemical Engineering **1**: 581-588.

[48] Bayat, B. (2002). "Comparative study of adsorption properties of Turkish fly ashs I.The case of nickel(II),copper(II) and zinc(II)." Journal of Hazardous Materials **B95**: 251-273.

[49] Wingenfelder, U., Hansen, C., Furrer, G. and Schulin., R. (2005). "Removal of Heavy Metals from Mine Waters by Natural Zeolites." Environmental Science and Technology **39**: 4606-4613.

[50] Sari, A., Tuzen, M., Citak, D. and Soylak, M. (2007). "Adsorption characteristics of Cu(II) and Pb(II) onto perlite from aqueous solution." Journal of Hazardous Materials **148**: 387-394.

[51] G.McKay (1984). "The adsorption of basic dye onto silica from aqueous -solution solid diffusion-model." Chemical Engineering Science **39**: 129-138.

[52] Ho Y.S., and McKay G. (1999). "Pseudo-second order model for sorption processes." Processes in Biochemistry **34**: 451.

[53] Taty-Costodes, V. C., Fauduet, H., Porte, C. and Delacroix, A. (2003). "Removal of Cd(II) and Pb(II) ions, from aqueous solutions,by adsorption onto sawdust of Pinus sylvestris." Journal of Hazardous Materials **B105**: 121-142.

[54] Benguela, B. B. and Benaissa H. (2002). "Cadmium removal from aqueous solution by chitin : kinetic and equilibrium studies." Water Research **36**: 2463.

[55] V. Christian Taty-Costodes , H., Catherine Porte and Alain Delacroix. "Removal of Cd(II) and Pb(II) ions, from aqueous solutions, by adsorption onto sawdust of Pinus sylvestris." Journal of Hazardous Materials. **B 105**: 121-142.

[56] Bayat B. (2002). "Comparative study of adsorption properties of Turkish fly ashes II.The case of nickel (II),copper(II) and zinc(II)." Journal of Hazardous Materials **B95**: 251-273.

[57] H. Wang, X. B., T. Teng,K Wang and K Ladwig (2006). "Impacts of pH and ammonia on the leaching of Cu(II) and Cd(II) from coal fly ash." Chemosphere **64**: 1892-1898.

[58] Chaiyasith S., Chaiyasith P. and Septhum C. (2006). "Removal of cadmium and nickel from aqueous solution by adorption onto treated fly ash from Thailand." Thammasat International of Science and Technology **11**: 13-20.

[59] Yueming Ren, N. Y., Qing Wen,Zhuangjun Fan,Tong Wei,Milin Zhang and Jun Ma (2011). "Graphene/-$MnO_2$ composite as adsorbent for the removal of Nickel ions from wastewater." Chemical Engineering Journal **175**: 1-7.

[60] Faust D. S. and Osman M. Aly. (1987). Adsorption processes for water treatment, Butterworth, Stoneham, 1987.

[61] Visa, M., Heavy metals removal on dye -modified fly ash substrates, World of coal ash (WOCA), www.flyash.info, Denver,Co,USA, 2011.

[62] Huang, S. H. and Chen, D. H. (2009). "Rapid removal of heavy metal cations and anions from aqueuos solutions by an amino-functionalized magnetic nano-adsorbent." Journal of Hazardous Materials **163**: 174-179.

[63] Chao, H. P., C.K.Lee, L.C.Juan and Y.L.Han (2013). "Sorption of organic ,oxyanions and heavy metal ions on surfactant modified titanate nanotubes." Industrial Engineering Chemical Research **52**(29): 9843-9850.

[64] Liang, P., Shi, T. and Li, J. (2004). "Nanometer-size titanium dioxide separation / preconcentration and FAAS determination of trace Zn and Cd in water sample." Internatinal Journal of Environmental Analytical Chemistry **84**(4): 315-321.

[65] Shawabheh, R., Al-Harahsheh, A., Hami, M. and Khlaifat, A. (2004). "Conversion of oil shale sh into zeolite for cadmium and lead removal from wastewater." Fuel **83**: 981-985.

[66] Ali, I. "Water treatment by adsorption columns: Evaluation at Ground Level." Separation and Purification Reviews **43**(3): 175-205.

[67] Karthikeyan, B., Selvaraj, R. and Saravanan, S. (2015). "Mechanical properties of foam concrete." International Journal of Earth Sciences and Engineering **8**(2): 115-119.

[68] Just, A. and Middendorf, B. (2009). "Microstructure of high-strength foam concrete." Materials Characterisation **60**: 741-748.

[69] Ibrahim, N. M., Salehuddin, S., Amat, R. C., Rahim, N. L. and Izhar, T. N. T. (2013). "Performance of lightweight foamed concrete with waste clay brick as coarse aggregate." APCBEE Procedia. **5**: 497-501.
[70] Luping, T. (1986). " A study of the quantitative relationship between strength and pore size distribution of porous materials." Cement Concrete Resources **16**: 87-96.
[71] Kalyani, S., Priya, J. A., Rao, P. S. and Krishnaiah, A. (2005). "Removal of copper and nickel from aqueous solutions using chitosan coated on perlite as biosorbent." Separation Science Technology **40**: 1483-1495.
[72] Inoue, K., Baba, Y. and Yoshizuka, K. (1988). "Selectivity series in the adsorption of metal ions on a resin prepared by crosslinking copper(II) - complexed chitosan." Chemistry Letters **9**: 1281-1284.
[73] Panayotova, M. and Velikov, B. (2003). "Influence of zeolite transformation in a homoionic form on the removal of some heavy metal ions from wastewater." Journal of Environmental Science and Health **A38**(3): 545-554.
[74] Nabi, S. A., Shahadat, M., Shalla, A. and Khan., A. M. (2011). "Removal of heavy metals from synthetic mixtures as well as pharmaceutical sample via cation exchange resin modified with Rhodamin B: It thermodynamic and kinetic studies. Clean -Soil Air Water **39**: 1120- 1128.